2020

CHEMICAL SYNTHESIS AND BIOLOGICAL EVALUATION OF BENZIMIDAZOLES AS CHEMOTHERAPEUTICS

Leonard Barasa
Saint John's University, Jamaica New York

CHEMICAL SYNTHESIS AND BIOLOGICAL EVALUATION OF BENZIMIDAZOLES AS CHEMOTHERAPEUTICS

A dissertation submitted in partial fulfillment
of the requirements for the degree of

DOCTOR OF PHILOSOPHY

to the faculty of the

DEPARTMENT OF GRADUATE DIVISION

of

COLLEGE OF PHARMACY AND HEALTH SCIENCES

at

ST. JOHN'S UNIVERSITY
New York
by
Leonard Barasa

Date Submitted _____ Date Approved _____

_____ _____

LEONARD BARASA PROF. SABESAN YOGANATHAN

ABSTRACT

CHEMICAL SYNTHESIS AND BIOLOGICAL EVALUATION OF BENZIMIDAZOLES AS CHEMOTHERAPEUTICS

Leonard Barasa

Nitrogen-containing heterocycles are among the most important structural motifs of chemical substances, which are well represented among natural products, and pharmaceuticals. The presence of nitrogen in heterocycles help to modulates physicochemical properties and the pKa profile of therapeutic leads.

Benzimidazole is a heterocyclic structure and a privileged scaffold that is routinely used during drug discovery efforts. The benzimidazole scaffold has structural similarity to purine which makes it a useful structural motif for the development of pharmaceutical or biological interesting molecules. Benzimidazole derivatives possess a wide variety of biological activities, including anti-bacterial, anti-cancer, and anti-inflammatory activities. Development of synthetic methods to access benzimidazoles have become a focus of synthetic organic chemists, as they are useful building blocks for drug discovery efforts. We have developed two new synthetic methodologies to access benzimidazoles and one new method to chemo-selectively alkylate indole-benzimidazole scaffold. We used these synthetic methodologies to synthesize new, drug-like benzimidazole compounds and evaluated their anticancer activity, and their ability to modulate Bone Morphogenetic Proteins (BMPs).

Our results indicate that several indole-based, lipid-based, and bis- benzimidazoles exhibit promising anticancer activity against several cancer cell lines. A new class of bis-

benzimidazoles, show topoisomerase II inhibitory activity. In addition, substituted aryl benzimidazoles have been identified as new class of small molecules with promising BMP receptor agonistic activity, where they stimulated downstream cascade canonical Smad-signaling pathways in C2C12 cells. Our findings suggest that further development of these scaffolds could provide drug leads towards new chemotherapeutic agents and a new class of small molecule activators of BMP signaling pathway for the treatment of bone-fracture.

ACKNOWLEDGEMENTS

With a sense of utmost gratitude, I would like to sincerely thank several people whose efforts have immensely contributed to the conclusion of my thesis during my term at St. John's University as a graduate student.

I would like to thank my mentor, Dr. Sabesan Yoganathan for his continuous support all through my research. I also thank him for the knowledge he has provided me with and encouragement to think critically, which developed a skill for troubleshooting within me. His approach toward perceiving results and to develop on the results has led to a strong foundation in my research. I am forever grateful for him for mentoring me in this long journey toward achieving my Ph.D. degree. I am also grateful to Dr. Vijaya Korlipara, Dr. Sandra Reznik, Dr. Tanaji T. Talele and Dr. Aaron Muth for serving as committee members in my defense. I am thankful to Dr. Vikas V. Dukhande, Dr. Woon-Kai Low, Dr. Jeanette C. Perron and Dr. Sandra Reznik for their collaboration in bioassays of the synthesized compounds. I am grateful to Dr. Korlipara, Dr. Talele and Dr. Muth for providing me access to their equipment and chemicals from their labs. I am thankful to Dr. Vivek Gupta, Dr. Steven M. Graham and Dr. Raymond S. Ochs for giving me an opportunity to work with their LC-MS related projects. I am also thankful to lab mates for their support throughout my research.

My sincere thanks go to St. John's University and especially the College of Pharmacy and Health Sciences, and the Department of Pharmaceutical Sciences for providing me support through weekly budgets, equipment for my research and also for providing me funding to complete my program. I am grateful to Dr. Carvalho, my supervisors Susana Solis, Joyce

Festa and Pratibha Agdern, for providing me the opportunity and a great experience in teaching, both as an assistant and as a fellow. I also thank Suzette Weiss from the science supply department for her support in ordering supplies in a timely manner and for always being available for any help related to lab supplies.

TABLE OF CONTENTS

LIST OF TABLES

LIST OF FIGURES

LIST OF ABBREVIATIONS

ATP	Adenosine Triphosphate
ALK	Anaplastic Lymphoma Kinase
BMP	Bone Morphogenetic proreins
BMPRI	Bone Morphogenetic proreins Receptor I
BMPRII	Bone Morphogenetic proreins Receptor II
BMD	Bone Marrow Density
CLL	Chronic Lymphocytic Leukemia
Cbz	Carboxybenzyl
DNA	Deoxyribonucleic Acid
DMF	Dimethylformamide
DM	Dorsomorphin
RNA	Ribonucleic acid
ºC	Degree centigrade
$CDCl_3$	Deuterated Chlorofoam
CH_3CN	Acetonitrile
DIPEA	*N*,*N*-disopropylethylamine
DMSO	Dimethyl sulfoxide
DMSO-d6	Deuterated Dimethyl sulfoxide
DIC	*N*,*N'*-diisopropylcarbodiimide
EDCI	1-ethyl-3-(3-dimethylaminopropyl) carbodiimide
h	hour
Hz	Hertz
HBTU	*O*-(benzotriazole-1-yl)-*N*,*N*,*N'*,*N'*-tetramethyluronium hexafluorophosphate
HCTU	*O*-(1*H*-6-chlorobenzotriazole-1-yl)-1,1,3,3-tetramethyluronium hexafluorophosphate

HOBt	1-hydroxybenzotriazole
HOCt	7-chloro-1-hydroxybenzotriazole
HOAt	7-aza-1-hydroxybenzotriazole
HRMS	High resolution mass spectometry
PyBOP	Tripyrrolidinophosphonium hexafluorophosphate
J	Coupling Constant
min	Minutes
NHS	*N*-hydroxysuccinimide
$NaHCO_3$	Sodium hydrogen carbonate
rt	Room Temperature
TLC	Thin layer chromatography
μM	Micro Molar

CHAPTER I. INTRODUCTION

1.1 Nitrogen-Containing Heterocycles

Nitrogen-containing heterocycles are the building blocks of life. They are the key constituents of both DNA and RNA.[1] Nitrogen-containing heterocycles are among the most important structural motifs of chemical substances, which are well represented among natural products, key component of biologically active structures and among the most significant structural components of pharmaceuticals.[2–8] The presence of nitrogen in heterocyclic motifs help to modulates the physicochemical properties and the pKa profile of therapeutic leads.[7,9] Nitrogen-containing heterocycles (**Figure 1.1**), in light of their importance, have drawn considerable attention of researchers and their synthesis has always been a topic of interest to organic and medicinal chemists.

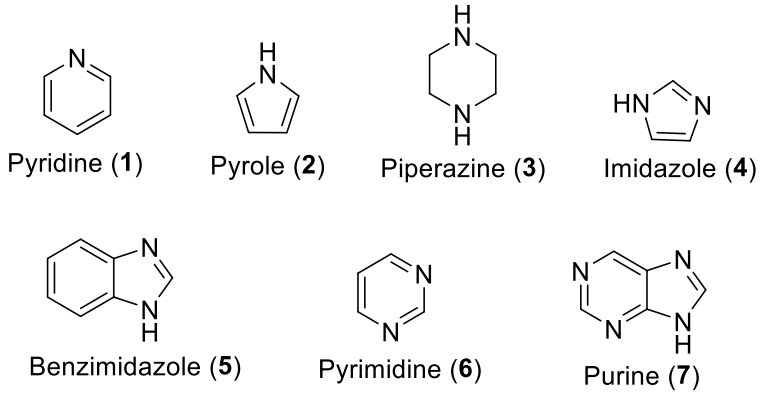

Figure 1.1 Structures of common nitrogen-containing heterocycles.

1.2 Benzimidazole: A Privileged Pharmacophore

Benzimidazole is a heterocyclic aromatic organic compound. It is an important scaffold and a privileged structure that is routinely used in drug discovery.[10] Benzimidazole core

(**5**, **Figure 1.1**) is bicyclic in nature that consists of a fused benzene and an imidazole rings. The heterocyclic benzimidazole scaffold has structural similarity to purine (**7**, **Figure 1.1**) which makes it a useful structural motif for the development of molecules of pharmaceutical or biological interest.[2,3] Benzimidazole derivatives possess a wide variety of biological activities,[10–29] including anti-bacterial,[30–40] anti-HIV,[41] anti-cancer,[42–54] analgesic,[55] anti-inflammatory activities,[56] anti-ulcer,[57] acetylcholinesterase inhibitors,[58] anti-tubercular,[59] anti-viral agent,[60] anthelmintic,[61–64] anti-malarial agent,[65] and anti-hypertensive activities.[66] In addition, chemotherapeutic leads containing benzimidazole core are known to target several biological molecules, including topoisomerases, nucleic acids (DNA), polyADP ribose polymerase (PARP), microtubule, epidermal growth factor receptors (EGFR), protein tyrosine kinases, and protein tyrosine phosphatases.[12,67–70] The benzimidazole nucleus is used as a drug lead and many benzimidazole drugs are in the market domain with Triclabendazole[71] (**12**) being the latest benzimidazole derivative drug to be approved by the FDA in the year 2019 for the treatment of fascioliasis (**Figure 1.2**).

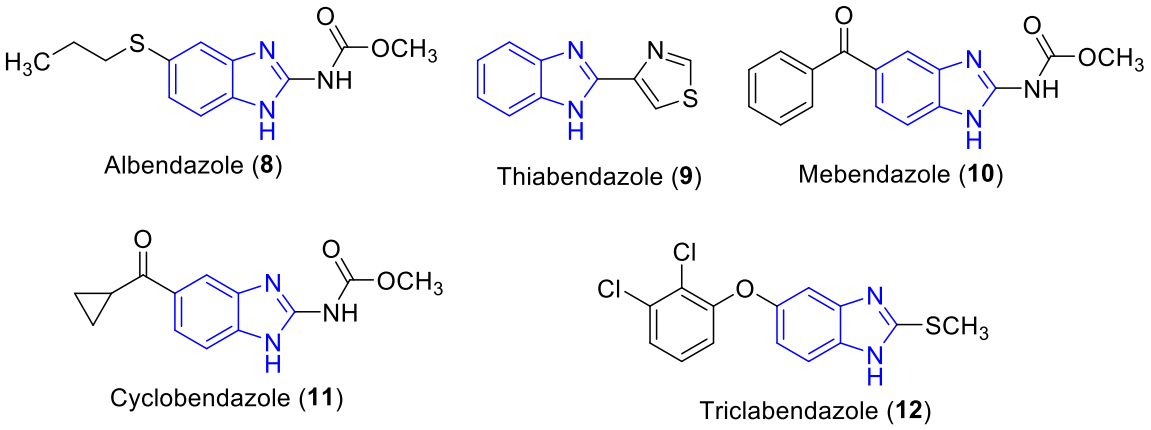

Figure 1.2 Marketed drugs with benzimidazole scaffold.

1.3 Synthetic limitations to access benzimidazoles

Development of synthetic methods to access benzimidazoles have become a focus of synthetic organic chemists, as they are useful building blocks for drug discovery efforts.[72] Various synthetic approaches are employed to generate structurally diverse benzimidazoles to better understand SAR and optimize the desired medicinal properties of drug leads.[73–90] One of the common synthetic approaches employed to access benzimidazoles involves condensation-dehydration sequence of an *o*-phenylenediamine with an aldehyde substrate[72,87,91,92] in the presence of a catalyst or a promoter. Another classical approach involves reaction of an *o*-phenylenediamine with a carboxylic acid substrate under forcing conditions, in the presence of a mineral acid or acetic acid, and under refluxing temperatures.[93] Other recent methods for the preparation of benzimidazole derivatives have focused on the use of transition metal-catalysts.[91,92,94–108]

The classically used approach (Phillip's method)[109] involves the condensation of an *o*-phenylenediamine with carboxylic acids or its derivatives, including heating the reagents together in the presence of aqueous hydrochloric acid (**Scheme 1.1**). Although effective, this method is limited to structurally simple substrates that can withstand the acidic medium at high temperatures.

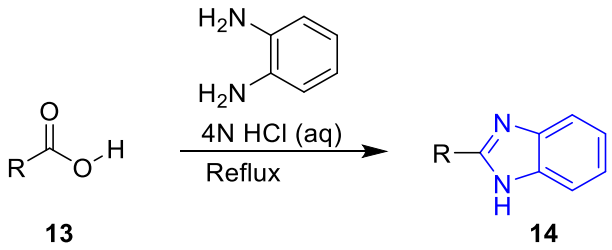

13 **14**

Scheme 1.1 A most commonly used synthetic method of benzimidazoles.

Due to the harsh reaction condition, the classical method shows very limited substrate scope, and cannot tolerate sensitive functional groups. In addition, limited availability of aldehyde substrates often hinders the application other available methods during medicinal chemistry efforts. Owing to the limited synthetic utility of existing methods, we envisioned developing a mild, functional group tolerant method for accessing diverse class of benzimidazole synthons (**Scheme 1.2**). In our proposed strategy, the substrates containing carboxylic acid are coupled with 1,2-diaminobenzene derivatives using standard carbodiimide-based coupling conditions and then the amide precursor is converted into the benzimidazoles via a dehydrative cyclization step under a mild reaction condition.

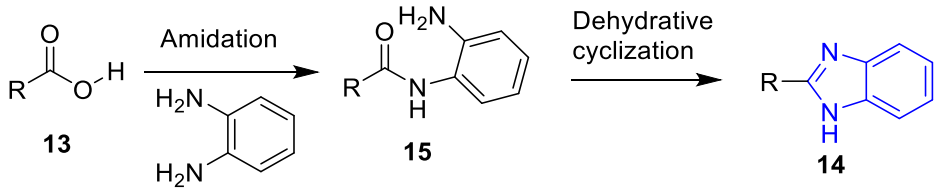

Scheme 1.2. Proposed one-pot, two step synthesis of benzimidazole derivatives

1.4 Synthetic limitation to N-alkylated 2-indolylbenzimidazoles

Indolylbenzimidazole, a hybrid benzimidazole derivative has emerged as an important scaffold during drug discovery efforts. *N*-alkylated indolylbenzimidazole scaffolds with different *N*-alkylation pattern have been found to be promising anticancer agents,[110] anti-bacteria agents,[38] and highly effective reversible inhibitors of protein arginine deiminase 4 (PAD4, **Figure 1.3**).[111–113] PAD4 enzyme mediates the transformation of protein arginine into citrulline.[112] Citrullination of proteins has normal roles in gene regulation and pathological roles in immunological and inflammatory diseases.

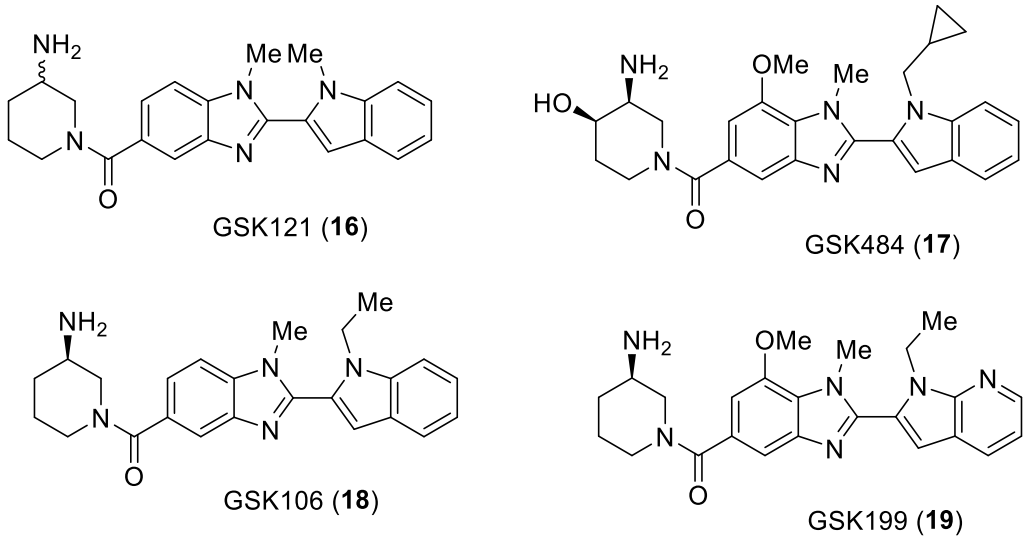

Figure 1.3 Structures of PAD4 inhibitors.

N-alkylation of indoles or benzimidazoles is typically carried out with strong bases, such as potassium hydroxide. Such reagents that cannot differentiate the reactivity of an indole, benzimidazole or any other reactive functional groups within a complex molecule.[37,110,114] This reactivity profile makes it nearly impossible to chemo-selectively alkylate indolyl-benzimidazole hybrids. *N*-alkylation of indolyl-benzimidazoles generally involves the separate *N*-alkylation of an indole's or benzimidazole's nitrogen prior to joining the two nuclei to form indolyl-benzimidazole hybrid structures (**Scheme 1.3**).[37,110] Such strategies require a series of protecting group manipulations and are deemed less economical. Other available methods for *N*-alkylation of heterocycles have typically focused on the use of ionic-liquids, other surfactant-type additives or metal catalyzed construction of heterocycles.[115–118]

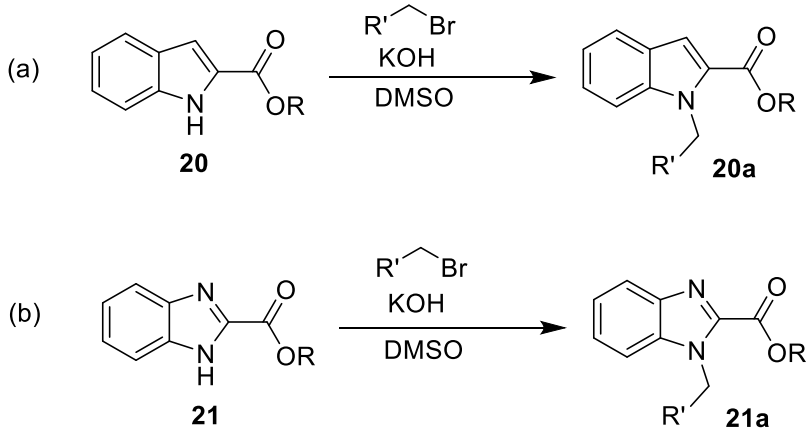

Scheme 1.3. Separate *N*-alkylation of indole (**20**) and benzimidazole (**21**) motifs.

We envision developing a simple chemical method to chemo-selectively alkylate the indolylbenzimidazole scaffold. The method is a late-stage alkylation and takes advantage of the pKa differences between the indolyl-nitrogen and the benzimidazole nitrogen.

1.5 Benzimidazoles as Anti-Cancer Agents

1.5.1 Cancer and Current Treatment Options

Cancer is a major public health problem worldwide and is the second leading cause of death in the United States.[119] Cancer is a group of diseases characterized by the uncontrolled growth and spread of abnormal cells, with the ability to spread to other parts of the body. If the spread is not controlled, it can lead to death.[120] According to the American Cancer Society, approximately 21.7 million new cancer cases are expected by 2030.[121] The mainstream treatment modalities,[122] chemotherapy, radiotherapy, surgery and immunotherapy have experienced set-backs in the hard fought battle against cancer, with toxicity and multidrug resistance (MDR) being the greatest stumbling blocks.[123–125]

Therefore, there is an urgent need for the development of new anti-cancer agents that exhibit improved efficacy and low adverse effects.

Many different types of drugs are used to treat cancer – either alone or in combination with other drugs or treatment options.[126] These drugs are very different in their chemical composition, how they are administered, how useful they are in treating certain types of cancer, and the side effects they exhibit.[127] Chlorambucil, an alkylating agent that works by disrupting DNA replication process.[128,129] Side effects include bone marrow suppression, nausea, mouth irritation, vomiting, skin reactions, hair loss, infertility, and diarrhea. Chlorambucil resistance in tumor cells has been reported to be secondary to: alterations in the transport of this agent, alterations in the kinetics of the DNA cross-links formed by this agent; cytoplasmic metabolism of the chloroethyl alkylating moiety to the inactive hydroxyethyl derivative via GSH/GST; and overexpression of metallothionein, which confers resistance to cis-platinum and cross-resistance to melphalan.[130] 5-Fluorouracil is an antimetabolite that interfere with DNA and RNA by acting as a substitute for the normal building blocks of RNA and DNA.[131] Side effects include nausea, vomiting, hair loss, persistent hiccups, mucositis, and headache. Resistance to fluoropyrimidines is a multifactorial event,[132] which includes transport mechanisms, metabolism, molecular mechanisms, protection from apoptosis, and resistance via cell cycle kinetics. Etoposide is a topoisomerase II inhibitor,[133] forms a ternary complex with DNA and the topoisomerase II enzyme, prevents re-ligation of the DNA strands, and by doing so causes DNA strands to break. Side effects include hair loss, low blood pressure, bone marrow suppression, and metallic food taste. Drug resistance towards Etoposide in human melanoma cells is associated with drug-dependent apoptosis deficiency.[134]

1.5.2 Benzimidazole-based Anti-Cancer Drugs

Nitrogen-containing heterocyclic ring systems are employed to treat different types of cancer, and benzimidazole is one of them as exemplified by benzimidazole based anti-cancer drugs[135,136] such as bendamustine (**22**)[137], is used for treatment of chronic lymphocytic leukemia (CLL), veliparib (**23**)[138] is an anti-cancer PARP inhibitor, selumetinib (**24**)[139] is an ATP-independent inhibitor of mitogen-activated protein kinase (MEK or MAPK/ERK kinase) 1 and 2, galeterone (**25**)[140] is a steroidal anti-androgen which is used for the treatment of prostate cancer, and nocodazole (**26**)[141] is a synthetic tubulin-binding agent that disrupts microtubule dynamics and this prevents mitosis and induces apoptosis in tumor cells (**Figure 1.4**).

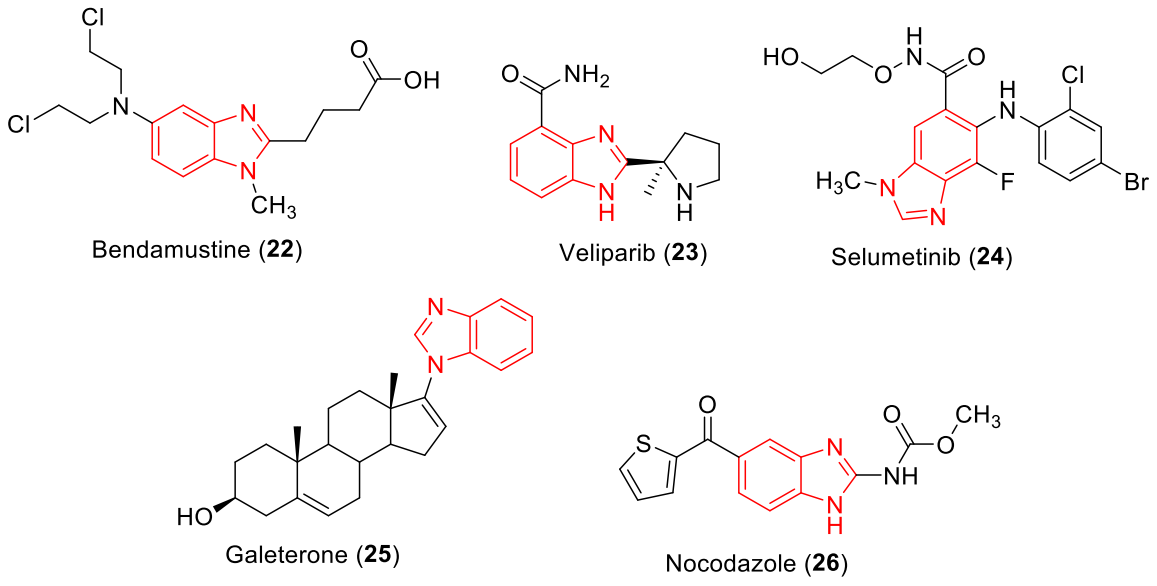

Figure 1.4 Benzimidazole-based anti-cancer drugs.

In an attempt to overcome adverse toxicity, drug-resistance and cancer-type based specificity, scientists are striving to find new and better anti-cancer agents.[135] Since potent

anticancer activity is associated with benzimidazole pharmacophore, it serves as a promising template for the design of new anti-cancer leads. Current research efforts have been heavily focused on the development of 2-substituted benzimidazoles, such as 2-aryl- and 2-heteroaryl benzimidazoles as drug leads.[12,38] Moreover, 2-substituted bis-benzimidazoles have been reported to exhibit remarkable cytotoxicity against various cancer cell lines as well.[12,16,142,143]

1.6 Benzimidazoles as Bone Morphogenetic Proteins (BMP) Modulators

1.6.1 Bone Morphogenetic Proteins

Bone Morphogenetic Proteins (BMPs) are a group of signaling molecules, which belong to the TGF-β superfamily.[144,145] The bone morphogenetic protein (BMP) family of ligands plays important roles in a multitude of processes during embryonic development and adult homeostasis by regulating cellular lineage commitment, morphogenesis, differentiation, proliferation, and apoptosis of various types of cells throughout the body.[146–148] BMPs are promising molecules for tissue engineering and bone therapy.[149,150] Alternative strategy to enhance BMP signaling by use of small molecules such as benzimidazoles[151] have been reported. The use of small molecules which are simpler to synthesize and more cost-effective is preferred alternative to clinical use of recombinant BMPs. The recombinant BMPs require harmful doses to achieve efficacy and is costly to synthesize the complex BMPs proteins.

Initially discovered for their ability to induce bone formation, BMPs are now known to play crucial roles in all organ systems.[152] BMPs are important morphogens in

embryogenesis and development, and in maintenance of adult tissue homeostasis. Many processes in early development are dependent on BMP signaling for cell growth, apoptosis, and differentiation.[153] Due to their ubiquitous expression and importance as regulators throughout the body, deficiency in BMP production or functionality usually leads to marked defects or severe pathologies.[145] BMPs signal through cell surface receptor complexes that consist of two distinct transmembrane serine/threonine kinase receptors, type I (BMPRI) and type II (BMPRII) which activate downstream signaling cascades (**Figure 1.5**) in many developmental, physiological, and pathophysiological processes.[154] Intracellular signals for bone morphogenetic proteins (BMPs) and other members in the transforming growth factor (TGF)-β superfamily are mediated by Smad proteins.[155] Receptor-regulated Smads (R-Smads) are activated by serine/threonine kinase receptors upon ligand binding. R-Smads then form hetero-oligomeric complexes with a common-mediator Smad 4 (co-Smad).[156] This complex is then translocated into the nucleus to regulate the transcription of genes, broadly influencing growth and differentiation. Smads 1, 5, and 8 are R-Smads activated by BMP receptors, whereas Smads 2 and 3 are activated by TGF-β and activin receptors.[153] Smad 4 is the only co-Smad isolated in mammals and is shared by BMP and TGF-β/activin signaling pathways. Smads 6 and 7 are anti-Smads, which block signals by preventing the activation of R-Smads by serine/threonine kinase receptors. Anti-Smads are induced by ligand stimulation, suggesting that they constitute a negative feedback loop in the signal transduction pathways of the TGF-β superfamily.[152,155–159]

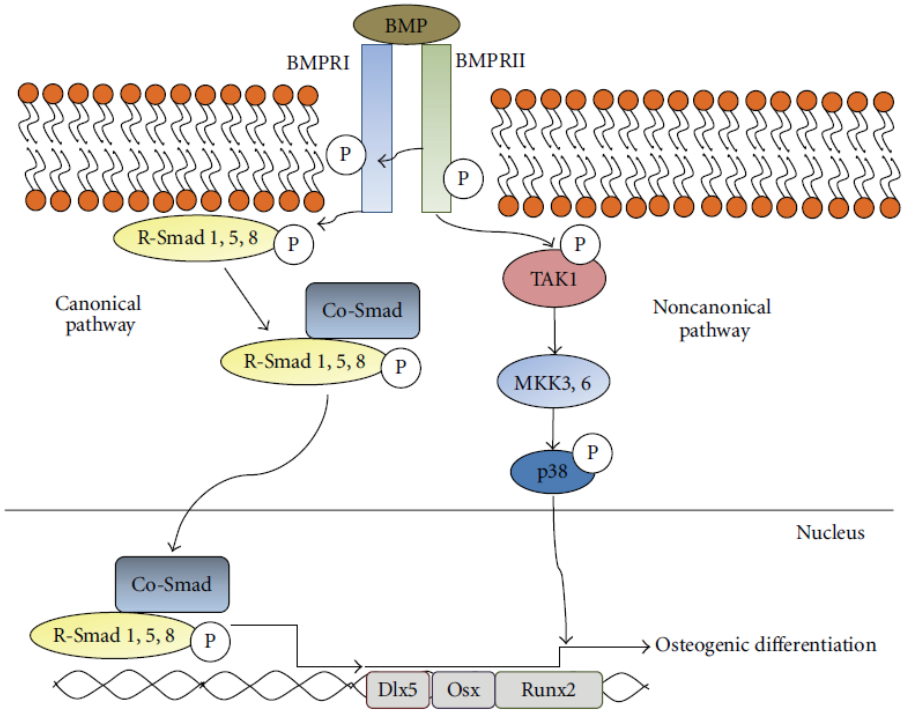

Figure 1.5. The canonical Smad-mediated and Smad-independent p38 MAPK pathways for BMP signal transduction are shown [Image adapted from Chenard K. E *et al*., *J. Biomed. Biotechnol*. **2012**].[153]

1.6.2 Bone Morphogenetic Proteins in Fracture Repair

Osteoporosis is a systemic disorder characterized as the depletion of bone mass with structural deterioration of bone tissue.[161] This results in a decrease in bone mineral density (BMD) and a predisposition to fragility fractures. It is a widespread chronic metabolic disease of the bone[162] and has been suggested to influence populations with different ethnic backgrounds, and the elderly are a high-risk group.[163] Osteoporotic fracture presents biomechanically impaired healing and seriously threatens human health as the global population ages.[164] It is reported that about 21 million males and 137 million females age

50 years and older around the world are at high risk of osteoporotic fracture and these numbers are predicted to double by 2040.[165] Moreover, the World Health Organization predicted that half of global osteoporotic hip fractures will occur in Asia by 2050.[166] Bisphosphonates[167] are the most widely used drugs for the prevention and treatment of osteoporosis but the main concerns limiting their use are the rare side-effects, such as a typical femur fractures and osteonecrosis of the jaw, and unproven efficacy after 5 years of treatment. Therefore, determining reasonable and effective approaches for diagnosis and treatment for osteoporotic fracture is of great significance.

BMPs are unique growth factors that can induce the formation of bone tissue individually, and can induce the differentiation of bone marrow mesenchymal stem cells into osteoblastic lineage and promote the proliferation of osteoblasts and chondrocytes.[168] BMPs stimulate the target cells by specific membrane-bound receptors and signal transduced through mothers against decapentaplegic (Smads) and mitogen-activated protein kinase (MAPK) pathways. It has been demonstrated that BMP-2, BMP-4, BMP-6, BMP-7, and BMP-9 play an important role in bone formation and healing.[179–182] However, BMP-based therapy for fracture healing require high doses, costly to produce, and major side-effects have been reported and their therapeutic use have been recently revisited.[172]

1.6.3 Small Molecules as Inhibitors of BMPs and their Therapeutic Application

Synthetic small molecules have been widely used to control developmental signaling pathways, as functional agonists or antagonists.[173] Compared to recombinant proteins, synthetic small molecules can be more stable, easier to quantify for reproducible activity

and dose-response, and far less expensive to produce.[173,174] To date, most of the small molecules discovered to regulate BMP signaling are antagonists.[175] Recent work suggests a role for BMP signals in regulating expression of hepcidin, a peptide hormone and central regulator of systemic iron balance.[176–178] Hepcidin binds and promotes degradation of ferroportin, the sole iron exporter in vertebrates. Loss of ferroportin activity prevents mobilization of iron to the bloodstream from intracellular stores in enterocytes, macrophages and hepatocytes.[179] Dorsomorphin (**27, Figure 1.6**) is the first known small-molecule inhibitor of BMP signaling, which inhibits BMP signals required for embryogenesis and iron metabolism.[175,180] Dorsomorphin selectively inhibits the BMP type I receptors ALK2, ALK3 and ALK6 and thus blocks BMP-mediated SMAD1/5/8 phosphorylation, target gene transcription and osteogenic differentiation.[181] The role of dorsomorphin in BMP signaling in iron homeostasis has been examined.[175,182] *In vitro*, dorsomorphin inhibits BMP-, hemojuvelin- and interleukin 6-, stimulated expression of the systemic iron regulator hepcidin, which suggests that BMP receptors regulate hepcidin induction by all of these stimuli. *In vivo*, systemic challenge with iron rapidly induced SMAD1/5/8 phosphorylation and hepcidin expression in the liver, whereas treatment with dorsomorphin blocked SMAD1/5/8 phosphorylation, normalized hepcidin expression and increased serum iron levels. These findings suggest an essential physiological role for hepatic BMP signaling in iron-hepcidin homeostasis.

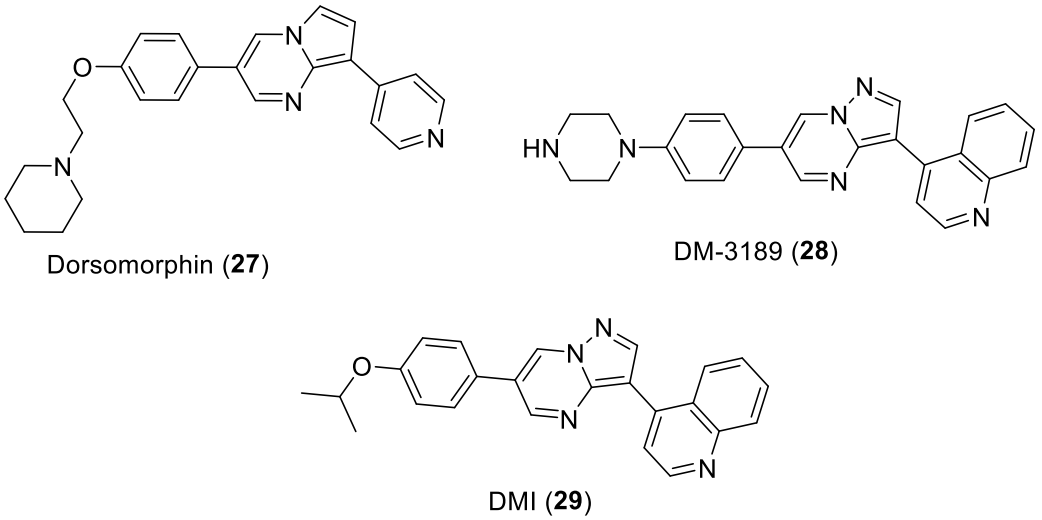

Figure 1.6 BMP signaling inhibitors of SMAD 1/5/8 phosphorylation.

1.6.4 Small Molecules as Activators of BMPs and their Therapeutic Application

Recently, several small molecules have been identified as activators of the BMP pathway (**Figure 1.7**). PD407824 (**30**) is a BMP sensitizer for human embryonic stem differentiation.[173] Quinoline derivative KM11073 (**31**) enhances BMP-2-dependent osteogenic differentiation of C2C12 cells *via* activation of p38 signaling and exhibits *in vivo* bone forming activity.[183] A01 (**32**) increases BMP-2 responsiveness by inhibiting Smurf1-mediated Smad1/5 degradation.[184] SJ000063181 (**33**), SJ000291942 (**34**) and SJ000370178 (**35**) are activators of the canonical BMP signaling pathway.[147] Sb 4 (**36**), Sb 5 (**37**), and Sb 6 (**38**) have been recently identified as agonists of BMP signaling pathways.[151] However, most of the reported compounds show relatively low activity and fail to induce the generation of mature osteoblasts, which limits their therapeutic potential. Thus, we screened an in-house library of small molecules to discovery more effective BMP activators. During the same time, we found a paper that reported a class of benzimidazole-

based BMP agonists[151] (**37** and **38**) that are similar to the aryl-benzimidazoles we identified. Based on this literature validity, we focused our efforts in designing and synthesizing 2-substituted aryl benzimidazoles as potential agonists of BMPs signaling pathways.

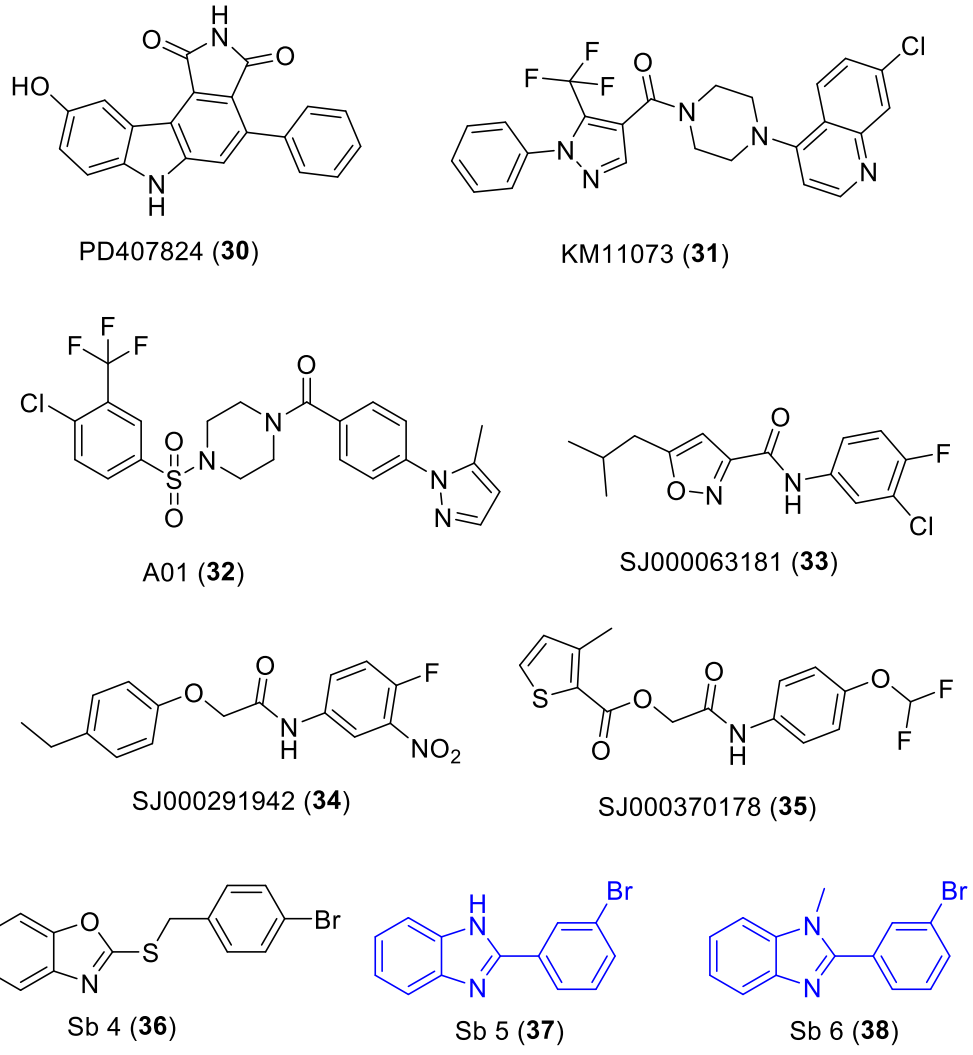

Figure 1.7. BMPs activators or sensitizers in stem cell differentiation.

CHAPTER II. DESIGN RATIONALE

Benzimidazoles have revolutionized the drug discovery process by their diverse range of biological activities, which makes this scaffold an indispensable anchor for innovative drug discovery efforts. Therapeutic potential of benzimidazoles has attracted researchers to design and synthesize more potent derivatives with a wide range of pharmacological activities. We have used benzimidazole nucleus in designing different classes of benzimidazole derivatives as drug leads with the aim of exploring their biological activities with regards to structure activity relationships (SAR) and if possible, deciphering their mode of action.

2.1 Benzimidazole derivatives as potential anti-cancer agents.

In our effort to address the challenges related to anti-cancer drug development, 2-substituted and bis-benzimidazole derivatives have been reported as remarkable cytotoxicity against various cancer cell lines.[12,16] With this understanding, we have designed two classes of benzimidazole derivatives as potential anti-cancer leads.

2.1.1 2-substituted benzimidazole derivatives as potential anti-cancer agents

Indole-based benzimidazoles have attracted the attention of medicinal chemists,[185,186] and our focus was to design this type of molecules as potential drug leads (**Figure 2.1**).

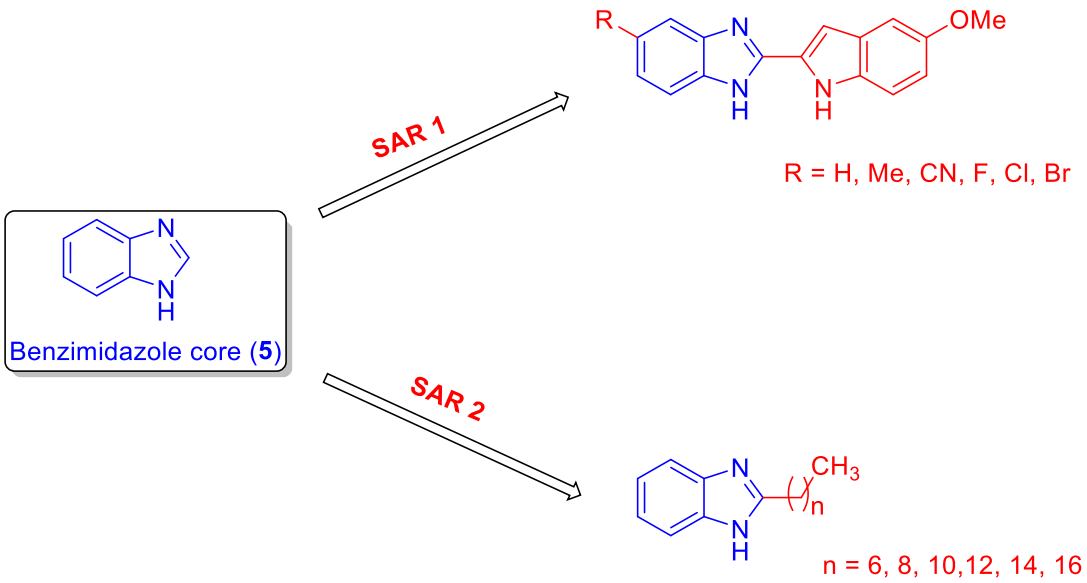

Figure 2.1. 2-aryl and alkyl substituted benzimidazoles.

In addition to indolyl-benzimidazoles derivatives, we also designed lipid-based benzimidazoles (**Figure 2.1**) with the aim of studying the effect of lipid chain on the activity of the benzimidazole scaffold. Lipid based benzimidazole derivatives is a new area of research that is yet to be explored.

2.1.2 Bis-benzimidazole derivatives as potential topoisomerase II inhibitors

Development of new anti-cancer Topo II inhibitors is necessary for improving cancer treatment.[187] Several benzimidazole derivatives are reported as novel Topo II inhibitors[188,189] and based on this information, we designed and synthesized a series of bis-benzimidazoles as potential topoisomerase II inhibitors (**Figure 2.2**).

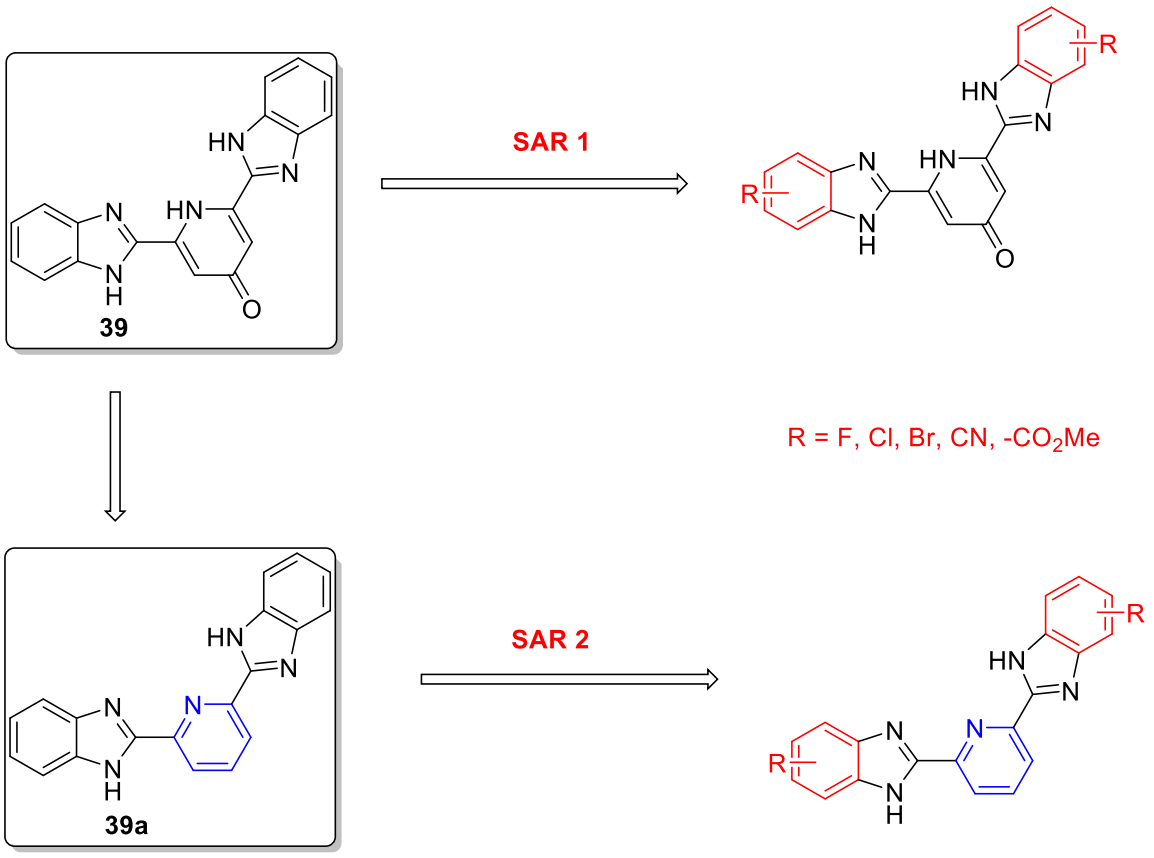

Figure 2.2. Design strategy for bis-benzimidazole derivatives as potential Topo II inhibitors.

2.2 Benzimidazole derivatives as BMPs agonists

Following a screening of a small set of aryl-benzimidazoles from an in-house library, we identified 2-substituted aryl-benzimidazoles as promising agonists of BMP signaling pathway. During the same time, benzimidazoles Sb 5 (**37**) and Sb 6 (**38**) (**Figure 2.3**) were reported as potential BMP agonists. However, these compounds are characterized by low activity and failed to induce the generation of mature osteoblasts, which limits their application to activate BMP signaling. We designed and synthesized a focused library of

2-arylbenzimidazole derivatives (**Figure 2.3**) to identify more effective agonists of BMP signaling pathway.

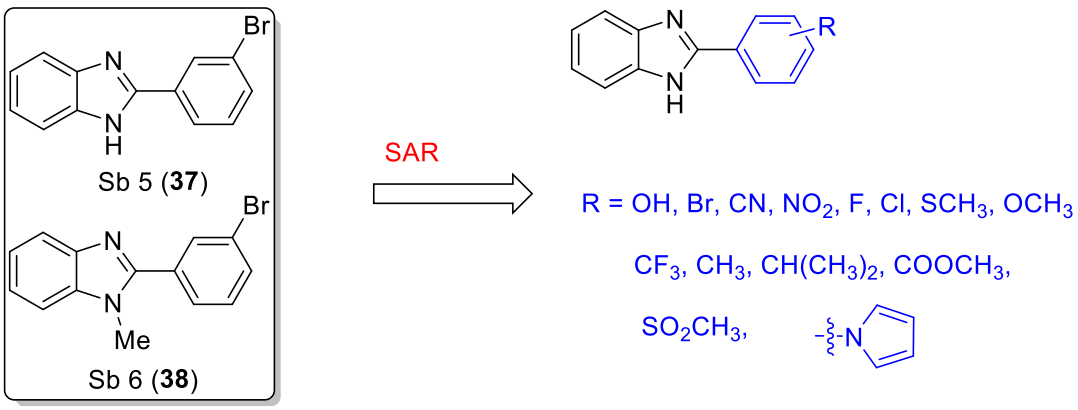

Figure 2.3. Design strategy for aryl-benzimidazole derivatives as potential BMPs agonists.

CHAPTER III. EXPERIMENTAL

3. 1 Chemical Synthesis.

3.1.1 Materials and Instrumentation.

All chemicals were procured from VWR International (Radnor, PA), Fisher Scientific (Hampton, NH), AK Scientific, Inc. (CA), Acros Organics (Geel, Belgium), Aldrich Chemical Co. (Milwaukee, WI), Alfa Aesar (Ward Hill, MA), Arkpharm, Inc. (Arlington Heights, IL), Chem-Impex Int. Inc. (Wood Dale, IL), and were used without additional purification. Qualitative analysis of reactions was performed by thin layer chromatography (TLC) with silica gel G as the adsorbent (250 microns) on aluminum backed plates (Agela Technologies) and Ultraviolet (UV) light at 254 nm or 365 nm for visualization purposes. ^{1}H NMR experiments were performed using a Bruker 400 Ultrashield™ spectrometer (at 400 MHz) equipped with a *z*-axis gradient probe. ^{1}H NMR chemical shifts were reported downfield from tetramethylsilane (TMS, an internal standard) in parts per million (δ ppm) for majority of the intermediates and all the target compounds. The ^{1}H NMR data are depicted as: chemical shift (multiplicity s (singlet), bs (broad singlet), d (doublet), t (triplet), dd (doublet of doublets), dt (doublet of triplets), tt (triplet of triplets), m (multiplet), H (number of protons) and J (coupling constant). Column chromatography purifications were performed using silica gel (40-63 μm) purchased from Silicycle Inc. (Quebec City, CANADA). LR-LC/MS analyses were performed on single quadrupole an Agilent Technologies 1260 infinity series LC. The following method was used for verifying exact masses of compounds: Column = Agilent Poroshell 120 EC-C18 2.7 μm, 4.6 x 50 mm.; temperature = 300 K; solvent acetonitrile/water 70:30 (0.1% formic acid):

flow rate 0.5 mL/min; isocratic; 3 μL injection and each single run lasted for 5 min. Accurate mass measurements/high resolution mass spectra (HRMS) were obtained from the Columbia University Chemistry Department Mass Spectrometry Facility on a Waters Xevo G2-XS QToF mass spectrometer equipped with a H-Class UPLC inlet and a LockSpray ESI source.

3.1.2 General procedure for the synthesis of 41a – 41g, 43a – 43f, 45a – 45n, 46 – 50, 79a – 79f, 80a – 80f and 84a – 84n benzimidazole analogs

To a solution of commercially available carboxylic acid substrate (1.0 equiv) in 30 mL of toluene or DMF was added *N*-Diisopropylethylamine (1.9 equiv) and the solution was stirred for 10 min at room temperature. To the stirring solution, HBTU (2 equiv) was added and the reaction mixture stirred for another 10 min. To the stirring reaction mixture, O-phenylenediamine (1.0 equiv) was added and stirred for 3-4 hours. Thereafter, the reaction was heated under reflux for 3-4 hours. The reaction was cooled to room temperature. The solvent was removed *in vacuo* in the case of toluene, but for DMF, the reaction mixture was diluted with water and products were extracted using ethyl acetate (EtOAc). The organic layer was dried over anhydrous sodium sulfate, filtered and concentrated *in vacuo*. The crude product was purified using column chromatography using hexanes/EtOAc in an increasing polarity up to 1:1 mixture. The fractions containing the desired product were concentrated and crystallized in hexanes/EtOAc (1:1) to yield the product as a white solid.

Tert-butyl (1H-benzo[d]imidazol-2-yl)methylcarbamate (41a),

White solid, 0.47 g, 91%; R_f 0.22 (9:1/CH_2Cl_2:MeOH); IR: 3343.8, 2923.9, 1939.1, 1738.9, 1683.4, 1527.6 cm^{-1}; ^1H NMR (DMSO-d_6, 400 MHz): δ = 12.21 (s, 1H, NH), 8.33

(s, 1H, NH), 7.48 (m, 2H, Ar-H), 7.14 (m, 2H, Ar-H), 4.37 (d, *J*=5.9Hz, 2H, CH_2), 1.35 (s, 9H, $C(CH_3)_3$); ^{13}C NMR (DMSO-d_6, 100 MHz) δ 156.2, 153.2, 79.7, 78.7, 28.7. LC-MS: (ESI) *m/z* calculated for $C_{13}H_{17}N_3O_2$ $[M+H]^+$ 248.14, observed 248.20.

Tert-butyl (S)-1-(methoxycarbonyl)-2-(1H-benzo[d]imidazol-2-yl)ethylcarbamate (41b),

White solid, 0.40 g, 92%; R_f 0.41 (9:1/CH_2Cl_2:MeOH); IR: 3300.1, 2979.8, 2618.5, 1888.4, 1676.4, 1650.9cm^{-1}; ^1H NMR (DMSO-d_6, 400 MHz): δ = 12.21 (s, 1H, NH), 8.33 (s, 1H, NH), 7.49 (m, 2H, Ar-H), 7.27 (d, *J*=8.3Hz, 1H, Ar-H), 7.13 (m, 2H, Ar-H), 5.20 (q, *J*=6.4Hz, 1H, CH), 3.11 (dd, *J*=6.4, 6.4Hz, 1H, CH_2), 3.06 (s, 3H, OCH_3), 2.91 (dd, *J*=6.4, 6.4Hz, 1H, CH_2), 1.39 (s, 9H, $C(CH_3)_3$); ^{13}C NMR (DMSO-d_6, 100 MHz) δ 169.8, 155.9, 155.4, 125.3, 122.1, 79.7, 78.7, 60.2, 46.7, 37.4, 37.1, 35.3, 28.7, 21.2. LC-MS: (ESI) *m/z* calculated for $C_{16}H_{22}N_3O_4$ $[M+H]^+$ 320.16, observed 320.20.

2-nonyl-1H-benzo[d]imidazole (41c),

White solid, 0.24 g, 90%; R_f 0.47 (9:1/CH_2Cl_2:MeOH); IR: 2937.4, 2894.1, 2857.2, 2562.8, 1949.0, 1926.9, 1886.9, 1739.9cm^{-1}; ^1H NMR (DMSO-d_6, 400 MHz): δ = 12.17 (s, 1H, NH), 7.45 (m, 2H, Ar-H), 7.10 (m, 2H, Ar-H), 2.79 (t, 2H, CH_2), 1.75 (t, 2H, CH_2), 1.24 (s, 12H, CH_2), 0.85 (t, 3H, CH_3); ^{13}C NMR (DMSO-d_6, 100 MHz) δ 155.6, 121.4, 31.8, 29.4, 29.2, 29.1, 29.0, 28.0, 22.6, 14.4. LC-MS: (ESI) *m/z* calculated for $C_{16}H_{25}N_2$ $[M+H]^+$ 245.20, observed 245.20.

2-undecyl-1H-benzo[d]imidazole (41d),

White solid, 0.449 g, 92%; R_f 0.24 (9:1/CH_2Cl_2:MeOH); IR: 3296.9, 2952.9, 2921.1, 2848.8, 2775.9, 1935.9, 1738.8cm^{-1}; ^1H NMR (DMSO-d_6, 400 MHz): δ = 12.18 (s, 1H, NH), 7.45 (m, 2H, Ar-H), 7.09 (m, 2H, Ar-H), 2.79 (t, 2H, CH_2), 1.75 (t, 2H, CH_2), 1.22

(s, 16H, CH_2), 0.84 (t, 3H, CH_3); ^{13}C NMR (DMSO-d_6, 100 MHz) δ 155.6, 122.1, 31.9, 29.7, 29.7, 29.7, 29.5, 29.4, 29.4, 29.4, 22.7, 14.1. **LC-MS**: (ESI) *m/z* calculated for $C_{18}H_{29}N_2$ $[M+H]^+$ 273.23, observed 273.20.

2-tridecyl-1H-benzo[d]imidazole (41e),

White solid, 0.46 g, 90%; R_f 0.26 (9:1/CH_2Cl_2:MeOH); IR: 3048.6, 2952.9, 2919.5, 2849.0, 1897.4, 1778.9cm^{-1}; ^1H NMR (DMSO-d_6, 400 MHz): δ = 12.15 (s, 1H, NH), 7.45 (m, 2H, Ar-H), 7.10 (m, 2H, Ar-H), 2.78 (t, 2H, CH_2), 1.75 (t, 2H, CH_2), 1.26 (s, 21H, CH_2), 0.85 (t, 3H, CH_3); ^{13}C NMR (DMSO-d_6, 100 MHz) δ 155.6, 122.1, 31.9, 29.7, 29.7, 29.7, 29.5, 29.4, 29.4, 29.4, 22.7, 14.1. **LC-MS**: (ESI) *m/z* calculated for $C_{20}H_{33}N_2$ $[M+H]^+$ 301.26, observed 301.30.

2-phenethyl-1H-benzo[d]imidazole (41f),

White solid, 1.1 g, %; R_f 0.24 (9:1/CH_2Cl_2:MeOH); IR: 3028.9, 2677.1, 1928.2, 1644.1, 1623.9, 1591.2cm^{-1}; ^1H NMR (DMSO-d_6, 400 MHz): δ = 12.26 (s, 1H, NH), 7.48 (m, 2H, Ar-H), 7.28 (m, 2H, Ar-H), 7.20 (m, 2H, Ar-H), 7.11 (m, 2H, Ar-H), 3.12 (s, 4H, $(-CH_2)_2$); ^{13}C NMR (DMSO-d_6, 100 MHz) δ 154.8, 141.5, 128.8, 128.8, 126.5, 33.8, 30.9. **LC-MS**: (ESI) *m/z* calculated for $C_{15}H_{15}N_2$ $[M+H]^+$ 223.12, observed 223.10.

Benzyl 1-((1H-benzo[d]imidazol-2-yl)methylcarbamoyl)-2-phenylethylcarbamate (41g),

White solid, 0.22 g, 68%; R_f 0.38 (9:1/CH_2Cl_2:MeOH); IR: 3280.7, 1691.9, 1648.3, 1539.5, 1439.8cm^{-1}; ^1H NMR (DMSO-d_6, 400 MHz): δ = 12.21 (s, 1H, NH), 8.77 (d, *J*=5.0Hz, 1H, NH), 8.33 (s, 1H, NH), 7.52 (m, *J*=8.2, 3H, Ar-H), 7.22 (m, 14H, Ar-H), 4.93 (m, 2H, CH_2), 4.45 (s, 2H, CH_2), 4.33 (m, 1H, CH), 3.095 (dd, *J*=3.4, 3.8Hz, 1H, CH_2), 2.84 (dd, J=3.4, 3.8 Hz, 1H, $-CH_2$); ^{13}C NMR (DMSO-d_6, 100 MHz) δ 172.3, 156.4, 152.3,

138.6, 137.5, 129.7, 128.7, 128.5, 127.9, 126.7, 122.0, 79.7, 65.7, 49.1, 37.9, 37.7. **LC-MS**: (ESI) *m/z* calculated for $C_{25}H_{25}N_4O_3$ $[M+H]^+$ 429.19, observed 429.20.

2-(5-methoxy-1H-indol-2-yl)-1H-benzo[d]imidazole (43a),

White solid, 0.46 g, 92%; R_f 0.47 (9:1/CH_2Cl_2:MeOH); IR: 2991.5, 2829.5, 1705.8, 1674.6, 1623.9, 1602.3cm^{-1}; ^{1}H NMR (DMSO-d_6, 400 MHz): δ = 12.93 (s, 1H, NH), 11.86 (s, 1H, NH), 7.67 (d, *J*=7.2Hz, 1H, Ar-H), 7.56 (d, 1H, Ar-H), 7.34 (dd, *J*=8.8, 8.8Hz, 1H, Ar-H), 7.23 (m, 2H, Ar-H), 6.83 (dd, *J*=8.8, 8.8Hz, 1H, Ar-H), 3.79 (s, 3H, OCH_3); ^{13}C NMR (DMSO-d_6, 100 MHz) δ 154.3, 146.7, 144.2, 135.2, 132.9, 129.4, 128.7, 122.9, 122.1, 118.9, 114.9, 114.1, 113.3, 113.2, 111.6, 102.2, 101.9, 55.7. **LC-MS**: (ESI) *m/z* calculated for $C_{16}H_{14}N_3O$ $[M+H]^+$ 264.11, observed 264.10.

5-fluoro-2-(5-methoxy-1H-indol-2-yl)-1H-benzo[d]imidazole (43b),

White solid, 0.19 g, 53%; R_f 0.38 (1:1/hexanes:EtOAc); IR: 3437.4, 3036.9, 1866.5, 1620.4, 1605.2, 1576.2 cm^{-1}; ^{1}H NMR (DMSO-d_6, 400 MHz): δ = 13.06 (s, 1H, NH), 11.86 (s, 1H, NH), 7.59 (s, 1H, Ar-H), 7.41 (s, 1H, Ar-H), 7.35 (d, *J*=8.8Hz, 1H, Ar-H), 7.15 (s, 1H, Ar-H), 7.06 (t, *J*=7.9Hz, 2H, Ar-H), 6.84 (dd, *J*=2.4, 2.4Hz, 1H, Ar-H), 3.78 (s, 3H, OCH_3); ^{13}C NMR (DMSO-d_6, 100 MHz) δ 154.3, 132.9, 129.1, 128.6, 114.2, 113.2, 102.2, 102.1, 55.7. **LC-MS**: (ESI) *m/z* calculated for $C_{16}H_{13}FN_3O$ $[M+H]^+$ 282.10, observed 282.10.

5-chloro-2-(5-methoxy-1H-indol-2-yl)-1H-benzo[d]imidazole (43c),

White solid, 0.21 g, 59%; R_f 0.47 (1:1/hexanes:EtOAc); IR: 3445.4, 2993.3, 2836.7, 1870.7, 1618.2, 1576.3 cm^{-1}; ^{1}H NMR (DMSO-d_6, 400 MHz): δ = 13.14 (s, 1H, NH), 11.91 (s, 1H, NH), 7.69 (s, 1H, Ar-H), 7.65 (dd, J=8.6, 8.6Hz, 1H, Ar-H), 7.55 (dd, *J*=8.6, 8.6Hz,

1H, Ar-H), 7.34 (d, *J*=8.8Hz, 1H, Ar-H), 7.23 (m, 2H, Ar-H), 6.84 (dd, *J*=2.4, 2.4Hz, 1H, Ar-H), 3.78 (s, 3H, OCH_3); ^{13}C NMR (DMSO-d_6, 100 MHz) δ 154.3, 133.0, 128.8, 128.6, 114.4, 113.2, 102.4, 102.2, 79.7, 55.7. **LC-MS**: (ESI) *m/z* calculated for $C_{16}H_{13}ClN_3O$ $[M+H]^+$ 298.07, observed 298.10.

5-bromo-2-(5-methoxy-1H-indol-2-yl)-1H-benzo[d]imidazole (43d),

White solid, 0.25 g, 70%; R_f 0.42 (1:1/hexanes:EtOAc); IR: 3315.3, 2938.2, 2832.4, 1738.1, 1628.0, 1569.4 cm^{-1}; ^1H NMR (DMSO-d_6, 400 MHz): δ = 13.14 (s, 1H, NH), 11.90 (s, 1H, NH), 7.8 (s, 1H, Ar-H), 7.71 (s, 1H, Ar-H), 7.60 (dd, J=8.6, 8.4Hz, 1H, Ar-H), 7.50 (dd, *J*=8.6, 8.4 Hz, 1H, Ar-H), 7.35 (m, 2H, Ar-H), 7.15 (dd, *J*=2.4, 1.7Hz, 2H, Ar-H), 6.83 (dd, *J*=2.4, 2.4Hz, 1H, Ar-H), 3.79 (s, 3H, OCH_3); ^{13}C NMR (DMSO-d_6, 100 MHz) δ 154.3, 148.0, 147.7, 145.7, 143.3, 136.5, 134,4, 133.0, 128.7, 125.6, 125.1, 121.1, 120.4, 115.1, 114.4, 113.2, 102.4, 102.2, 55.7. **LC-MS**: (ESI) *m/z* calculated for $C_{16}H_{13}BrN_3O$ $[M+H]^+$ 342.02, observed 342.10.

2-(5-methoxy-1H-indol-2-yl)-1H-benzo[d]imidazole-5-carbonitrile (43e),

White solid, 0.25 g, 70%; R_f 0.40 (1:1/hexanes:EtOAc); IR: 3453.1, 3387.2, 3240.1, 2970.2, 2218.1, 1738.0, 1623.1, 1595.9 cm^{-1}; ^1H NMR (DMSO-d_6, 400 MHz): δ = 13.49 (s, 1H, NH), 11.97 (s, 1H, NH), 8.13 (s, 1H, Ar-H), 7.73 (d, *J*=7.1 Hz, 1H, Ar-H), 7.61 (d, *J*=8.2 Hz, 1H, Ar-H), 7.34 (d, *J*=8.8 Hz, 1H, Ar-H), 7.23 (s, 1H, Ar-H), 7.15 (s, 1H, Ar-H), 6.85 (dd, *J*=2.4, 2.4Hz, 1H, Ar-H), 3.79 (s, 3H, OCH_3); ^{13}C NMR (DMSO-d_6, 100 MHz) δ 154.3, 133.3, 128.6, 128.2, 120.5, 114.9, 113.4, 104.3, 103.4, 102.3, 55.7. **LC-MS**: (ESI) *m/z* calculated for $C_{17}H_{13}N_4O$ $[M+H]^+$ 289.11, observed 289.10.

2-(5-methoxy-1H-indol-2-yl)-5-methyl-1H-benzo[d]imidazole (43f),

White solid, 0.32 g, 89%; R_f 0.42 (9:1/CH_2Cl_2:MeOH); IR: 3461.6, 3009.7, 2970.5, 1738.0, 1626.7, 1572.2 cm^{-1}; ^1H NMR (DMSO-d_6, 400 MHz): δ = 12.75 (s, 1H, NH), 11.79 (s, 1H, NH), 7.52 (dd, *J*=8.2, 8.2Hz, 1H, Ar-H), 7.45 (s, 1H, Ar-H), 7.41 (dd, *J*=8.2, 8.2Hz, 1H, Ar-H), 7.33 (s, 1H, Ar-H), 7.13 (d, *J*=2.2Hz, 1H, Ar-H), 7.07 (s, 1H, Ar-H), 7.02 (m, 1H, Ar-H), 6.81 (dd, *J*=2.4, 2.4Hz, 1H, Ar-H), 3.78 (s, 3H, OCH_3), 2.45 (s, 3H, -CH_3); ^{13}C NMR (DMSO-d_6, 100 MHz) δ 154.3, 146.6, 144.5, 133.2, 132.8, 131.0, 129.6, 124.4, 123.6, 118.6, 113.9, 111.3, 102.2, 101.6, 79.7, 55.7. **LC-MS**: (ESI) *m/z* calculated for $C_{17}H_{16}N_3O$ $[M+H]^+$ 278.13, observed 278.10.

Tert-butyl 1-(1H-benzo[d]imidazol-2-yl)-3-methylbutylcarbamate (45a)**,** White solid, 0.48 g, 96%; R_f 0.40 (1:1/hexanes:EtOAc); IR: 3345.2, 2958.5, 1680.1, 1524.6, 1443.6, 1365.3, 1316.2 cm^{-1}; ^1H NMR (DMSO-d_6, 400 MHz): δ = 12.16 (s, 1H, NH), 7.50 (m, 2H, Ar-H), 7.30 (d, 1H, *J*=8.1Hz, Ar-H), 7.14 (m, 2H, Ar-H), 4.84 (m, 1H, CH), 3.37 (s, 1H, NH), 1.74 (m, 2H, CH_2), 1.60 (m, 1H, CH), 1.34 (s, 9H, $C(CH_3)_3$), 0.92 (s, 6H, $C(CH_3)_2$); ^{13}C NMR (DMSO-d_6, 100 MHz) δ 156.6, 155.8, 143.5, 134.5, 122.1, 121.4, 118.9, 111.7, 78.5, 48.1, 43.5, 28.7, 24.8, 23.2, 22.3. **LC-MS**: (ESI) *m/z* calculated for $C_{17}H_{26}N_3O_2$ $[M+H]^+$ 304.20, observed 304.20.

Tert-butyl 1-(1H-benzo[d]imidazol-2-yl)-2-methylbutylcarbamate (45b), White solid, 0.48 g, 96%; R_f 0.56 (1:1/hexanes:EtOAc); IR: 3323.4, 2965.7, 1681.3, 1526.9, 1443.3, 1364.9, 1331.9cm^{-1}; ^1H NMR (DMSO-d_6, 400 MHz): δ = 12.17 (s, 1H, NH), 7.51 (m, 2H, Ar-H), 7.21 (d, 1H, *J*=8.8Hz, Ar-H), 7.15 (m, 2H, Ar-H), 4.64 (t, 1H, *J*=8.2Hz, CH), 3.39 (s, 1H, NH), 1.74 (m, 2H, CH_2), 1.60 (m, 1H, CH), 1.34 (s, 9H, $C(CH_3)_3$), 0.86 (d, 3H,

J=2.2Hz, C(CH_3)), 0.74 (d, 3H, *J*=6.7Hz, C(CH_3)); ^{13}C NMR (DMSO-d_6, 100 MHz) δ 156.0, 155.8, 155.5, 121.9, 118.9,111.8, 78.5, 54.4, 53.8, 38.8, 28.6, 26.2, 25.3, 16.0, 15.4, 11.8, 11.5. **LC-MS**: (ESI) *m/z* calculated for $C_{17}H_{26}N_3O_2$ $[M+H]^+$ 304.20, observed 304.20.

Tert-butyl 1-(1H-benzo[d]imidazol-2-yl)-2-methylpropylcarbamate (45c), White solid, 0.48 g, 94%; R_f 0.56 (1:1/hexanes:EtOAc); IR: 3325.7, 2964.0, 1681.4, 1529.7, 1443.3, 1365.3, 1302.5cm^{-1}; ^{1}H NMR (DMSO-d_6, 400 MHz): δ = 12.16 (s, 1H, NH), 7.51 (m, 2H, Ar-H), 7.19 (d, 1H, *J*=8.8Hz, Ar-H), 7.14 (m, 2H, Ar-H), 4.57 (t, 1H, *J*=7.8Hz, CH), 3.37 (s, 1H, NH), 2.21 (m, 1H, C(CH)), 1.38 (s, 9H, C(CH_3)$_3$), 0.92 (d, 3H, *J*=5.4Hz, C(CH_3)), 0.79 (d, 3H, *J*=5.2Hz, C(CH_3); ^{13}C NMR (DMSO-d_6, 100 MHz) δ 155.9, 155.5, 121.6, 118.9, 111.7, 78.5, 55.7, 32.6, 28.6, 19.7, 19.1. **LC-MS**: (ESI) *m/z* calculated for $C_{16}H_{24}N_3O_2$ $[M+H]^+$ 290.19, observed 290.20.

Tert-butyl 2-(1H-benzo[d]imidazol-2-yl)pyrrolidine-1-carboxylate (45d), White solid, 1.0 g, 98%; R_f 0.38 (1:1/hexanes:EtOAc); IR: 2976.3, 1696.1, 1660.9, 1428.3, 1383.9, 1360.1, 1322.9, 1307.7cm^{-1}; ^{1}H NMR (DMSO-d_6, 400 MHz): δ = 8.34 (s, 1H, NH), 7.49 (m, 2H, Ar-H), 7.13 (m, 2H, Ar-H), 4.95 (dd, 1H, *J*=6.7, 3.6Hz, CH), 3.61 (m, 1H, CH_2), 3.41 (m, 1H, CH_2), 2.29 (m, 2H, CH_2), 1.94 (m, 2H, CH_2), 1.39 (s, 9H, C(CH_3)$_3$); ^{13}C NMR (DMSO-d_6, 100 MHz) δ 157.5, 156.9, 154.3, 153.8, 121.7, 115.2, 79.7, 79.2, 78.8, 56.2, 55.7, 47.2, 46.9, 38.7, 33.7, 32.4, 28.6, 28.2, 24.3, 23.6. **LC-MS**: (ESI) *m/z* calculated for $C_{16}H_{22}N_3O_2$ $[M+H]^+$ 288.17, observed 288.20.

Tert-butyl 1-(1H-benzo[d]imidazol-2-yl)-2-(4-(benzyloxy)phenyl)ethylcarbamate (45e), White solid, 0.42 g, 84%; R_f 0.40 (1:1/hexanes:EtOAc); IR: 3325.7, 2982.9, 1676.9,

1511.5, 1447.4, 1367.3, 1309.9, 1277.7, 1240.9, 1170.7, 1071.1, 1017.7, 962.1, 863.3, 813.8, 738.6cm^{-1}; ^{1}H NMR (DMSO-d$_6$, 400 MHz): δ = 12.22 (s, 1H, NH), 7.41 (m, 8H, Ar-H), 7.16 (m, 4H, Ar-H), 6.90 (d, 2H, *J*=7.7Hz, Ar-H), 5.04 (s, 2H, CH_2), 4.95 (q, 1H, *J*=6.4Hz, CH_2), 3.40 (s, 1H, NH), 3.29 (m, 1H, CH_2), 3.02 (t, 1H, *J*=12.9Hz, CH), 1.32 (s, 9H, $C(CH_3)_3$); ^{13}C NMR (DMSO-d$_6$, 100 MHz) δ 157.4, 155.8, 155.6, 137.7, 130.7, 128.9, 128.2, 128.1, 114.9, 78.5, 69.6, 51.5, 28.6. **LC-MS**: (ESI) *m/z* calculated for $C_{27}H_{30}N_3O_3$ $[M+H]^+$ 444.23, observed 444.20.

Tert-butyl 1-(1H-benzo[d]imidazol-2-yl)-2-(benzyloxy)ethylcarbamate (45f), White solid, 0.42 g, 84%; R_f 0.34 (1:1/hexanes:EtOAc); IR: 3295.8, 2869.7, 1687.7, 1532.4, 1454.2, 1366.6, 1309.5cm^{-1}; ^{1}H NMR (DMSO-d$_6$, 400 MHz): δ = 12.29 (s, 1H, NH), 7.52 (m, 2H, Ar-H), 7.37 (d, 2H, *J*=8.2Hz, Ar-H), 7.29 (m, 4H, 7.4Hz, Ar-H), 7.16 (m, 2H, Ar-H), 5.08 (m, 1H, CH), 4.53 (s, 1H, NH), 3.86 (m, 2H, CH_2), 3.38 (s, 2H, CH_2), 1.41 (s, 9H, $C(CH_3)_3$); ^{13}C NMR (DMSO-d$_6$, 100 MHz) δ 155.8, 153.8, 138.7, 128.6, 127.9, 78.8, 72.4, 71.4, 49.7, 28.7. **LC-MS**: (ESI) *m/z* calculated for $C_{21}H_{26}N_3O_3$ $[M+H]^+$ 368.20, observed 368.20.

Tert-butyl 1-(1H-benzo[d]imidazol-2-yl)-2-(benzylthio)ethylcarbamate (45g), White solid, 1.0 g, 98 %; R_f 0.45 (1:1/hexanes:EtOAc); IR: 3316.1, 2980.9, 1672.6, 1515.4, 1441.1cm^{-1}; ^{1}H NMR (DMSO-d$_6$, 400 MHz): δ = 12.32 (s, 1H, NH), 7.58 (d, 1H, *J*=7.4Hz, Ar-H), 7.48 (m, 2H, Ar-H), 7.44 (m, 4H, Ar-H), 7.22 (m, 1H, Ar-H), 7.18 (m, 2H, Ar-H), 5.01 (q, 1H, *J*=6.6Hz, CH), 3.75 (s, 2H, CH_2), 3.11 (dd, 1H, *J*=6.2, 6.1Hz, CH_2), 2.85 (dd, 1H, J=8.3, 8.3Hz, CH_2), 1.43 (s, 9H, $C(CH_3)_3$); ^{13}C NMR (DMSO-d$_6$, 100 MHz) δ 155.8, 154.7, 143.4, 138.8, 134.6,129.4, 128.8, 127.3, 122.5, 121.7, 119.1, 111.9, 78.9, 49.4, 35.7,

35.4, 28.7. **LC-MS**: (ESI) *m/z* calculated for $C_{21}H_{26}N_3O_2S$ $[M+H]^+$ 384.17, observed 384.20.

Tert-butyl 1-(1H-benzo[d]imidazol-2-yl)-3-(benzyloxy)butylcarbamate (45h)**,** White solid, 0.47 g, 94%; R_f 0.40 (1:1/hexanes:EtOAc); IR: 3324.3, 2977.1, 1678.7, 1528.7cm^{-1}; ^{1}H NMR (DMSO-d_6, 400 MHz): δ = 12.25 (s, 1H, NH), 7.49 (m, 2H, Ar-H), 7.30 (d, 1H, *J*=9.4Hz, Ar-H), 7.18 (m, 6H, Ar-H), 7.03 (d, 1H, *J*=8.9Hz, Ar-H), 5.02 (m, 1H, CH), 4.94 (m, 1H, CH), 4.47 (m, 2H, CH_2), 4.01 (m, 1H, NH), 3.37 (m, 2H, CH_2), 1.34 (s, 9H, $C(CH_3)_3$), 1.13 (d, 3H, *J*=5.6Hz, CH_3); ^{13}C NMR (DMSO-d_6, 100 MHz) δ 155.9, 154.1, 139.1, 138.9, 128.5, 127.9, 127.8, 127.7, 79.6, 78.9, 76.5, 76.4, 70.7, 70.5, 53.4, 28.6, 17.0, 16.6. **LC-MS**: (ESI) *m/z* calculated for $C_{22}H_{28}N_3O_3$ $[M+H]^+$ 382.21, observed 382.20.

Compound (45i), White solid, 1.00 g, 96%; R_f 0.29 (1:1/hexanes:EtOAc); IR: 3317.9, 1693.9, 1677.2, 1530.9, 1439.8, 1393.0, 1364.3cm^{-1}; ^{1}H NMR (DMSO-d_6, 400 MHz): δ = 12.15 (s, 1H, NH), 7.50 (m, 2H, Ar-H), 7.28 (d, 1H, *J*=7.3Hz, Ar-H), 7.14 (m, 2H, Ar-H), 6.79 (s, 1H, NH), 4.73 (m, 1H, CH), 3.37 (s, 1H, NH), 2.90 (m, 2H, CH_2), 1.84, (m, 2H, CH_2), 1.38 (s, 9H, $C(CH_3)_3$); ^{13}C NMR (DMSO-d_6, 100 MHz) δ 156.3, 156.0, 155.8, 121.8, 78.6, 77.8, 49.9, 34.1, 29.6, 28.7, 28.7, 23.3. **LC-MS**: (ESI) *m/z* calculated for $C_{22}H_{35}N_4O_4$ $[M+H]^+$ 419.27, observed 419.30.

Tert-butyl 2-(phenoxycarbonyl)-1-(1H-benzo[d]imidazol-2-yl)ethylcarbamate (45j), White solid, 0.45 g, 90%; R_f 0.46 (1:1/hexanes:EtOAc); IR: 3320.1, 2980.3, 1737.4, 1679.4, 1524.8, 1440.8, 1391.5, 1367.3, 1337.2cm^{-1}; ^{1}H NMR (DMSO-d_6, 400 MHz): δ = 12.30 (s, 1H, NH), 7.56 (d, 1H, *J*=8.00Hz, Ar-H), 7.47 (m, 2H, Ar-H), 7.31 (m, 5H, Ar-H), 7.16 (m, 2H, Ar-H), 5.21 (q, 1H, *J*=7.4Hz, CH), 5.10 (s, 2H, CH_2), 3.40 (s, 1H, NH),

3.22 (m, 1H, CH_2), 2.95 (m, 1H, CH_2), 1.41 (s, 9H, $C(CH_3)_3$); ^{13}C NMR (DMSO-d_6, 100 MHz) δ 170.6, 155.5, 154.6, 136.6, 134.9, 128.8, 128.3, 128.1, 121.6, 119.1, 111.9, 79.7, 78.9, 65.9, 46.6, 38.6, 28.7. **LC-MS**: (ESI) *m/z* calculated for $C_{22}H_{26}N_3O_4$ $[M+H]^+$ 396.19, observed 396.20.

Tert-butyl 3-((benzyloxy)carbonyl)-1-(1H-benzo[d]imidazol-2-yl)propylcarbamate (45k), White solid, 0.40 g, 80%; R_f 0.33 (1:1/hexanes:EtOAc); IR: 3312.3, 2977.1, 1737.5, 1677.3, 1525.8, 1453.8, 1391.4, 1366.9cm^{-1}; ^1H NMR (DMSO-d_6, 400 MHz): δ = 12.22 (s, 1H, NH), 7.57 (dd, 1H, *J*=6.9, 6.9Hz, Ar-H), 7.46 (dd, 1H, *J*=6.9, 6.9Hz, Ar-H), 7.39 (m, 5H, Ar-H), 7.15 (m, 2H, Ar-H), 5.08 (s, 2H, CH_2), 4.85 (m, 1H, CH), 3.38 (s, 1H, NH), 2.49 (d, 2H, *J*=12.0Hz, CH_2), 2.29 (m, 1H, CH_2), 2.09 (m, 1H, CH_2), 1.40 (s, 9H, $C(CH_3)_3$); ^{13}C NMR (DMSO-d_6, 100 MHz) δ 172.7, 155.8, 155.5, 143.4, 136.6, 134.7, 128.9, 128.4, 128.4, 122.3, 121.5, 119.0, 111.8, 79.7, 78.7, 65.9, 49.0, 30.6, 29.3, 28.7. **LC-MS**: (ESI) *m/z* calculated for $C_{23}H_{28}N_3O_4$ $[M+H]^+$ 410.21, observed 410.20.

Tert-butyl 1-(1H-benzo[d]imidazol-2-yl)-2-carbamoylethylcarbamate (45l), White solid, 0.48 g, 96%; R_f 0.41 (1:1/hexanes:EtOAc); IR: 3296.2, 2983.9, 1728.0, 1676.4, 1526.9, 1446.2, 1394.7, 1371.1, 1303.5cm^{-1}; ^1H NMR (DMSO-d_6, 400 MHz): δ = 12.43 (s, 1H, NH), 8.32 (d, 1H, *J*=1.2Hz, NH), 7.79 (d, 1H, *J*=8.3Hz, Ar-H), 7.60 (dd, 1H, *J*=7.2, 7.4Hz, Ar-H), 7.48 (dd, 1H, *J*=7.2, 7.4Hz, Ar-H), 7.19 (t, 1H, *J*=7.6Hz, Ar-H), 5.19 (m, 1H, CH), 3.39 (s, 2H, NH_2), 3.13 (m, 1H, CH_2), 1.44 (s, 9H, $C(CH_3)_3$); ^{13}C NMR (DMSO-d_6, 100 MHz) δ 155.5, 152.9, 143.1, 134.9, 122.8, 121.8, 119.2, 118.8, 112.0, 79.6, 79.3, 46.5, 28.6, 22.5. **LC-MS**: (ESI) *m/z* calculated for $C_{15}H_{21}N_4O_3$ $[M-NH^+_4]$ 305.16, observed 287.20.

1,2,3,4-Tetrahydro-1-oxo-pyrido[1,2a]benzimidazole (45m), White solid, 0.48 g, 96%; R_f 0.53 (1:1/hexanes:EtOAc); IR: 3376.1, 2973.6, 1738.1, 1682.0, 1610.6, 1548.1, 1514.3, 1445.9, 1356.8, 1330.4, 1303.4cm^{-1}; ^{1}H NMR (DMSO-d_6, 400 MHz): δ = 8.14 (m, 1H, Ar-H), 7.71 (m, 1H, Ar-H), 7.56 (d, 1H, *J*=8.5Hz, Ar-H), 7.39 (m, 2H, Ar-H), 5.12 (m, 1H, CH), 3.04 (m, 1H, NH), 2.88 (m, 1H, CH), 2.17 (m, 2H, CH_2), 1.45 (s, 9H, $C(CH_3)_3$), 0.92 (s, 6H, $C(CH_3)_2$); ^{13}C NMR (DMSO-d_6, 100 MHz) δ 169.6, 155.6, 155.5, 142.7, 131.6, 125.4, 125.3, 119.9, 115.2, 78.9, 45.9, 31.8, 28.7, 27.6. **LC-MS**: (ESI) *m/z* calculated for $C_{16}H_{19}N_3O_3$ $[M+H]^+$ 302.15, observed 334.20.

Tert-butyl 1-(1H-benzo[d]imidazol-2-yl)-2-phenylethylcarbamate (45n), White solid, 1.0 g, 99%; R_f 0.40 (1:1/hexanes:EtOAc); IR: 3307.6, 1681.9, 1531.8, 1457.6, 1433.8, 1367.1, 1335.5, 1311.8cm^{-1}; ^{1}H NMR (DMSO-d_6, 400 MHz): δ = 12.22 (s, 1H, NH), 7.51 (m, 1H, Ar-H), 7.40 (d, 1H, *J*=8.3Hz, Ar-H), 7.20 (m, 7H, Ar-H), 4.99 (m, 1H, CH), 3.36 (s, 1H, NH), 3.07 (t, 1H, *J*=11.6Hz, CH_2), 1.21 (s, 9H, $C(CH_3)_3$); ^{13}C NMR (DMSO-d_6, 100 MHz) δ 155.8, 155.6, 138.6, 138.9, 129.7, 128.5, 126.7, 78.5, 51.3, 28.6. **LC-MS**: (ESI) *m/z* calculated for $C_{20}H_{24}N_3O_2$ $[M+H]^+$ 338.19, observed 338.20.

Tert-butyl 2-(4-(benzyloxy)phenyl)-1-(5-chloro-1H-benzo[d]imidazol-2-yl) ethylcarbamate (46), White solid, 0.45 g, 90%; R_f 0.47 (7:3/hexanes:EtOAc); IR: 3318.2, 2930.1, 1675.5, 1607.9, 1510.4, 1445.3, 1371.1cm^{-1}; ^{1}H NMR (DMSO-d_6, 400 MHz): δ = 12.41 (s, 1H, NH), 8.15 (s, 1H, Ar-H), 7.82 (m, 1H, Ar-H), 7.71 (m, 1H, Ar-H), 7.48 (m, 9H, Ar-H), 7.11 (m, 4H, Ar-H), 5.05 (m, 1H, CH), 3.37 (s, 2H, CH_2), 3.27 (m, 1H, CH_2), 3.01 (m, 1H, CH_2), 1.31 (s, 9H, $C(CH_3)_3$); ^{13}C NMR (DMSO-d_6, 100 MHz) δ 157.4, 137.7,

130.7, 128.9, 128.2, 128.1, 118.4, 114.9, 78.6, 69.6, 28.6. **LC-MS**: (ESI) *m/z* calculated for $C_{27}H_{29}ClN_3O_3$ $[M+H]^+$ 478.19, observed 478.20.

Tert-butyl 2-(4-(benzyloxy)phenyl)-1-(5-bromo-1H-benzo[d]imidazol-2-yl)ethylcarbamate (47), White solid, 0.46 g, 92%; R_f 0.47 (7:3/hexanes:EtOAc); IR: 3314.6, 2914.3, 1675.6, 1613.5, 1512.9, 1443.4, 1371.9cm^{-1}; ^1H NMR (DMSO-d_6, 400 MHz): δ = 12.44 (s, 1H, NH), 7.77 (s, 1H, Ar-H), 7.60 (d, *J*=8.3Hz, 1H, Ar-H), 7.48 (m, 7H, Ar-H), 7.15 (dd, *J*=8.1, 8.2Hz, 2H, Ar-H), 6.89 (dd, *J*=8.1, 8.2Hz, 2H, Ar-H), 5.05 (m, 1H, CH), 3.37 (s, 2H, CH_2), 3.27 (m, 1H, CH_2), 3.01 (m, 1H, CH_2), 1.31 (s, 9H, $C(CH_3)_3$); ^{13}C NMR (DMSO-d_6, 100 MHz) δ 157.4, 155.7, 144.9, 137.7, 130.7, 133.7, 129.4, 128.9, 128.2, 128.1, 124.9, 121.4, 120.7, 114.9, 114.5, 78.6, 69.6, 51.5, 38.9, 28.6. **LC-MS**: (ESI) *m/z* calculated for $C_{27}H_{29}BrN_3O_3$ $[M+H]^+$ 522.14, observed 522.10.

Benzyl 1-(1H-benzo[d]imidazol-2-yl)-2-carbamoylethylcarbamate (48), White solid, 0.41 g, 82%; R_f 0.40 (1:1/hexanes:EtOAc); IR: 3303.1, 1693.3, 1528.7, 1440.3, 1328.9cm^{-1}; ^1H NMR (DMSO-d_6, 400 MHz): δ = 12.52 (s, 1H, NH), 8.31 (d, 1H, *J*=9.2Hz, NH), 7.61 (dd, 1H, *J*=7.6, 7.6Hz, Ar-H), 7.49 (dd, 1H, *J*=7.6, 7.6Hz, Ar-H), 7.33 (m, 5H, Ar-H), 7.23 (m, 1H, Ar-H), 7.18(m, 2H, Ar-H), 5.27 (q, 1H, *J*=7.4Hz, CH), 5.13 (q, 2H, *J*=12.7Hz, CH_2), 3.38 (s, 4H, NH_2, CH_2), 3.33 (d, 1H, *J*=5.0Hz, CH), 3.18 (m, 1H); ^{13}C NMR (DMSO-d_6, 100 MHz) δ 156.3, 152.6, 143.0, 137.2, 135.0, 128.9, 128.4, 128.3, 122.9, 121.9, 119.2, 118.8, 112.0, 66.4, 47.0, 22.4. **LC-MS**: (ESI) *m/z* calculated for $C_{18}H_{19}N_4O_3$ $[M+H]^+$ 339.15, observed 321.10.

Benzyl 1-(1H-benzo[d]imidazol-2-yl)-2-phenylethylcarbamate (49), White solid, 1.0 g, 98%; R_f 0.54 (1:1/hexanes: EtOAc); IR: 3303.2, 1685.8, 1524.9, 1454.9, 1429.8, 1335.8cm^{-1}; ^{1}H NMR (DMSO-d$_6$, 400 MHz): δ = 12.33 (s, 1H, NH), 7.99 (d, 1H, *J*=8.2Hz, Ar-H), 7.53 (m, 2H, Ar-H), 7.25 (m, 13H, Ar-H), 5.00 (q, 2H, *J*=12.7Hz, CH), 3.40 (s, 4H, CH_2), 3.11 (t, 1H, *J*=12.0Hz, NH); ^{13}C NMR (DMSO-d$_6$, 100 MHz) δ 156.3, 155.5, 138.6, 137.5, 129.7, 128.8, 128.6, 128.1, 127.9, 126.8, 65.7, 51.9. **LC-MS**: (ESI) *m/z* calculated for $C_{23}H_{22}N_3O_2$ $[M+H]^+$ 372.17, observed 372.20.

Benzyl 1-(1H-benzo[d]imidazol-2-yl)-3-methylbutylcarbamate (50), White solid, 0.45 g, 90%; R_f 0.40 (1:1/hexanes: EtOAc); IR: 3255.3, 1693.1, 1530.7, 1326.9cm^{-1}; ^{1}H NMR (DMSO-d$_6$, 400 MHz): δ = 12.25 (s, 1H, NH), 7.83 (d, 1H, *J*=8.2Hz, Ar-H), 7.41 (m, 6H, Ar-H), 7.15 (m, 2H, Ar-H), 5.06 (q, 2H, *J*=12.6Hz, CH_2), 4.89 (q, 1H, *J*=7.7Hz, NH), 3.37 (s, 2H, CH_2), 1.79 (m, 1H, CH), 1.63 (m, 1H, CH), 0.92 (s, 6H, $C(CH_3)_2$); ^{13}C NMR (DMSO-d$_6$, 100 MHz) δ 156.5, 156.4, 137.5, 128.8, 128.3, 128.2, 66.0, 48.6, 43.1, 24.8, 23.2, 22.2. **LC-MS**: (ESI) *m/z* calculated for $C_{20}H_{24}N_3O_2$ $[M+H]^+$ 338.19, observed 338.20.

2,6-di(1H-benzo[d]imidazol-2-yl)pyridin-4(1H)-one (79a), a white solid, 0.16 g, 92 %; ^{1}H NMR (DMSO-d$_6$, 400MHz): δ = 8.09 (s, 1H, Ar-H), 7.88 (d, *J*=6.2 Hz, 2H, Ar-H), 7.56 (d, J=6.2 Hz, 2H, Ar-H); ^{13}C NMR (DMSO-d$_6$, 100MHz) δ = 167.4, 148.0, 134.0,126.2, 115.2, 112.7 . **HRMS** (ESI) *m/z* calculated for $C_{19}H_{14}N_5O$ $[M+H]^+$ 328.1193, observed 328.1207.

2,6-bis(5-fluoro-1H-benzo[d]imidazol-2-yl)pyridin-4(1H)-one (79b), a white solid, 0.20 g, 93 %; ^{1}H NMR (DMSO-d$_6$, 400MHz): δ = 7.91 (s, 1H, Ar-H), 7.82 (s, 1H, Ar-H), 7.65 (d, J=8.6 Hz, 1H, Ar-H), 7.52 (d, *J*=8.6 Hz, 1H, Ar-H); ^{13}C NMR (DMSO-d$_6$, 100MHz) δ

= 167.2, 149.2, 145.6, 136.1, 133.9, 128.5, 117.7, 116.9, 112.3. **HRMS** (ESI) *m/z* calculated for $C_{19}H_{12}F_2N_5O$ $[M+H]^+$ 364.1004, observed 364.1012.

2,6-bis(5-chloro-1H-benzo[d]imidazol-2-yl)pyridin-4(1H)-one (79c), a white solid, 0.15 g, 89 %; ^{1}H NMR (DMSO-d_6, 400MHz): δ = 8.24 (s, 1H, Ar-H), 7.88 (d, *J*=8.2 Hz, 1H, Ar-H), 7.80 (s, 1H, Ar-H), 7.69 (d, *J*=8.2 Hz, 1H, Ar-H); ^{13}C NMR (DMSO-d_6, 100MHz) δ = 162.4, 150.2, 150.0, 149.4, 144.7, 140.6, 136.2, 134.1, 129.7, 129.6, 125.8, 124.6, 116.8, 114.9. **HRMS** (ESI) *m/z* calculated for $C_{19}H_{12}Cl_2N_5O$ $[M+H]^+$ 396.0413, observed 396.0420.

2,6-bis(5-bromo-1H-benzo[d]imidazol-2-yl)pyridin-4(1H)-one (79d), a white solid, 0.10 g, 90 %; ^{1}H NMR (DMSO-d_6, 400MHz): δ = 7.91 (s, 1H, Ar-H), 7.82 (s, 1H, Ar-H), 7.65 (d, J=8.6 Hz, 1H, Ar-H), 7.52 (d, *J*=8.6 Hz, 1H, Ar-H); ^{13}C NMR (DMSO-d_6, 100MHz) δ = 167.2, 149.2, 145.6, 136.1, 133.9, 128.5, 117.7, 116.9, 112.3. **HRMS** (ESI) *m/z* calculated for $C_{19}H_{12}Br_2N_5O$ $[M+H]^+$ 483.9403, observed 483.9420, 487.9384.

Compound (79e), a white solid, 0.13 g, 85 %; ^{1}H NMR (DMSO-d_6, 400MHz): δ = 8.24 (s, 1H, Ar-H), 7.88 (d, *J*=8.2 Hz, 1H, Ar-H), 7.80 (s, 1H, Ar-H), 7.69 (d, *J*=8.2 Hz, 1H, Ar-H); ^{13}C NMR (DMSO-d_6, 100MHz) δ = 166.8, 153.2, 148.2, 127.1, 120.1, 110.9, 105.5. **HRMS** (ESI) *m/z* calculated for $C_{21}H_{12}N_7O$ $[M+H]^+$ 378.1098, observed 378.1096.

Compound (79f), a white solid, 0.2 g, 90 %; ^{1}H NMR (DMSO-d_6, 400MHz): δ = 8.24 (s, 1H, Ar-H), 7.88 (d, *J*=8.2 Hz, 1H, Ar-H), 7.80 (s, 1H, Ar-H), 7.69 (d, *J*=8.2 Hz, 1H, Ar-H), 3.87 (s, 3H, OCH_3); ^{13}C NMR (DMSO-d_6, 100MHz) δ = 167.2, 166.1, 150.4, 150.0,

145.6, 127.9, 126.4, 126.1, 125.8, 116.8, 115.2, 112.5, 112.4, 52.7, 52.7. **HRMS** (ESI) *m/z* calculated for $C_{23}H_{18}N_5O_5$ $[M+H]^+$ 444.1302, observed 444.1312.

2-(6-(1H-benzo[d]imidazol-2-yl)pyridin-2-yl)-1H-benzo[d]imidazole (80a), a white solid, 0.2 g, 95 %; ^{1}H NMR (DMSO-d_6, 400MHz): δ = 8.77 (d, *J*=7.8, Hz, 1H, Ar-H), 8.38 (t, *J*=7.8, 7.8 Hz, 1H, Ar-H), 7.85 (m, 2H, Ar-H), 7.56 (m, 2H, Ar-H); ^{13}C NMR (DMSO-d_6, 100MHz) δ = 165.3, 148.8, 147.4, 143.2, 140.6, 133.3, 127.5, 126.8, 126.6, 125.5, 115.2. **HRMS** (ESI) *m/z* calculated for $C_{19}H_{14}N_5$ $[M+H]^+$ 312.1244, observed 312.1257.

5-fluoro-2-(6-(5-fluoro-1H-benzo[d]imidazol-2-yl)pyridin-2-yl)-1H-benzo[d]imidazole (80b), a white solid, 0.18 g, 84 %; ^{1}H NMR (DMSO-d_6, 400MHz): δ = 8.54 (d, *J*=7.9 Hz, 1H, Ar-H), 8.35 (t, *J*=7.8, 8.0 Hz, 1H, Ar-H), 7.81 (dd, *J*=2.3, 4.6 Hz, 1H, Ar-H), 7.56 (d, *J*=8.7 Hz, 1H, Ar-H), 7.34 (t, *J*=9.4, 9.2 Hz, 1H, Ar-H); ^{13}C NMR (DMSO-d_6, 100MHz) δ = 161.5,159.1, 149.7, 145.0, 140.6, 124.2, 116.8, 114.2, 113.9, 101.6, 101.4. **HRMS** (ESI) *m/z* calculated for $C_{19}H_{12}F_2N_5$ $[M+H]^+$ 348.1055, observed 348.1056.

5-chloro-2-(6-(5-chloro-1H-benzo[d]imidazol-2-yl)pyridin-2-yl)-1H-benzo[d]imidazole (80c), a white solid, 0.17 g, 89 %; ^{1}H NMR (DMSO-d_6, 400MHz): δ = 11.00 (s, 1H, NH), 8.54 (d, *J*=7.9 Hz, 1H, Ar-H), 8.35 (t, *J*=7.8, 8.0 Hz, 1H, Ar-H), 7.81 (dd, *J*=2.3, 4.6 Hz, 1H, Ar-H), 7.56 (d, *J*=8.7 Hz, 1H, Ar-H), 7.34 (t, *J*=9.4, 9.2 Hz, 1H, Ar-H); ^{13}C NMR (DMSO-d_6, 100MHz) δ = 161.5,159.1, 149.7, 145.0, 140.6, 124.2, 116.8, 114.2, 113.9, 101.6, 101.4. **HRMS** (ESI) *m/z* calculated for $C_{19}H_{12}Cl_2N_5$ $[M+H]^+$ 380.0464, observed 380.0464.

5-bromo-2-(6-(5-bromo-1H-benzo[d]imidazol-2-yl)pyridin-2-yl)-1H-benzo[d]imidazole (80d), a white solid, 0.18 g, 88 %; ^{1}H NMR (DMSO-d_6, 400MHz): δ = 8.54 (d, *J*=7.9 Hz,

1H, Ar-H), 8.35 (t, *J*=7.8, 8.0 Hz, 1H, Ar-H), 7.81 (dd, *J*=2.3, 4.6 Hz, 1H, Ar-H), 7.56 (d, *J*=8.7 Hz, 1H, Ar-H), 7.34 (t, *J*=9.4, 9.2 Hz, 1H, Ar-H); ^{13}C NMR (DMSO-d_6, 100MHz) δ = 161.5,159.1, 149.7, 145.0, 140.6, 124.2, 116.8, 114.2, 113.9, 101.6, 101.4. **HRMS** (ESI) *m/z* calculated for $C_{19}H_{12}Br_2N_5$ $[M+H]^+$ 467.9454, observed 467.9480, 471.9442.

Compound (80e), a white solid, 0.14 g, 88 %; ^{1}H NMR (DMSO-d_6, 400MHz): δ = 8.54 (d, *J*=7.9 Hz, 1H, Ar-H), 8.35 (t, *J*=7.8, 8.0 Hz, 1H, Ar-H), 7.81 (dd, *J*=2.3, 4.6 Hz, 1H, Ar-H), 7.56 (d, *J*=8.7 Hz, 1H, Ar-H), 7.34 (t, *J*=9.4, 9.2 Hz, 1H, Ar-H); ^{13}C NMR (DMSO-d_6, 100MHz) δ = 161.5,159.1, 149.7, 145.0, 140.6, 124.2, 116.8, 114.2, 113.9, 101.6, 101.4. **HRMS** (ESI) *m/z* calculated for $C_{21}H_{12}N_7$ $[M+H]^+$ 362.1149, observed 362.1150.

Compound (80f), a white solid, 0.12 g, 91 %; ^{1}H NMR (DMSO-d_6, 400MHz): δ = 8.77 (d, *J*=7.8, Hz, 1H, Ar-H), 8.38 (t, *J*=7.8, 7.8 Hz, 1H, Ar-H), 7.85 (m, 2H, Ar-H), 7.56 (m, 2H, Ar-H), 3.92 (s, 3H, OCH_3); ^{13}C NMR (DMSO-d_6, 100MHz) δ = 168.1, 167.1, 152.9, 147.8, 147.7, 1140.0, 125.9, 122.9, 122.9, 52.0. **HRMS** (ESI) *m/z* calculated for $C_{23}H_{18}N_5O_4$ $[M+H]^+$ 428.1353, observed 428.1363.

3-(1H-benzo[d]imidazol-2-yl)phenol (84a), White solid, 0.85 g, 92%; R_f 0.40 (1:1/Hexanes: EtOAc); ^{1}H NMR (DMSO-d_6, 400MHz): δ = 12.85 (s, 1H, NH), 9.78 (s, 1H, OH), 7.61 (m, 4H, Ar-H), 7.33 (m, 3H, Ar-H), 6.9 (d, *J*=7.3 Hz, 1H, Ar-H); ^{13}C NMR (DMSO-d_6, 100MHz) δ 158.2, 151.8, 131.9, 130.5, 117.7, 117.4, 113.8. **HRMS**: (ESI) *m/z* calculated for $C_{13}H_{11}N_2O$ $[M+H]^+$ 211.0866, observed 211.0867.

2-(3-bromophenyl)-1H-benzo[d]imidazole (84b), White solid, 1.2 g, 95%; R_f 0.61 (7:3/Hexanes: EtOAc); ^{1}H NMR (DMSO-d_6, 400MHz): δ = 13.06 (s, 1H, NH), 8.39 (s, 1H, Ar-H), 8.20 (d, *J*=7.8 Hz, 1H, Ar-H), 7.55 (m, 4H, Ar-H), 7.23 (m, 2H, Ar-H); ^{13}C NMR

(DMSO-d_6, 100MHz) δ 150.1, 132.9, 132.9, 131.7, 129.4, 125.8, 122.7. **HRMS**: (ESI) *m/z* calculated for $C_{13}H_{11}BrN_2$ $[M+H]^+$ 273.0022, observed 273.0033, 275.0015.

3-(1H-benzo[d]imidazol-2-yl)benzonitrile (84c), White solid, 2.1 g, 96%; R_f 0.49 (7:3/Hexanes: EtOAc); ^{1}H NMR (DMSO-d_6, 400MHz): δ = 13.15 (s, 1H, NH), 8.56 (s, 1H, Ar-H), 8.50 (d, *J*=7.8 Hz, 1H, Ar-H), 7.96 (d, *J*=7.6 Hz, 1H, Ar-H), 7.70 (m, 3H, Ar-H), 7.25 (m, 2H, Ar-H); ^{13}C NMR (DMSO-d_6, 100MHz) δ 149.7, 133.5, 131.8, 131.4, 130.8, 130.2, 118.9, 112.6. **HRMS**: (ESI) *m/z* calculated for $C_{14}H_{10}N_3$ $[M+H]^+$ 220.0869, observed 220.0874.

2-m-tolyl-1H-benzo[d]imidazole (84d), White solid, 0.8 g, 89%; R_f 0.51 (7:3/Hexanes: EtOAc); ^{1}H NMR (DMSO-d_6, 400MHz): δ = 12.91 (s, 1H, NH), 8.05 (s, 1H, Ar-H), 8.00 (d, *J*=7.8 Hz, 1H, Ar-H), 7.55 (m, 3H, Ar-H), 7.30 (d, *J*=7.5 Hz, 1H, Ar-H), 7.20 (m, 2H, Ar-H), 2.42 (s, 3H, CH_3); ^{13}C NMR (DMSO-d_6, 100MHz) δ 151.8, 138.6, 130.9, 130.6, 129.3, 127.5, 124.1, 21.5. **HRMS**: (ESI) *m/z* calculated for $C_{14}H_{13}N_2$ $[M+H]^+$ 209.1073, observed 209.1084.

2-(3-nitrophenyl)-1H-benzo[d]imidazole (84e), White solid, 2.1 g, 82%; R_f 0.34 (7:3/Hexanes: EtOAc); ^{1}H NMR (DMSO-d_6, 400MHz): δ = 13.33 (s, 1H, NH), 9.02 (s, 1H, Ar-H), 8.60 (d, *J*=7.8 Hz, 1H, Ar-H), 8.30 (d, *J*=8.1 Hz, 1H, Ar-H), 7.85 (m, 4H, Ar-H), 7.25 (m, 2H, Ar-H); ^{13}C NMR (DMSO-d_6, 100MHz) δ 149.5, 148.8, 132.9, 132.2, 131.1, 124.7, 121.3. **HRMS**: (ESI) *m/z* calculated for $C_{13}H_{10}N_3O_2$ $[M+H]^+$ 240.0768, observed 240.0768.

2-(3-fluorophenyl)-1H-benzo[d]imidazole (84f), White solid, 0.21 g, 78%; R_f 0.45 (7:3/Hexanes: EtOAc); ^{1}H NMR (DMSO-d_6, 400MHz): δ = 13.05 (s, 1H, NH), 8.03 (d, *J*=7.9 Hz, 1H, Ar-H), 7.96 (m, 1H, Ar-H), 7.60 (m, 3H, Ar-H), 7.35 (m, 1H, Ar-H), 7.23 (m, 2H, Ar-H); ^{13}C NMR (DMSO-d_6, 100MHz) δ 150.4, 150.4, 133.0, 132.9, 131.7, 131.7, 123.0, 122.9. **HRMS**: (ESI) *m/z* calculated for $C_{13}H_{10}FN_2$ $[M+H]^+$ 213.0823, observed 213.0824.

2-(3-chlorophenyl)-1H-benzo[d]imidazole (84g), White solid, 0.21 g, 78%; R_f 0.45 (7:3/Hexanes: EtOAc); ^{1}H NMR (DMSO-d_6, 400MHz): δ = 13.06 (s, 1H, NH), 8.24 (s, 1H, Ar-H), 8.15 (d, *J*=7.2 Hz, 1H, Ar-H), 7.60 (m, 4H, Ar-H), 7.23 (m, 2H, Ar-H); ^{13}C NMR (DMSO-d_6, 100MHz) δ 150.2, 134.2, 132.7, 131.4, 130.0, 126.5, 125.5, 122.9. **HRMS**: (ESI) *m/z* calculated for $C_{13}H_{10}ClN_2$ $[M+H]^+$ 229.0527, observed 229.0535.

2-(3-(methylthio)phenyl)-1H-benzo[d]imidazole (84h), White solid, 0.32 g, 85%; R_f 0.47 (7:3/Hexanes: EtOAc); ^{1}H NMR (DMSO-d_6, 400MHz): δ = 12.98 (s, 1H, NH), 8.07 (s, 1H, Ar-H), 7.96 (d, *J*=7.8 Hz, 1H, Ar-H), 7.50 (m, 3H, Ar-H), 7.37 (d, *J* =7.8 Hz, 1H, Ar-H), 7.21 (m, 2H, Ar-H); ^{13}C NMR (DMSO-d_6, 100MHz) δ 151.2, 139.7, 131.3, 129.9, 127.5, 123.5, 123.4, 15.1. **HRMS**: (ESI) *m/z* calculated for $C_{14}H_{13}N_2S$ $[M+H]^+$ 241.0794, observed 241.0786.

2-(3-methoxyphenyl)-1H-benzo[d]imidazole (84i), White solid, 0.22 g, 94%; R_f 0.53 (7:3/Hexanes: EtOAc); ^{1}H NMR (DMSO-d_6, 400MHz): δ = 12.92 (s, 1H, NH), 7.79 (s, 1H, Ar-H), 7.66 (m, 2H, Ar-H), 7.45 (m, 2H, Ar-H), 7.21 (m, 2H, Ar-H), 7.05 (d, J=7.7 Hz, 1H, Ar-H), 3.87 (s, 3H, OCH_3); ^{13}C NMR (DMSO-d_6, 100MHz) δ 160.1, 151.5, 131.9,

130.6, 119.2, 116.3, 111.9, 55.8. **HRMS**: (ESI) *m/z* calculated for $C_{14}H_{13}N_2O[M+H]^+$ 225.1022, observed 225.1032.

2-(3-(trifluoromethyl)phenyl)-1H-benzo[d]imidazole (84j), White solid, 0.22 g, 82%; R_f 0.50 (7:3/Hexanes: EtOAc); ^{1}H NMR (DMSO-d_6, 400MHz): δ = 13.18 (s, 1H, NH), 8.54 (s, 1H, Ar-H), 8.50 (d, *J*=7.8 Hz, 1H, Ar-H), 7.80 (m, 4H, Ar-H), 7.24 (m, 2H, Ar-H); ^{13}C NMR (DMSO-d_6, 100MHz) δ 150.1, 131.6, 130.6, 130.1, 126.7, 126.6, 125.9, 123.3, 123.2. **HRMS**: (ESI) *m/z* calculated for $C_{14}H_{10}F_3N_2$ $[M+H]^+$ 263.0791, observed 263.0784.

2-(3-isopropylphenyl)-1H-benzo[d]imidazole (84k), White solid, 0.35 g, 90%; R_f 0.42 (7:3/Hexanes: EtOAc); ^{1}H NMR (DMSO-d_6, 400MHz): δ = 12.92 (s, 1H, NH), 8.11 (s, 1H, Ar-H), 8.01 (d, *J*=7.8 Hz, 1H, Ar-H), 7.50 (m, 3H, Ar-H), 7.34 (d, *J*=7.8 Hz, 1H, Ar-H), 7.21 (m, 2H, Ar-H), 3.00 (m, 1H, -CH-), 1.27 (s, 6H, $(CH_3)_2$); ^{13}C NMR (DMSO-d_6, 100MHz) δ 151.9, 149.6, 130.6, 129.4, 128.5, 124.8, 124.5, 49.1, 33.9, 24.3. **HRMS**: (ESI) *m/z* calculated for $C_{16}H_{17}N_2$ $[M+H]^+$ 237.1386, observed 237.1389.

Methyl 3-(1H-benzo[d]imidazol-2-yl)benzoate (84l), White solid, 0.35 g, 90%; R_f 0.42 (7:3/Hexanes: EtOAc); ^{1}H NMR (DMSO-d_6, 400MHz): δ = 13.17 (s, 1H, NH), 8.82 (s, 1H, Ar-H), 8.45 (d, *J*=8.2 Hz, 1H, Ar-H), 8.06 (d, *J*=8.0 Hz, 1H, Ar-H), 7.70 (m, 3H, Ar-H), 7.24 (m, 2H, Ar-H); ^{13}C NMR (DMSO-d_6, 100MHz) δ 166.3, 150.6, 131.3, 131.2, 130.9, 130.7, 130.0, 127.5, 52.8. **HRMS**: (ESI) *m/z* calculated for $C_{15}H_{13}N_2O_2$ $[M+H]^+$ 253.0972, observed 253.1028.

2-(3-(methylsulfonyl)phenyl)-1H-benzo[d]imidazole (84m), White solid, 0.3 g, 96%; R_f 0.23 (7:3/Hexanes: EtOAc); ^{1}H NMR (DMSO-d_6, 400MHz): δ = 13.25 (s, 1H, NH), 8.74

(s, 1H, Ar-H), 8.51 (d, *J*=7.9 Hz, 1H, Ar-H), 8.05 (d, *J*= 8.0 Hz, 1H, Ar-H), 7.86 (t, *J*= 7.8, 7.8 Hz, 1H, Ar-H), 7.72 (d, *J*=7.6 Hz, 1H, Ar-H), 7.58 (d, *J*=7.4 Hz, 1H, Ar-H), 7.25 (m, 2H, Ar-H), 3.38 (s, 3H, SO_2CH_3); ^{13}C NMR (DMSO-d_6, 100MHz) δ 150.0, 144.1, 142.3, 135.6, 131.8, 131.5, 130.8, 128.4, 125.2, 123.6, 122.5, 119.6, 112.1, 44.0. **HRMS**: (ESI) *m/z* calculated for $C_{14}H_{13}N_2O_2S$ $[M+H]^+$ 273.0692, observed 273.0692.

2-(3-(1H-pyrrol-1-yl)phenyl)-1H-benzo[d]imidazole (84n), White solid, 0.4 g, 91%; R_f 0.45 (7:3/Hexanes: EtOAc); ^{1}H NMR (DMSO-d_6, 400MHz): δ = 13.00 (s, 1H, NH), 8.34 (s, 1H, Ar-H), 8.06 (d, *J*=7.7 Hz, 1H, Ar-H), 7.72 (m, 3H, Ar-H), 7.45 (m, 3H, Ar-H), 7.24 (m, 2H, Ar-H), 6.35 (m, 2H, Ar-H); ^{13}C NMR (DMSO-d_6, 100MHz) δ 151.1, 140.9, 132.0, 130.9, 123.7, 120.9, 119.5, 117.4, 111.3. **HRMS**: (ESI) *m/z* calculated for $C_{17}H_{14}N_3$ $[M+H]^+$ 260.1182, observed 260.1193.

3.1.3 General procedure for the synthesis of 64a – 64r, 66a – 66e, and 68a – 68k benzimidazole analogs.

The amide substrates were semi-synthetically prepared using carbodiimide-based coupling conditions. The amide substrate was dissolved in 30 mL of toluene or DMF, and added *N,N*-diisopropylethylamine (1.0 equiv), HBTU (1.0 equiv), and heated to reflux for 6 hours. The reaction was cooled to room temperature. The solvent was removed *in vacuo* in the case of toluene, but for DMF, the reaction mixture was diluted with water and products were extracted using ethyl acetate (EtOAc). The organic layer was dried over anhydrous sodium sulfate, filtered and concentrated *in vacuo*. The crude product was purified using column chromatography using hexanes/EtOAc in an increasing polarity up to 1:1 mixture. The impure fractions containing the desired product were concentrated and crystallized in

hexanes/EtOAc 1:1 to yield the product as a white solid. All the products were characterized by 1D (^{1}H and ^{13}C) NMR, and HRMS.

2-phenyl-1H-benzo[d]imidazole (64a), White solid, 0.23 g, 96%; R_f 0.61 (1:1/Hexanes: EtOAc); ^{1}H NMR (DMSO-d_6, 400MHz): δ = 12.94 (s, 1H, NH), 8.20 (d, 2H, *J*=7.4Hz, Ar-H), 7.54 (m, 5H, Ar-H), 7.21 (m, 2H, Ar-H); ^{13}C NMR (DMSO-d_6, 100MHz) δ 151.7, 130.7, 130.3, 129.4, 126.9. **HRMS**: (ESI) *m/z* calculated for $C_{13}H_{11}N_2$ $[M+H]^+$ 195.0917, observed 195.0918.

2-p-tolyl-1H-benzo[d]imidazole (64b), White solid, 0.21 g, 94%; R_f 0.56 (1:1/Hexanes: EtOAc); ^{1}H NMR (DMSO-d_6, 400MHz): δ = 12.84 (s, 1H, NH), 8.08 (d, 2H, *J*=8.1 Hz, Ar-H), 7.59 (m, 2H, Ar-H), 7.35 (d, 2H, *J*=8.1 Hz, Ar-H), 7.20 (m, 2H, Ar-H), 2.38 (s, 3H, CH_3); ^{13}C NMR (DMSO-d_6, 100MHz) δ 151.9, 140.0, 129.9, 127.9, 126.9, 21.4. **HRMS**: (ESI) *m/z* calculated for $C_{14}H_{13}N_2$ $[M+H]^+$ 209.1073, observed 209.1074.

2-(4-ethylphenyl)-1H-benzo[d]imidazole (64c), White solid, 0.23 g, 88%; R_f 0.26 (1:1/Hexanes: EtOAc); ^{1}H NMR (DMSO-d_6, 400MHz): δ = 12.85 (s, 1H, NH), 8.11 (d, 2H, *J*=8.0 Hz, Ar-H), 7.59 (m, 2H, Ar-H), 7.38 (d, 2H, *J*=8.0 Hz, Ar-H), 7.20 (m, 2H, Ar-H), 2.65 (q, 2H, *J*=12, 4 Hz CH_2), 1.22 (t, 3H, *J*=12, 4 Hz, CH_3); ^{13}C NMR (DMSO-d_6, 100MHz) δ 151.9, 146.2, 128.8, 128.2, 126.9, 28.5, 15.8. **HRMS**: (ESI) *m/z* calculated for $C_{15}H_{15}N_2$ $[M+H]^+$ 223.1230, observed 223.1238.

2-(3,4-dimethoxyphenyl)-1H-benzo[d]imidazole (64d), White solid, 0.32 g, 86%; R_f 0.57 (1:1/Hexanes: EtOAc); ^{1}H NMR (DMSO-d_6, 400MHz): δ = 12.69 (s, 1H, NH), 7.76 (m, 2H, Ar-H), 7.57 (m, Ar-H), 7.17 (m, 3H, Ar-H), 3.88 (s, 3H, OCH_3), 3.84 (s, 3H, OCH_3); ^{13}C NMR (DMSO-d_6, 100MHz) δ 152.0, 150.7, 149.4, 123.3, 122.2, 119.7, 112.3, 110.2,

56.1, 56.0. **HRMS**: (ESI) *m/z* calculated for $C_{15}H_{15}N_2O_2$ $[M+H]^+$ 255.1128, observed 255.1129.

2-(1H-benzo[d]imidazol-2-yl)-5-methoxyphenol (64e), White solid, 0.12g, 47%; R_f 0.23 (1:1/Hexanes: EtOAc); ^{1}H NMR (DMSO-d_6, 400MHz): δ = 13.39 (s, 1H, NH), 7.96 (d, 1H, *J*=8.6 Hz, Ar-H), 7.60 (m, 2H, Ar-H), 7.25 (m, 2H, Ar-H), 6.62 (m, 2H, Ar-H), 3.81 (s, 3H, OCH_3), 3.37 (s, 1H, OH); ^{13}C NMR (DMSO-d_6, 100MHz) δ 162.7, 160.4, 152.6, 127.7, 106.9, 106.2, 101.9, 55.8. **HRMS**: (ESI) *m/z* calculated for $C_{14}H_{13}N_2O_2$ $[M+H]^+$ 241.0972, observed 241.0988.

2-(3,4,5-trimethoxyphenyl)-1H-benzo[d]imidazole (64f), White solid, 0.11g, 82%; R_f 0.27 (1:1/Hexanes: EtOAc); ^{1}H NMR (DMSO-d_6, 400MHz): δ = 12.86 (s, 1H, NH), 7.67 (d, 1H, *J*=7.5 Hz, Ar-H), 7.54 (m, 2H, Ar-H), 7.21 (m, 2H, Ar-H), 3.91 (s, 6H, OCH_3), 3.38 (s, 3H, OCH_3); ^{13}C NMR (DMSO-d_6, 100MHz) δ 153.7, 151.7, 144.2, 139.4, 135.4, 125.9, 122.9, 122.1, 119.2, 111.6, 104.3, 60.6, 56.5. **HRMS**: (ESI) *m/z* calculated for $C_{16}H_{17}N_2O_3$ $[M+H]^+$ 285.1234, observed 285.1236.

2-(4-fluorophenyl)-1H-benzo[d]imidazole (64g), White solid, 0.15 g, 80%; R_f 0.34 (1:1/Hexanes: EtOAc); ^{1}H NMR (DMSO-d_6, 400MHz): δ = 12.94 (s, 1H, NH), 8.25 (m, 2H, Ar-H), 7.65 (m, 2H, Ar-H), 7.42 (m, 2H, Ar-H), 7.20 (m, 2H, Ar-H); ^{13}C NMR (DMSO-d_6, 100MHz) δ 164.8, 162.3, 150.7, 144.3, 135.5, 131.8, 130.8, 130.7, 129.2, 129.1, 127.3, 127.3, 123.0, 122.2, 119.3, 116.6, 116.4, 116.1, 115.9, 111.8. **HRMS**: (ESI) *m/z* calculated for $C_{13}H_{10}FN_2$ $[M+H]^+$ 213.0823, observed 213.0829.

2-(4-nitrophenyl)-1H-benzo[d]imidazole (64h), White solid, 0.17 g, 79%; R_f 0.61 (1:1/Hexanes: EtOAc); ^{1}H NMR (DMSO-d_6, 400MHz): δ = 13.29 (s, 1H, NH), 8.42 (m,

4H, Ar-H), 7.72 (d, 1H, *J*=7.6 Hz, Ar-H), 7.60 (d, 1H, *J*=7.6 Hz, Ar-H), 7.23 (m, 2H, Ar-H); ^{13}C NMR (DMSO-d_6, 100MHz) δ 149.5, 148.3, 144.3, 136.5, 135.7, 127.8, 124.7, 124.0, 122.8, 119.9, 112.3. **LC-MS**: (ESI) *m/z* calculated for $C_{13}H_{10}N_3O_2$ $[M+H]^+$ 240.0768, observed 240.0771.

2-(4-bromophenyl)-1H-benzo[d]imidazole (64i), White solid, 0.30 g, 94%; R_f 0.51 (1:1/Hexanes: EtOAc); ^{1}H NMR (DMSO-d_6, 400MHz): δ = 13.01 (s, 1H, NH), 8.14 (d, 2H, *J*=9.1 Hz, Ar-H), 7.61 (m, 2H, Ar-H), 7.22 (m, 2H, Ar-H); ^{13}C NMR (DMSO-d_6, 100MHz) δ 150.7, 132.4, 129.9, 128.8, 123.7, 123.3, 122.4, 119.4, 111.9. **HRMS**: (ESI) *m/z* calculated for $C_{13}H_{10}BrN_2$ $[M+H]^+$ 273.0022, observed 273.0016, 274.9995.

2-(4-methoxyphenyl)-1H-benzo[d]imidazole (64j), White solid, 0.54 g, 90%; R_f 0.63 (1:1/Hexanes: EtOAc); ^{1}H NMR (DMSO-d_6, 400MHz): δ = 12.77 (s, 1H, NH), 8.14 (d, 2H, *J*=6.8 Hz, Ar-H), 7.57 (m, 2H, Ar-H), 7.18 (m, 2H, Ar-H), 7.11 (d, 2H, J=6.8 Hz, Ar-H), 3.84 (s, 3H, OCH_3); ^{13}C NMR (DMSO-d_6, 100MHz) δ 161.1, 151.8, 128.5, 123.2, 114.8, 55.8. **HRMS**: (ESI) *m/z* calculated for $C_{14}H_{13}N_2O[M+H]^+$ 225.1022, observed 225.1025.

2-(3,5-dimethoxy-4-methylphenyl)-1H-benzo[d]imidazole (64k), White solid, 0.61 g, 88 %; R_f 0.701 (1:1/Hexanes: EtOAc); ^{1}H NMR (DMSO-d_6, 400MHz): δ = 12.90 (s, 1H, NH), 7.66 (d, 2H, *J*=7.4 Hz, Ar-H), 7.55 (d, 2H, *J*=7.4 Hz, Ar-H), 7.49 (s, 2H, Ar-H), 7.20 (m, 2H, Ar-H), 3.91 (s, 6H, OCH_3), 2.07 (s, 3H, CH_3); ^{13}C NMR (DMSO-d_6, 100MHz) δ 158.5, 152.0, 144.2, 135.4, 129.0, 122.9, 122.1, 119.2, 115.4, 111.6, 102.3, 56.2, 8.9. **HRMS**: (ESI) *m/z* calculated for $C_{16}H_{17}N_2O_2[M+H]^+$ 269.1285, observed 269.1298.

2-(3-iodo-4-methylphenyl)-1H-benzo[d]imidazole (64l), White solid, 0.71 g, 86 %; R_f 0.67 (1:1/Hexanes: EtOAc); ^{1}H NMR (DMSO-d_6, 400MHz): δ = 12.96 (s, 1H, NH), 8.64 (s,1H, Ar-H), 8.10 (d, 2H, *J*=7.9 Hz, Ar-H), 7.66 (d, 1H, *J*=7.4 Hz, Ar-H), 7.52 (d, 1H, J=7.4 Hz, Ar-H), 7.49 (d, 1H, j=7.9 Hz, Ar-H), 7.20 (m, 2H, Ar-H), 2.43 (s, 3H, CH_3); ^{13}C NMR (DMSO-d_6, 100MHz) δ 150.0, 144.1, 143.0, 136.6, 135.4, 130.8, 130.0, 129.9, 126.9, 126.7, 123.2, 122.3, 119.3, 111.8, 102.2, 27.9. **HRMS**: (ESI) *m/z* calculated for $C_{14}H_{12}IN_2[M+H]^+$ 335.0040, observed 335.0065.

2-(3-bromo-4-methylphenyl)-1H-benzo[d]imidazole (64m), White solid, 0.93 g, 82 %; R_f 0.58 (1:1/Hexanes: EtOAc); ^{1}H NMR (DMSO-d_6, 400MHz): δ = 12.98 (s, 1H, NH), 8.40 (s,1H, Ar-H), 8.10 (d, 2H, *J*=7.9 Hz, Ar-H), 7.66 (d, 1H, *J*=7.4 Hz, Ar-H), 7.52 (d, 1H, J=7.4 Hz, Ar-H), 7.49 (d, 1H, j=7.9 Hz, Ar-H), 7.20 (m, 2H, Ar-H), 2.43 (s, 3H, CH_3); ^{13}C NMR (DMSO-d_6, 100MHz) δ 150.0, 144.1, 139.5, 132.1, 130.3, 130.1, 126.0, 125.1, 123.2, 122.3, 119.4, 111.9, 22.8. **HRMS**: (ESI) *m/z* calculated for $C_{14}H_{12}BrN_2[M+H]^+$ 287.0178, observed 287.0201, 289.0182.

2-(2,3-dimethoxyphenyl)-1H-benzo[d]imidazole (64n), White solid, 0.22 g, 91%; R_f 0.51 (1:1/Hexanes: EtOAc); ^{1}H NMR (DMSO-d_6, 400MHz): δ = 12.23 (s, 1H, NH), 7.85(m,1H, Ar-H), 7.64 (m, 2H, Ar-H), 7.21 (m, 4H, Ar-H), 3.85 (s, 6H, OCH_3); ^{13}C NMR (DMSO-d_6, 100MHz) δ 152.4, 149.0, 148.8, 119.2, 118.1, 114.4, 112.9, 56.2. **HRMS**: (ESI) *m/z* calculated for $C_{15}H_{15}N_2O_2[M+H]^+$ 255.1128, observed 255.1144.

2-(6-chloropyridin-2-yl)-1H-benzo[d]imidazole (64o), White solid, 0.16 g, 87%; R_f 0.49 (1:1/Hexanes: EtOAc); ^{1}H NMR (DMSO-d_6, 400MHz): δ = 12.53 (s, 1H, NH), 7.63 (m, 4H, Ar-H), 7.22 (m, 2H, Ar-H), 6.72 (d, 1H, *J*=8.0Hz, Ar-H); ^{13}C NMR (DMSO-d_6,

100MHz) δ 159.1, 151.9, 146.7, 144.5, 141.5, 138.6, 135.1, 125.6, 123.2, 122.1, 120.9, 119.5, 112.4, 109.3, 107.3. **HRMS**: (ESI) *m/z* calculated for $C_{12}H_9ClN_3[M+H]^+$ 230.0480, observed 230.0499.

2-(3,5-dimethoxyphenyl)-1H-benzo[d]imidazole (64p), White solid, 0.32 g, 84%; R_f 0.51 (1:1/Hexanes: EtOAc); ^{1}H NMR (DMSO-d_6, 400MHz): δ = 12.90 (s, 1H, NH), 7.44 (m, 4H, Ar-H), 7.21 (m, 3H, Ar-H), 3.85 (s, 6H, OCH_3); ^{13}C NMR (DMSO-d_6, 100MHz) δ 161.3, 151.5, 132.4, 104.7, 102.5, 56.0. **HRMS**: (ESI) *m/z* calculated for $C_{15}H_{15}N_2O_2[M+H]^+$ 255.1128, observed 255.1128.

4-(1H-benzo[d]imidazol-2-yl)benzene-1,3-diol (64q), White solid, 0.12g, 47%; R_f 0.23 (1:1/Hexanes: EtOAc); ^{1}H NMR (DMSO-d_6, 400MHz): δ = 13.39 (s, 1H, NH), 7.96 (d, 1H, *J*=8.6 Hz, Ar-H), 7.60 (m, 2H, Ar-H), 7.25 (m, 2H, Ar-H), 6.62 (m, 2H, Ar-H), 3.81 (s, 3H, OCH_3), 3.37 (s, 1H, OH); ^{13}C NMR (DMSO-d_6, 100MHz) δ 162.7, 160.4, 152.6, 127.7, 106.9, 106.2, 101.9, 55.8. HRMS: (ESI) *m/z* calculated for $C_{13}H_{11}N_2O_2$ $[M+H]^+$ 227.0815, observed 227.0827.

2-(1H-benzo[d]imidazol-2-yl)benzene-1,3-diol (64r), White solid, 0.12g, 47%; R_f 0.23 (1:1/Hexanes: EtOAc); ^{1}H NMR (DMSO-d_6, 400MHz): δ = 13.39 (s, 1H, NH), 7.96 (d, 1H, *J*=8.6 Hz, Ar-H), 7.60 (m, 2H, Ar-H), 7.25 (m, 2H, Ar-H), 6.62 (m, 2H, Ar-H), 3.81 (s, 3H, OCH_3), 3.37 (s, 1H, OH); ^{13}C NMR (DMSO-d_6, 100MHz) δ 162.7, 160.4, 152.6, 127.7, 106.9, 106.2, 101.9, 55.8. LC-MS: (ESI) *m/z* calculated for $C_{13}H_{11}N_2O_2$ $[M+H]^+$ 227.0815, observed 227.0827.

2-(1H-indol-2-yl)-1H-benzo[d]imidazole (66a), White solid, 0.19g, 96 %; R_f 0.203 (1:1/Hexanes: EtOAc); ^{1}H NMR (DMSO-d_6, 400MHz): δ = 12.98 (s, 1H, NH), 12.03 (s,

1H, NH), 7.66 (m, 2H, Ar-H), 7.56 (d, *J*=7.4 Hz, 1H, Ar-H), 7.48 (m, 1H, Ar-H), 7.24 (m, 4H, Ar-H), 7.05 (m, 1H, Ar-H); ^{13}C NMR (DMSO-d_6, 100MHz) δ 146.6, 144.2, 137.7, 135.2, 129.1, 128.3, 123.3, 123.1, 122.2, 121.3, 120.2, 118.9, 112.4, 111.6, 102.1. **HRMS**: (ESI) *m/z* calculated for $C_{15}H_{12}N_3[M+H]^+$ 234.1026, observed 234.1039.

2-(1H-indol-3-yl)-1H-benzo[d]imidazole (66b), White solid, 0.2 g, 84%; R_f 0.201 (1:1/Hexanes: EtOAc); ^{1}H NMR (DMSO-d_6, 400MHz): δ = 13.07 (s, 1H, NH), 12.04 (s, 1H, NH), 8.53 (m, 1H, Ar-H), 8.15 (s, 1H, Ar-H), 7.52 (m, 2H, Ar-H), 7.15 (m, 3H, Ar-H); ^{13}C NMR (DMSO-d_6, 100MHz) δ 150.0, 136.9, 126.5, 125.7, 122.7, 121.9, 121.6, 120.7, 112.4, 107.1. **HRMS**: (ESI) *m/z* calculated for $C_{15}H_{12}N_3[M+H]^+$ 234.1026, observed 234.1028.

2-(1H-indol-5-yl)-1H-benzo[d]imidazole (66c), White solid, 0.19g, 94 %; R_f 0.302 (1:1/Hexanes: EtOAc); ^{1}H NMR (DMSO-d_6, 400MHz): δ = 12.75 (s, 1H, NH), 11.37 (s, 1H, NH), 8.42 (s, 1H, Ar-H), 8.00 (d, 1H, *J*=8.6 Hz, Ar-H), 7.52 (m, 4H, Ar-H), 7.16 (m, 2H, Ar-H), 6.58 (t, 1H, *J*=7.4, 2.2 Hz, Ar-H); ^{13}C NMR (DMSO-d_6, 100MHz) δ 153.6, 137.3, 128.2, 127.2, 121.9, 121.7, 120.5, 119.2, 112.3, 102.4. **HRMS**: (ESI) *m/z* calculated for $C_{15}H_{12}N_3[M+H]^+$ 234.1026, observed 234.1040.

2-(1H-indol-6-yl)-1H-benzo[d]imidazole (66d), White solid, 0.41 g, 96%; R_f 0.20 (1:1/Hexanes: EtOAc); ^{1}H NMR (DMSO-d_6, 400MHz): δ = 12.81 (s, 1H, NH), 11.47 (s, 1H, NH), 8.11 (d, 2H, *J*=8.0 Hz, Ar-H), 7.59 (m, 2H, Ar-H), 7.38 (d, 2H, *J*=8.0 Hz, Ar-H), 7.20 (m, 2H, Ar-H), 6.52 (m, 2H, Ar-H); ^{13}C NMR (DMSO-d_6, 100MHz) δ 153.4, 143.5, 136.3, 135.7, 130.5, 129.5, 127.9, 126.9, 124.6, 123.5, 120.8, 119.9, 119.0, 118.2, 116.9,

116.8, 112.3, 110.4, 101.9, 101.8, 79.7. **HRMS**: (ESI) *m/z* calculated for $C_{15}H_{12}N_3$ $[M+H]^+$ 234.1026, observed 234.1026.

2-(1H-indol-7-yl)-1H-benzo[d]imidazole (66e), White solid, 0.5g, 90%; R_f 0.302 (1:1/Hexanes: EtOAc); ^{1}H NMR (DMSO-d_6, 400MHz): δ = 13.07 (s, 1H, NH), 11.47 (s, 1H, NH), 7.95 (d, 1H, *J*=7.4 Hz, Ar-H), 7.76 (m, 2H, Ar-H), 7.55 (m, 2H, Ar-H), 7.24 (m, 3H, Ar-H), 6.58 (t, 1H, *J*=7.4, 2.2 Hz, Ar-H); ^{13}C NMR (DMSO-d_6, 100MHz) δ 151.8, 133.5, 129.3, 127.2, 123.1, 122.9, 122.1, 119.4, 119.1, 113.3, 111.7, 101.9. **HRMS**: (ESI) *m/z* calculated for $C_{15}H_{12}N_3[M+H]^+$ 234.1026, observed 234.1033.

2-heptadecyl-1H-benzo[d]imidazole (68a), White solid, 1.5 g, 96 %; R_f 0.62 (9:1/CH_2CL_2:MeOH); ^{1}H NMR ($CDCl_3$, 400MHz): δ = 7.55 (m, 2H, Ar-H), 7.23 (m, 2H, Ar-H), 2.91 (t, 2H, *J*=15.2, 7.2Hz, CH_2), 1.84 (m, 2H, CH_2), 1.26 (s, 28H, CH_2), 0.89 (t, 3H, *J*=12.6, 5.8Hz, CH_3); ^{13}C NMR ($CDCl_3$, 100MHz) δ 155.6, 122.1, 31.9, 29.7, 29.7, 29.7, 29.5, 29.4, 29.4, 29.4, 22.7, 14.1. **HRMS**: (ESI) *m/z* calculated for $C_{24}H_{41}N_2$ $[M+H]^+$ 357.3264, observed 357.3277.

2-pentadecyl-1H-benzo[d]imidazole (68b), White solid, 1.2 g, 92 %; R_f 0.56 (9:1/CH_2CL_2:MeOH); ^{1}H NMR ($CDCl_3$, 400MHz): δ = 7.55 (m, 2H, Ar-H), 7.23 (m, 2H, Ar-H), 2.91 (t, 2H, *J*=15.2, 7.2Hz, CH_2), 1.84 (m, 2H, CH_2), 1.26 (s, 28H, CH_2), 0.89 (t, 3H, *J*=12.6, 5.8Hz, CH_3); ^{13}C NMR ($CDCl_3$, 100MHz) δ 155.6, 138.3, 122.1, 114.6, 31.9, 29.7, 29.7, 29.7, 29.5, 29.4, 29.4, 29.4, 22.7, 14.1. **HRMS**: (ESI) *m/z* calculated for $C_{22}H_{37}N_2$ $[M+H]^+$ 329.2951, observed 329.2958.

2-heptyl-1H-benzo[d]imidazole (68c), White solid, 0.92 g, 94 %; R_f 0.61 (9:1/CH_2CL_2:MeOH); ^{1}H NMR (DMSO-d_6, 400MHz): δ = 12.18 (s, 1H, NH), 7.45 (m,

2H, Ar-H), 7.10 (m, 2H, Ar-H), 2.78 (t, 2H, *J*=15.2, 7.2Hz, CH_2), 1.75 (m, 2H, CH_2), 1.26 (s, 8H, CH_2), 0.85 (t, 3H, J=12.6, 5.8Hz, CH_3); ^{13}C NMR (DMSO-d_6, 100MHz) δ 155.6, 122.1, 31.9, 29.7, 29.7, 29.7, 29.5, 29.4, 29.4, 29.4, 22.7, 14.1. **LC-MS**: (ESI) *m/z* calculated for $C_{14}H_{21}N_2$ $[M+H]^+$ 217.1699, observed 217.1698.

Tert-butyl 2-(1H-benzo[d]imidazol-2-yl)ethylcarbamate (68d), White solid, 0.36 g, 92 %; R_f 0.67 (9:1/CH_2CL_2:MeOH); ^1H NMR (DMSO-d_6, 400MHz): δ = 12.24 (s, 1H, NH), 7.45 (m, 2H, Ar-H), 7.10 (m, 3H, Ar-H), 3.38 (m, 2H, CH_2), 2.94 (t, 2H, *J*=7.6, 14.8Hz, CH_2), 1.38 (s, 9H, CH_3); ^{13}C NMR (DMSO-d_6, 100MHz) δ 162.8, 155.9, 153.2, 134.3, 127.7, 121.6, 120.8, 117.1, 112.3, 102.9, 94.3, 78.2, 29.8, 28.7. **HRMS**: (ESI) *m/z* calculated for $C_{14}H_{20}N_3O_2$ $[M+H]^+$ 262.1550, observed 262.1552.

2-(but-3-enyl)-1H-benzo[d]imidazole (68e), White solid, 0.75 g, 92 %; R_f 0.44 (9:1/CH_2CL_2:MeOH); ^1H NMR (DMSO-d_6, 400MHz): δ = 12.23 (s, 1H, NH), 7.47 (m, 2H, Ar-H), 7.10 (m, 2H, Ar-H), 5.88 (m, 1H, CH), 5.11 (dd, 1H, *J*=4.0, 17.0Hz, CH), 5.00 (dd, 1H, J=4.0, 17.0Hz, CH), 2.90 (t, 2H, *J*=7.2, 15.2Hz, CH_2), 2.52 (m, 2H, CH_2); ^{13}C NMR (DMSO-d_6, 100MHz) δ 154.9, 137.9, 121.6, 115.9, 32.0, 28.4. **HRMS**: (ESI) *m/z* calculated for $C_{11}H_{13}N_2$ $[M+H]^+$ 173.1073, observed 173.1075.

2-(3-phenylpropyl)-1H-benzo[d]imidazole (68f), White solid, 0.28 g, 95%; R_f 0.410 (1:1/Hexanes: EtOAc); ^1H NMR (DMSO-d_6, 400MHz): δ = 12.24 (s, 2H, NH), 7.45 (m, 2H, Ar-H), 7.21 (m, 8H, Ar-H), 2.82 (t, *J*=15.0, 7.4Hz, 2H, CH_2), 2.66 (t, *J*=15.0, 7.4Hz, 2H, CH_2), 2.10 (p, *J*=15.0, 7.4Hz, 2H, CH_2); ^{13}C NMR (DMSO-d_6, 100MHz) δ 155.3, 142.1, 128.9, 128.8, 126.3, 121.5, 35.1, 29.7, 28.5. **HRMS**: (ESI) *m/z* calculated for $C_{16}H_{17}N_2[M+H]^+$ 237.1386, observed 237.1387.

2-(4-nitrobenzyl)-1H-benzo[d]imidazole (68g), White solid, 0.21 g, 90%; R_f 0.57 (1:1/Hexanes: EtOAc); ^{1}H NMR (DMSO-d_6, 400MHz): δ = 12.42 (s, 2H, NH), 8.20 (d, 2H, *J*=6.8Hz, Ar-H), 7.62 (d, 2H, *J*=6.8Hz, Ar-H), 7.50 (m, 2H, Ar-H), 7.13 (m, 2H, Ar-H), 4.3 (s, 2H, CH_2); ^{13}C NMR (DMSO-d_6, 100MHz) δ 152.7, 146.8, 146.1, 130.7, 124.1, 122.0, 35.0. **HRMS**: (ESI) *m/z* calculated for $C_{14}H_{12}N_3O_2[M+H]^+$ 254.0924, observed 254.0936.

2-(4-bromobenzyl)-1H-benzo[d]imidazole (68h), White solid, 0.8 g, 92%; R_f 0.64 (1:1/Hexanes: EtOAc); ^{1}H NMR (DMSO-d_6, 400MHz): δ = 12.31 (s, 2H, NH), 7.50 (m, 4H, Ar-H), 7.21 (m, 4H, Ar-H), 4.17 (s, 2H, CH_2); ^{13}C NMR (DMSO-d_6, 100MHz) δ 153.5, 137.5, 131.5, 121.8, 120.2, 34.7. **HRMS**: (ESI) *m/z* calculated for $C_{14}H_{12}BrN_2[M+H]^+$ 287.0178, observed 287.0177, 289.0158.

2-(2-bromobenzyl)-1H-benzo[d]imidazole (68i), White solid, 1.2 g, 94%; R_f 0.51 (1:1/Hexanes: EtOAc); ^{1}H NMR (DMSO-d_6, 400MHz): δ = 12.30 (s, 2H, NH), 7.64 (d, 1H, *J*=8.0Hz, Ar-H), 7.44 (m, 2H, Ar-H), 7.34 (d, 1H, *J*=8.0Hz, Ar-H), 7.21 (m, 3H, Ar-H), 4.32 (s, 2H, CH_2); ^{13}C NMR (DMSO-d_6, 100MHz) δ 152.6, 137.3, 133.0, 132.0, 129.3, 128.4, 124.5, 35.8. **HRMS**: (ESI) *m/z* calculated for $C_{14}H_{12}BrN_2$ $[M+H]^+$ 287.0178, observed 287.0182, 289.0165.

2-(2-(1H-indol-3-yl)ethyl)-1H-benzo[d]imidazole (68j), White solid, 0.36 g, 93%; R_f 0.70 (1:1/Hexanes: EtOAc); ^{1}H NMR (DMSO-d_6, 400MHz): δ = 12.28 (s, 1H, NH), 10.81 (s, 1H, NH), 7.57 (d, 1H, *J*=7.8 Hz, Ar-H), 7.47 (m, 2H, Ar-H), 7.60 (d, 1H, *J*=7.8 Hz, Ar-H), 7.10 (m, 4H, Ar-H), 6.97 (t, 1H, *J*=7.4, 14.8Hz, Ar-H), 3.21 (m, 4H, CH_2); ^{13}C NMR (DMSO-d_6, 100MHz) δ 155.4, 136.7, 127.5, 122.7, 121.6, 121.4, 118.7, 118.7, 114.0,

111.8, 30.1, 23.9. **HRMS**: (ESI) *m/z* calculated for $C_{17}H_{16}N_3[M+H]^+$ 262.1339, observed 262.1339.

2-(2-(1H-indol-3-yl)propyl)-1H-benzo[d]imidazole (68k), White solid, 0.21g, 92%; R_f 0.52 (1:1/Hexanes: EtOAc); ^{1}H NMR (DMSO-d_6, 400MHz): δ = 12.25 (s, 1H, NH), 10.83 (s, 1H, NH), 7.53 (d, 1H, *J*=7.9 Hz, Ar-H), 7.48 (m, 1H, Ar-H), 7.360 (d, 1H, *J*=8.0 Hz, Ar-H), 7.10 (m, 4H, Ar-H), 6.97 (t, 1H, *J*=7.4, 14.8Hz, Ar-H), 2.89 (t, 2H, *J*=7.4, 15.2Hz, CH_2), 2.79 (t, 2H, *J*=7.4, 15.2Hz, CH_2), 2.17 (p, 2H, *J*=7.7, 15.1Hz, CH_2); ^{13}C NMR (DMSO-d_6, 100MHz) δ 155.6, 136.8, 127.7, 122.9, 121.5, 121.3, 118.8, 114.4, 111.8, 28.9, 28.9, 24.8. **HRMS**: (ESI) *m/z* calculated for $C_{18}H_{18}N_3[M+H]^+$ 276.1495, observed 276.1519.

3.1.4 General Procedure for the selective mono-alkylation of 2-indolyl-benzimidazoles 71a – 71j, 72a – 72f and 73a – 73e.

A solution of 2-indolylbenzimidazole derivative **66a** (1.0 equiv.) in acetonitrile (3 mL) was cooled to 0 ˚C in ice/water bath. To the solution was added potassium carbonate powder (3 equiv.) and allowed to stir for 20 min. Then, alkyl or benzyl bromide (1 equiv) was added and the reaction mixture allowed to stir for another 20 minutes at 0 ˚C before brought to room temperature. The reaction stirred for another 3 h. Upon the reaction completion, (as per TLC analysis), the reaction mixture was diluted with water and extracted using ethyl acetate (3 x 100 mL). The combined organic layer was dried over anhydrous sodium sulfate, filtered and concentrated *in vacuo*. The crude product was purified using column chromatography using hexanes/EtOAc in increasing polarity up to

7:3 mixture. The fractions containing the desired product were concentrated and crystallized in hexanes/EtOAc (7:3) to yield the desired products as off-white solid.

1-benzyl-2-(1H-indol-2-yl)-1H-benzo[d]imidazole (71a)*, a* white solid, 0.10 g, 90%; R_f 0.50 (1:1/Hexanes: EtOAc); ^{1}H NMR (DMSO-d_6, 400MHz): δ = 12.03 (s, 1H, NH), 7.66 (m, 1H, Ar-H), 7.56 (m, 3H, Ar-H), 7.25 (m, 5H, Ar-H), 7.05 (m, 5H, Ar-H), 5.83 (s, 2H, -CH_2); ^{13}C NMR (DMSO-d_6, 100MHz) δ 146.7, 143.0, 137.2, 136.8, 134.2, 128.4, 127.3, 126.4, 126.3, 126.1, 123.6, 123.3, 122.9, 121.4, 120.2, 119.3, 112.4, 111.2, 102.9, 79.7, 46.7. **HRMS**: (ESI) *m/z* calculated for $C_{22}H_{18}N_3[M+H]^+$ 324.1495, observed 324.1501.

Compound (71b)*,* a white solid, 0.19 g, 92%; R_f 0.60 (1:1/Hexanes: EtOAc); ^{1}H NMR (DMSO-d_6, 400MHz): δ = 12.14 (s, 1H, NH), 7.80 (m, 2H, Ar-H), 7.66 (m, 1H, Ar-H), 7.25 (m, 10H, Ar-H), 6.88 (s, 1H, Ar-H), 5.78 (s, 2H, -CH_2), 2.41 (s, 3H, -CH_3); ^{13}C NMR (DMSO-d_6, 100MHz) δ 147.3, 142.7, 137.7, 137.1, 136.5, 132.9,129.9, 128.5, 126.7, 126.0, 123.8, 123.3, 123.1, 121.3, 120.2, 119.4, 111.9, 110.1, 103.5, 48.3, 21.2. **HRMS**: (ESI) *m/z* calculated for $C_{23}H_{20}N_3[M+H]^+$ 338.1652, observed 338.1656.

1-(4-tert-butylbenzyl)-2-(1H-indol-2-yl)-1H-benzo[d]imidazole (71c)*,* a white solid, 0.2 g, 84%; R_f 0.64 (1:1/Hexanes: EtOAc); ^{1}H NMR (DMSO-d_6, 400MHz): δ = 12.03 (s, 1H, NH), 7.66 (m, 1H, Ar-H), 7.56 (m, 3H, Ar-H), 7.25 (m, 5H, Ar-H), 7.05 (m, 5H, Ar-H), 5.83 (s, 2H, -CH_2), 1.20 (s, 9H, (-CH_3)$_3$); ^{13}C NMR (DMSO-d_6, 100MHz) δ 150.3, 146.9, 143.0, 137.2, 136.8, 134.2, 128.4, 127.3, 126.4, 126.3, 126.1, 123.6, 123.3, 122.9, 121.4, 120.2, 119.3, 112.4, 111.2, 102.9, 79.7, 47.4, 34.6, 31.5, 22.6. **HRMS**: (ESI) *m/z* calculated for $C_{26}H_{26}N_3[M+H]^+$ 380.2121, observed 380.2121.

1-(4-(trifluoromethoxy)benzyl)-2-(1H-indol-2-yl)-1H-benzo[d]imidazole (71d), a white solid, 0.3 g, 89%; R_f 0.70 (1:1/Hexanes: EtOAc); ^{1}H NMR (DMSO-d_6, 400MHz): δ = 12.68 (s, 1H, NH), 7.80 (m, 2H, Ar-H), 7.66 (m, 1H, Ar-H), 7.25 (m, 10H, Ar-H), 6.88 (s, 1H, Ar-H), 5.81 (s, 2H, -CH_2); ^{13}C NMR (DMSO-d_6, 100MHz) δ 148.9, 148.9, 148.9, 147.4, 142.7, 137.3, 136.2, 134.6, 128.4, 127.6, 126.4, 124.3, 124.0, 123.5, 123.4, 121.8, 121.3, 120.4, 119.4. 119.2, 116.7, 112.1, 109.9, 103.4, 47.8. **HRMS**: (ESI) *m/z* calculated for $C_{23}H_{17}F_3N_3O[M+H]^+$ 480.1318, observed 408.1319.

1-(4-(trifluoromethylthio)benzyl)-2-(1H-indol-2-yl)-1H-benzo[d]imidazole (71e), a white solid, 0.5 g, 90%; R_f 0.60 (1:1/Hexanes: EtOAc); ^{1}H NMR (DMSO-d_6, 400MHz): δ = 12.06 (s, 1H, NH), 7.77 (m, 8H, Ar-H), 7.25 (m, 8H, Ar-H), 6.95 (s, 1H, Ar-H), 6.50 (m, 2H, -CH_2); ^{13}C NMR (DMSO-d_6, 100MHz) δ 146.8, 142.9, 141.2, 137.3, 137.2, 136.8, 128.5, 128.4, 128.1, 127.0, 123.7, 123.5, 123.2, 122.4, 121.4, 120.2, 119.4, 112.4, 111.1, 103.0, 47.3. **HRMS**: (ESI) *m/z* calculated for $C_{23}H_{17}F_3N_3S[M+H]^+$ 424.1090, observed 424.1090.

4-((2-(1H-indol-2-yl)-1H-benzo[d]imidazol-1-yl)methyl)benzonitrile (71f), a white solid, 0.4 g, 84%; R_f 0.50 (1:1/Hexanes: EtOAc); ^{1}H NMR (DMSO-d_6, 400MHz): δ = 12.06 (s, 1H, NH), 7.75 (m, 9H, Ar-H), 7.31 (m, 9H, Ar-H), 7.00 (s, 1H, Ar-H), 5.84 (s, 2H, -CH_2); ^{13}C NMR (DMSO-d_6, 100MHz) δ 146.8, 145.8, 144.6, 143.1, 142.9, 142.9, 138.1, 137.2, 136.7, 133.3, 133.2, 132.8, 128.4, 127.7, 127.6, 127.5, 127.5, 127.3, 126.9, 123.7, 123.5, 123.2, 121.9, 121.4, 120.2, 119.4, 119.0, 112.4, 111.6, 111.4, 111.0, 110.8, 110.3, 106.3, 103.0, 79.7, 47.5. **HRMS**: (ESI) *m/z* calculated for $C_{23}H_{17}N_4[M+H]^+$ 349.1448, observed 349.1451.

1-(4-nitrobenzyl)-2-(1H-indol-2-yl)-1H-benzo[d]imidazole (71g), a yellow solid, 0.7 g, 86%; R_f 0.43 (1:1/Hexanes: EtOAc); ^{1}H NMR (DMSO-d_6, 400MHz): δ = 12.08 (s, 1H, NH), 8.20 (d, *J*=8.8 Hz, 2H, Ar-H), 7.56 (m, 5H, Ar-H), 7.25 (m, 6H, Ar-H), 7.00 (m, 2H, Ar-H), 6.06 (s, 2H, -CH_2); ^{13}C NMR (DMSO-d_6, 100MHz) δ 147.3, 146.8, 145.2, 142.9, 137.3, 136.7, 128.3, 127.8, 126.9, 124.6, 123.7, 123.6, 123.3, 121.4, 120.2, 119.4, 112.4, 111.0, 103.1, 47.4. **HRMS**: (ESI) *m/z* calculated for $C_{22}H_{17}N_4O_2$ $[M+H]^+$ 369.1346, observed 369.1348.

1-(4-(methylsulfonyl)benzyl)-2-(1H-indol-2-yl)-1H-benzo[d]imidazole (71h), a white solid, 0.6 g, 86%; R_f 0.19 (1:1/Hexanes: EtOAc); ^{1}H NMR (DMSO-d_6, 400MHz): δ = 12.14 (s, 1H, NH), 7.97 (m, 2H, Ar-H), 7.66 (m, 1H, Ar-H), 7.25 (m, 8H, Ar-H), 6.72 (s, 1H, Ar-H), 5.87 (s, 2H, -CH_2), 3.09 (s, 3H, -CH_3); ^{13}C NMR (DMSO-d_6, 100MHz) δ 147.1, 142.7, 142.3, 140.4, 136.9, 136.1, 128.5, 128.3, 127.0, 126.2, 124.2, 123.7, 123.5, 121.3, 120.6, 119.6, 111.9, 109.7, 103.3, 48.0, 44.5. **HRMS**: (ESI) *m/z* calculated for $C_{23}H_{20}N_3O_2S[M+H]^+$ 402.1271, observed 402.1280.

Methyl 4-((2-(1H-indol-2-yl)-1H-benzo[d]imidazol-1-yl)methyl)benzoate (71i), a white solid, 0.9 g, 87%; R_f 0.45 (1:1/Hexanes: EtOAc); ^{1}H NMR (DMSO-d_6, 400MHz): δ = 12.01 (s, 1H, NH), 7.97 (m, 2H, Ar-H), 7.66 (m, 1H, Ar-H), 7.25 (m, 9H, Ar-H), 6.84 (s, 1H, Ar-H), 5.98 (s, 2H, -CH_2), 3.80 (s, 3H, -CH_3); ^{13}C NMR (DMSO-d_6, 100MHz) δ 166.3, 146.9, 142.9, 142.9, 137.2, 136.8, 130.3, 129.3, 128.3, 127.0, 126.8, 123.7, 123.5, 123.2, 121.4, 120.2, 119.4, 112.4, 111.1, 103.1, 79.7, 52.6. **HRMS**: (ESI) *m/z* calculated for $C_{24}H_{20}N_3O_2[M+H]^+$ 382.1550, observed 382.1556.

1-(4-(trifluoromethyl)benzyl)-2-(1H-indol-2-yl)-1H-benzo[d]imidazole (71j), a white solid, 0.2 g, 79%; R_f 0.60 (1:1/Hexanes: EtOAc); ^{1}H NMR (DMSO-d_6, 400MHz): δ = 12.06 (s, 1H, NH), 7.75 (m, 3H, Ar-H), 7.56 (m, 2H, Ar-H), 7.31 (m, 4H, Ar-H), 7.17 (m, 1H, Ar-H), 7.02 (m, 1H, Ar-H), 6.89 (m, 1H, Ar-H); ^{13}C NMR (DMSO-d_6, 100MHz) δ 146.8, 142.9, 142.2, 137.2, 136.8, 128.4, 128.4, 127.3, 126.9, 126.3, 126.3, 125.9, 123.7, 123.5, 123.2, 123.2, 121.4, 120.2, 119.4, 112.4, 111.1, 103.0, 47.4. **HRMS**: (ESI) *m/z* calculated for $C_{26}H_{26}N_3[M+H]^+$ 392.1369, observed 392.1369.

1-(cyclopropylmethyl)-2-(1H-indol-2-yl)-1H-benzo[d]imidazole (72a), a white solid, 0.3 g, 92%; R_f 0.53 (1:1/Hexanes: EtOAc); ^{1}H NMR (DMSO-d_6, 400MHz): δ = 12.00 (s, 1H, NH), 7.66 (m, 3H, Ar-H), 7.30 (m, 1H, Ar-H), 7.20 (m, 4H, Ar-H), 7.05 (m, 2H, Ar-H), 4.53 (d, *J*=6.6 Hz, 2H, -CH_2) 1.33 (m, 1H, -CH), 0.45 (m, 4H, $(CH_2)_2$); ^{13}C NMR (DMSO-d_6, 100MHz) δ 146.4, 142.9, 137.2, 136.8, 128.6, 127.6, 123.5, 123.0, 122.7, 121.5, 120.2, 119.1, 112.4, 111.4, 102.9, 79.7, 48.1, 11.6, 4.0. **HRMS**: (ESI) *m/z* calculated for $C_{19}H_{18}N_3[M+H]^+$ 288.1495, observed 288.1495.

1-(cyclohexylmethyl)-2-(1H-indol-2-yl)-1H-benzo[d]imidazole (72b), a white solid, 0.20 g, 89%; R_f 0.68 (1:1/Hexanes: EtOAc); ^{1}H NMR (DMSO-d_6, 400MHz): δ = 11.94 (s, 1H, NH), 7.66 (m, 3H, Ar-H), 7.50 (m, 1H, Ar-H), 7.25 (m, 3H, Ar-H), 7.05 (m, 2H, Ar-H), 4.43 (d, *J*=7.4 Hz, 2H, -CH_2) 1.92 (m, 1H, -CH), 1.54 (m, 5H, $(-CH)_5$), 1.09 (m, 5H, $(-CH)_5$); ^{13}C NMR (DMSO-d_6, 100MHz) δ 146.4, 142.9, 137.2, 137.1, 128.6, 127.7, 123.5, 122.9, 122.6, 121.5, 120.1, 119.1, 112.4, 111.6, 102.7, 79.7, 50.2, 30.6, 26.2, 25.7. **HRMS**: (ESI) *m/z* calculated for $C_{22}H_{24}N_3[M+H]^+$ 330.1965, observed 330.1965.

1-(cyclobutylmethyl)-2-(1H-indol-2-yl)-1H-benzo[d]imidazole (72c), a white solid, 0.40 g, 90%; R_f 0.62 (1:1/Hexanes: EtOAc); ^{1}H NMR (DMSO-d_6, 400MHz): δ = 12.00 (s, 1H, NH), 7.66 (m, 3H, Ar-H), 7.30 (m, 1H, Ar-H), 7.20 (m, 6H, Ar-H), 7.00 (s, 1H, Ar-H), 4.53 (d, *J*=6.6 Hz, 2H, -CH_2) 3.10 (m, 1H, -CH), 2.15 (m, 2H, -CH_2), 1.95 (m, 4H, (-CH_2)$_2$); ^{13}C NMR (DMSO-d_6, 100MHz) δ 146.7, 142.4, 136.8, 136.6, 128.6, 127.3, 123.7, 122.9, 122.7, 121.2, 120.2, 119.3, 111.9, 110.2, 102.9, 49.5, 36.1, 26.7, 18.5. **HRMS**: (ESI) *m/z* calculated for $C_{20}H_{20}N_3[M+H]^+$ 302.1652, observed 302.1652.

1-allyl-2-(1H-indol-2-yl)-1H-benzo[d]imidazole (72d), a white solid, 0.20 g, 94%; R_f 0.55 (1:1/Hexanes: EtOAc); ^{1}H NMR (DMSO-d_6, 400MHz): δ = 12.98 (s, 1H, NH), 12.03 (s, 1H, NH), 7.66 (m, 2H, Ar-H), 7.56 (d, *J*=7.4 Hz, 1H, Ar-H), 7.48 (m, 1H, Ar-H), 7.24 (m, 4H, Ar-H), 7.05 (m, 1H, Ar-H); ^{13}C NMR (DMSO-d_6, 100MHz) δ 146.9, 144.2, 137.7, 135.2, 129.1, 128.3, 123.3, 123.1, 122.2, 121.3, 120.2, 118.9, 112.4, 111.6, 102.1, 79.9, 47.7. **HRMS**: (ESI) *m/z* calculated for $C_{18}H_{16}N_3[M+H]^+$ 274.1339, observed 274.1339.

2-(1H-indol-2-yl)-1-phenethyl-1H-benzo[d]imidazole (72e), a white solid, 0.31 g, 88%; R_f 0.47 (1:1/Hexanes: EtOAc); ^{1}H NMR (DMSO-d_6, 400MHz): δ = 11.97 (s, 1H, NH), 7.66 (m, 4H, Ar-H), 7.48 (m, 10H, Ar-H), 4.77 (t, *J*= 7.5, 15.1 Hz, 2H, -CH_2), 3.16 (t, *J*= 7.6, 15.1 Hz, 2H, -CH_2); ^{13}C NMR (DMSO-d_6, 100MHz) δ 146.4, 142.8, 138.3, 137.2, 136.4, 129.4, 128.9, 128.5, 127.5, 127.1, 123.6, 122.9, 122.7, 121.5, 120.2, 120.1, 119.1, 112.4, 111.1, 102.9, 102.7, 45.9, 35.6. **HRMS**: (ESI) *m/z* calculated for $C_{23}H_{20}N_3[M+H]^+$ 338.1652, observed 338.1652.

1-(3-(benzyloxy)propyl)-2-(1H-indol-2-yl)-1H-benzo[d]imidazole (72f), a white solid, 0.15 g, 90%; R_f 0.49 (1:1/Hexanes: EtOAc); ^{1}H NMR (DMSO-d_6, 400MHz): δ = 11.59 (s,

1H, NH), 7.66 (m, 3H, Ar-H), 7.48 (m, 12H, Ar-H), 4.75 (t, *J*= 7.2, 14.44 Hz, 2H, -CH_2), 4.59 (s, 2H, -CH_2), 3.66 (t, *J*= 5.4, 10.96 Hz, 2H, -CH_2), 2.38 (p, *J*= 7.0, 12.96 Hz, 2H, -CH_2); ^{13}C NMR (DMSO-d_6, 100MHz) δ 146.5, 142.5, 138.1, 136.8, 136.4, 128.7, 128.6, 127.8, 127.7, 127.0, 123.8, 122.9, 122.8, 121.3, 120.2, 119.3, 111.7, 109.8, 103.2, 66.8, 41.9, 30.1. **HRMS**: (ESI) *m/z* calculated for $C_{25}H_{24}N_3O[M+H]^+$ 382.1914, observed 382.1916.

***1-benzyl-2-(5-methoxy-1H-indol-2-yl)-1H-benzo[d]imidazole (73a)**, a* white solid, 0.6 g, 92%; R_f 0.60 (1:1/hexanes:EtOAc); ^{1}H NMR (DMSO-d_6, 400 MHz): δ = 11.91 (s, 1H, NH), 7.76 (d, *J*=7.2Hz, 1H, Ar-H), 7.57 (d, *J*=7.4Hz, 1H, Ar-H), 7.36 (m, 6H, Ar-H), 7.34 (dd, *J*=8.8, 8.8Hz, 1H, Ar-H), 7.23 (m, 2H, Ar-H), 6.83 (dd, *J*=8.8, 8.8Hz, 1H, Ar-H), 5.86 (s, 2H, -CH_2-), 3.74 (s, 3H, OCH_3); ^{13}C NMR (DMSO-d_6, 100 MHz) δ 154.3, 147.0, 142.9, 137.3, 136.8, 132.5, 129.4, 128.7, 127.9, 127.4, 126.5, 123.3, 122.9, 119.2, 114.6, 113.2, 111.1, 102.8, 102.1, 79.7, 55.7, 47.7. **HRMS**: (ESI) *m/z* calculated for $C_{23}H_{20}N_3O$ $[M+H]^+$ 354.1601, observed 354.1601.

***1-(4-(trifluoromethyl)benzyl)-2-(5-methoxy-1H-indol-2-yl)-1H-benzo[d]imidazole (73b)**,* a white solid, 0.35 g, 90%; R_f 0.60 (1:1/hexanes:EtOAc); ^{1}H NMR (DMSO-d_6, 400 MHz): δ = 11.91 (s, 1H, NH), 7.76 (d, *J*=7.2Hz, 1H, Ar-H), 7.57 (d, *J*=7.4Hz, 1H, Ar-H), 7.36 (m, 6H, Ar-H), 7.34 (dd, *J*=8.8, 8.8Hz, 1H, Ar-H), 7.23 (m, 2H, Ar-H), 6.83 (dd, *J*=8.8, 8.8Hz, 1H, Ar-H), 5.86 (s, 2H, -CH_2-), 3.74 (s, 3H, OCH_3); ^{13}C NMR (DMSO-d_6, 100 MHz) δ 154.3, 147.0, 142.9, 137.3, 136.8, 132.5, 129.4, 128.7, 127.9, 127.4, 126.5, 123.3, 122.9, 119.2, 114.6, 113.2, 111.1, 102.8, 102.1, 79.7, 55.7, 47.7. **HRMS**: (ESI) *m/z* calculated for $C_{24}H_{19}F_3N_3O$ $[M+H]^+$ 422.1475, observed 422.1482.

1-(cyclohexylmethyl)-2-(5-methoxy-1H-indol-2-yl)-1H-benzo[d]imidazole (73c), a white solid, 0.6 g, 78%; R_f 0.68 (1:1/hexanes:EtOAc); ^{1}H NMR (DMSO-d_6, 400 MHz): δ = 11.86 (s, 1H, NH), 7.67 (d, *J*=7.2Hz, 1H, Ar-H), 7.56 (d, 1H, Ar-H), 7.34 (dd, *J*=8.8, 8.8Hz, 1H, Ar-H), 7.23 (m, 2H, Ar-H), 6.83 (dd, *J*=8.8, 8.8Hz, 1H, Ar-H), 4.41 (d, *J*=6.6Hz, 2H, -CH_2-), 3.79 (s, 3H, OCH_3), 1.7 (m, 1H, -CH-), 1.55 (m, 5H, -CH-), 1.1 (m, 5H, -CH-); ^{13}C NMR (DMSO-d_6, 100 MHz) δ 154.3, 146.7, 144.2, 135.2, 132.9, 129.4, 128.7, 122.9, 122.1, 118.9, 114.9, 114.1, 113.3, 113.2, 111.6, 102.2, 101.9, 55.7, 50.2, 38.5, 30.6, 26.2, 25.7. **HRMS**: (ESI) *m/z* calculated for $C_{23}H_{26}N_3O$ $[M+H]^+$ 360.2070, observed 360.2070.

1-(cyclopropylmethyl)-2-(5-methoxy-1H-indol-2-yl)-1H-benzo[d]imidazole (73d), a white solid, 0.46 g, 82%; R_f 0.53 (1:1/hexanes:EtOAc); ^{1}H NMR (DMSO-d_6, 400 MHz): δ = 12.93 (s, 1H, NH), 11.86 (s, 1H, NH), 7.67 (d, *J*=7.2Hz, 1H, Ar-H), 7.56 (d, 1H, Ar-H), 7.34 (dd, *J*=8.8, 8.8Hz, 1H, Ar-H), 7.23 (m, 2H, Ar-H), 6.83 (dd, *J*=8.8, 8.8Hz, 1H, Ar-H), 4.50 (d, *J*=6.6Hz, 2H, -CH_2-), 3.78 (s, 3H, OCH_3), 1.33 (m, 1H, -CH-), 0.48 (m. 4H, 2[-CH_2-]); ^{13}C NMR (DMSO-d_6, 100 MHz) δ 154.3, 146.7, 144.2, 135.2, 132.9, 129.4, 128.7, 122.9, 122.1, 118.9, 114.9, 114.1, 113.3, 113.2, 111.6, 102.2, 101.9, 79.8, 55.7, 48.1, 11.6, 4.0. **HRMS**: (ESI) *m/z* calculated for $C_{20}H_{20}N_3O$ $[M+H]^+$ 318.1601, observed 318.1601.

1-allyl-2-(5-methoxy-1H-indol-2-yl)-1H-benzo[d]imidazole (73e), a *w*hite solid, 0.25 g, 96%; R_f 0.56 (1:1/hexanes:EtOAc); ^{1}H NMR (DMSO-d_6, 400 MHz): δ = 11.86 (s, 1H, NH), 7.67 (d, *J*=7.2Hz, 1H, Ar-H), 7.56 (d, 1H, Ar-H), 7.34 (dd, *J*=8.8, 8.8Hz, 1H, Ar-H), 7.23 (m, 2H, Ar-H), 6.83 (dd, *J*=8.8, 8.8Hz, 1H, Ar-H), 6.21 (m, 1H, -CH-), 5.21 (m, 2H, -CH_2-), 4.88 (m, 1H, -CH-), 3.79 (s, 3H, OCH_3); ^{13}C NMR (DMSO-d_6, 100 MHz) δ 154.3,

146.7, 144.2, 135.2, 132.9, 129.4, 128.7, 122.9, 122.1, 118.9, 114.9, 114.1, 113.3, 113.2, 111.6, 102.2, 101.9, 55.7, 46.8. **HRMS**: (ESI) *m/z* calculated for $C_{19}H_{18}N_3O$ $[M+H]^+$ 304.1444, observed 304.1444.

3.1.5 General procedure for the synthesis of symmetrically or asymmetrically bis-alkylated 2-indolylbenzimidazoles 75a – 75c and 77a – 77d.

There were two steps. Step 1, a solution of 2-indolylbenzimidazole **66a** (1 equiv.) in 3 mL of CH_3CN was cooled to 0 ˚C in ice/water bath, potassium hydroxide powder (1 equiv.) was added and the reaction mixture was left to stir for 20 min. Thereafter, alkyl or benzyl bromide (1 equiv.) was added and the reaction mixture was stirred for 4 h at 0 ˚C. For the benzylation, the reaction was done at 0 ˚C for 4 h. For the cyclopropylmethylation reaction, the reaction was allowed to warm to rt and continued at rt for 6 h. Step 2, Once the mono-alkylation was complete, second equivalence of potassium hydroxide powder was added to the reaction mixture and stirred at 0 ˚C for 20 min. Then, alkyl bromide (1 equiv.) was added and the reaction mixture was stirred at 0 ˚C for another 20 min, and subsequently allowed to warm to rt and stirred for 7 h. Once the reaction was complete, crude reaction mixture was diluted with water and extracted using ethyl acetate (3 x 100 mL). The combined organic layer was dried over anhydrous sodium sulfate, filtered and concentrated *in vacuo*. The crude product was purified using column chromatography using hexanes/EtOAc in increasing polarity up to 7:3 mixture. The fractions containing the desired product were concentrated and crystallized in hexanes/EtOAc (7:3) to yield the desired products as off-white solid.

1-benzyl-2-(1-benzyl-1H-indol-2-yl)-1H-benzo[d]imidazole (75a)**,** a white solid, 0. 11g, 68%; R_f 0.71 (1:1/Hexanes: EtOAc); ^{1}H NMR (DMSO-d_6, 400MHz): δ = 7.78 (m, 1H, Ar-H), 7.66 (m, 1H, Ar-H), 7.25 (m, 2H, Ar-H), 7.12 (m, 6H, Ar-H), 7.03 (m, 6H, Ar-H), 5.92 (s, 2H, -CH_2), 5.45 (s, 2H, -CH_2); ^{13}C NMR (DMSO-d_6, 100MHz) δ 163.0, 162.8, 160.6, 160.4, 145.9, 142.9, 138.1, 135.6, 134.9, 134.9, 133.4, 133.4, 129.0, 128.9, 128.8, 128.7, 127.8, 127.3, 123.9, 123.8, 123.1, 121.8, 120.9, 120.0, 116.1, 116.0, 115.7, 115.5, 111.7, 111.5, 106.1, 79.7, 47.3, 46.7. **HRMS**: (ESI) *m/z* calculated for $C_{29}H_{22}N_3[M+H]^+$ 414.1965, observed 414.1966.

2-(1-benzyl-1H-indol-2-yl)-1-(cyclopropylmethyl)-1H-benzo[d]imidazole (77a), a white solid, 0.14 g, 62%; R_f 0.81 (1:1/Hexanes: EtOAc); ^{1}H NMR (DMSO-d_6, 400MHz): δ = 7.66 (m, 2H, Ar-H), 7.30 (m, 7H, Ar-H), 7.10 (m, 6H, Ar-H), 5.81 (s, 2H, -CH_2), 4.05 (d, *J*=6.6 Hz, 2H, -CH_2) 1.33 (m, 1H, -CH), 0.45 (m, 4H, $(CH_2)_2$); ^{13}C NMR (DMSO-d_6, 100MHz) δ 146.4, 142.9, 137.2, 136.8, 128.6, 127.6, 123.5, 123.0, 122.7, 121.5, 120.2, 119.1, 112.4, 111.4, 106.7, 49.1, 47.7, 29.7, 11.3, 4.4. **HRMS**: (ESI) *m/z* calculated for $C_{26}H_{24}N_3[M+H]^+$ 378.1965, observed 378.1968.

2-(1-(cyclopropylmethyl)-1H-indol-2-yl)-1-methyl-1H-benzo[d]imidazole (77b)**,** a white solid, 0.16 g, 66 %; R_f 0.53 (1:1/Hexanes: EtOAc); ^{1}H NMR ($CDCl_3$, 400MHz): δ = 7.66 (m, 2H, Ar-H), 7.56 (d, *J*=7.4 Hz, 1H, Ar-H), 7.48 (m, 1H, Ar-H), 7.24 (m, 4H, Ar-H), 7.05 (m, 1H, Ar-H), 6.86 (s,1H, Ar-H), 4.53 (d, *J*=6.6 Hz, 2H, -CH_2), 3.97 (s, 3H, N-CH_3), 1.33 (m, 1H, -CH), 0.35 (m, 4H, $(CH_2)_2$); ^{13}C NMR ($CDCl_3$, 100MHz) δ 146.6, 142.9, 137.9, 135.8, 127.6, 127.4, 123.1, 123.1, 122.6, 121.3, 120.2, 120.1, 110.5, 109.8, 106.2,

48.3, 31.4, 11.8, 3.6. **HRMS** (ESI) *m/z* calculated for $C_{20}H_{20}N_3[M+H]^+$ 302.1652, observed 302.1652.

1-methyl-2-(1-(prop-2-ynyl)-1H-indol-2-yl)-1H-benzo[d]imidazole (77c), a white solid, 0.11 g, 84 %; R_f 0.71 (1:1/Hexanes: EtOAc); ^{1}H NMR (DMSO-d_6, 400MHz): δ = 7.66 (m, 2H, Ar-H), 7.56 (d, *J*=7.4 Hz, 1H, Ar-H), 7.48 (m, 1H, Ar-H), 7.24 (m, 4H, Ar-H), 7.05 (m, 1H, Ar-H), 6.86 (s,1H, Ar-H), 5.56 (s, 2H, -CH_2), 4.00 (s, 3H, N-CH_3), 2.21 (s, 1H, -CCH); ^{13}C NMR (DMSO-d_6, 100MHz) δ 145.9, 142.9, 137.8, 135.9, 127.5, 127.2, 123.8, 123.3, 122.7, 121.5, 120.9, 120.1, 110.7, 109.8, 106.9, 78.8, 72.3, 33.9, 31.7. **HRMS** (ESI) *m/z* calculated for $C_{19}H_{16}N_3[M+H]^+$ 286.1339, observed 286.1352.

2-(1-methyl-1H-indol-2-yl)-1-(prop-2-ynyl)-1H-benzo[d]imidazole (77d), a white solid, 0.11 g, 71 %; R_f 0.73 (1:1/Hexanes: EtOAc); ^{1}H NMR (DMSO-d_6, 400MHz): δ = 7.66 (m, 2H, Ar-H), 7.56 (d, *J*=7.4 Hz, 1H, Ar-H), 7.48 (m, 1H, Ar-H), 7.24 (m, 4H, Ar-H), 7.05 (m, 1H, Ar-H), 6.86 (s,1H, Ar-H), 5.27 (s, 2H, -CH_2), 4.01 (s, 3H, N-CH_3), 3.57 (s, 1H, -CCH); ^{13}C NMR (DMSO-d_6, 100 MHz) δ 145.6, 142.9, 142.9, 138.7, 135.1, 127.9, 127.1, 123.7, 123.2, 121.6, 120.7, 119.9, 111.4, 111.0, 105.3, 79.2, 76.6, 34.8, 31.9. **HRMS** (ESI) *m/z* calculated for $C_{19}H_{16}N_3$ $[M+H]^+$ 286.1339, observed 286.1352.

3.2 Cell culture

HeLa (cervical cancer), A549 (lung cancer), HepG2(liver cancer), MCF-7 (human breast cancer), and MDAMB231 (triple negative breast cancer) cell lines in which were cultured in air-jacketed humidified incubator at 37 °C with 5% CO_2 in DMEM high glucose media supplemented with 10% FBS, 1% penicillin-streptomycin. 1000 cells per well in 96-well

plates were plated and then compounds were added to each well at indicated concentrations with carrier DMSO and incubated for 72 hours followed by MTT assay.

3.3. Cell viability determination (MTT assay)

The effect of the synthesized compounds on cellular viability was evaluated using the tetrazolium based calorimetric assay using 3-(4,5-dimethylthiazol-2-yl)-2,5-diphenyltetrazolium bromide (MTT, Acros Organics) dye on five different cancer cell lines HepG2, HeLa, MCF-7, MDA-MB231 and A549. MTT assay measures the activity of cellular NAD(P)H-dependent oxidoreductase enzymes reflecting the number of viable cells [190]. Briefly, cells were plated in sterile 96-well cell culture plates and allowed to reach ~70% confluency. Cells were then treated with benzimidazole derivatives. After 48 or 72 h of treatment, 0.05% v/v MTT dye was added and cells were incubated at 37 °C for 3-4 h. Formazan crystals formed from the reduction of MTT dye were dissolved in DMSO and the absorbance [191,192] was measured at 570 nm using the SpectraMax M5e plate reader (Molecular Devices).

3.4. Apoptosis / necrosis assay

A fluorescence dye-based apoptosis / necrosis assay was used to assess the mechanism of benzimidazole-induced cell death. This assay employs HO-33342 (HO), a DNA-binding dye that permeates healthy cells and propidium iodide (PI), a dye that can only penetrate cells with damaged membranes (necrotic cells). At the end of drug treatments for 24 h, HeLa cells were incubated with PI (25 µg/mL) for 10 min in the dark. Next, cells were washed with PBS and incubated with HO dye (11.25 µg/mL). Images were taken immediately using the EVOS FL Auto Imaging System (Thermo Fisher Scientific). The

percentage of apoptotic cells were determined by the number of bright HO-stained cells as a fraction of total HO-stained cells whereas PI-stained cells represent total necrotic cells.

3.5 Western blot analysis

HeLa cells treated with benzimidazole derivatives for 48 h were lysed in modified RIPA buffer (50 mM Tris pH 8.0, 150 mM NaCl, 1% v/v NP40, 0.5% w/v deoxycholate, 0.1% w/v SDS, 10 % v/v glycerol, 10 mM NaF, 0.4 mM EDTA) with protease inhibitors (Sigma-Aldrich). Lysates were collected using a scraper, transferred to microcentrifuge tubes, and cleared by centrifugation at 10,000g for 10 min. Next, Laemmli sample buffer containing SDS and β-mercaptoethanol was added and the samples were denatured by heating them at 95 °C for 10 min. Subsequently, samples were separated on polyacrylamide gels and transferred to PVDF membrane and processed for Western blot analysis with chemiluminescence detection. Images were obtained using Azure biosystems c500 imager and analyzed using ImageJ 1.8.0 software.

3.6 Human topoisomerase II assay

Human Topoisomerase II (topo II) activity assay was performed according to the protocol provided by the manufacturer (TopoGen). Briefly, the total reaction volume was fixed at 20 µL. For preparation of one complete reaction, 4 µL of a 1:1 mixture of buffer A (0.5 M Tris-HCl, pH 8, 1.5 M NaCl, 0.1M $MgCl_2$, 5 mM dithiothreitol, 300 µg/mL BSA) and Buffer B (20 mM ATP) were added to 14.75 µL of dH_2O and 1 µL of kinetoplast DNA substrate. Finally, 1 µL of benzimidazoles was added followed by topo II (2 units). After 45 min of incubation at 37 °C in a water bath, the reactions were stopped by the addition of 4 µL of stop buffer (5% sarkosyl, 0.0025% bromophenol blue, 25% glycerol). Next,

12.5 µL of a 125 µg/mL solution of proteinase K from *Tritirachium album* (Sigma Aldrich) was added to degrade the topoisomerase II from the decatenated DNA products. After an additional 15 min of incubation at 37 °C in a water bath, the reactions were analyzed on a 1% agarose gel by running at 120 V for 30 min in TAE buffer (40 mM Tris base, 1.1% glacial acetic acid, 20 mM disodium EDTA dihydrate). Gels were stained with SYBR Safe DNA gel stain (Invitrogen) and photographed under UV illumination using a c500 Azure Biosystems reader.

3.7 Materials for the BMP project

C2C12 mouse myoblast cells were obtained from American Type Culture Collection (ATCC®, Manassas, VA, USA; ATCC® CRL-1772). Dulbecco's Modified Eagle's Medium (DMEM), Penicillin/Streptomycin/Glutamine solution (PSG), Penicillin/Streptomycin solution (PS), 0.25% Trypsin-EDTA were purchased from Gibco by Life Technologies (Gaithersburg, MD, USA). Fetal Bovine Serum (FBS) was obtained from Atlanta Biologicals (Flowery Branch, GA, USA). Vascular Cell Basal medium, Endothelial Cell Growth Kit – BBE, Trypsin/ EDTA solution for Primary cells, Trypsin Neutralizing Solution were obtained from ATCC (Manassas, VA, USA). Acridine Orange/Propidium Iodide stain was purchased from Logos Biosystem (Annandale, VA, USA). Recombinant BMP7 was purchased from R&D Systems (Minneapolis, MN, USA). TGX Fast Cast Acrylamide gel kit (12%), 4X Laemmli Sample Buffer, 10X Tris/Glycine/SDS buffer (Running Buffer) and Precision Plus Protein Standard were obtained from Bio-Rad Laboratories (Hercules, California, USA). Amersham™ Protran™ 0.2 µm Nitrocellulose membrane was obtained from GE Healthcare Life Sciences (Pittsburgh, PA, USA). Bovine Serum Albumin (30% BSA solution) was from Alfa Aesar

(Ward Hill, MA, USA). Non-fat dry milk and Goat anti-rabbit IgG-HRP: sc-2004 were obtained from Santa Cruz Biotechnology, Inc. (Dallas, TX, USA). GeneTex Trident Pico Western HRP Substrate solutions for western blot imaging were bought from GeneTex (Irvine, CA, USA). Ponceau S solution, Poly-D-Lysine hydrobromide (PDL) and Tris-EDTA buffer solution were procured from Sigma Aldrich (St. Louis, MO, USA). Paraformaldehyde stock solution (16%) was from Electron Microscopy Sciences (Hatfield, PA, USA). Cy3-goat anti-rabbit IgG was obtained from Jackson ImmunoResearch Laboratories (West Grove, PA, USA). Vectashield Mounting Medium with DAPI was purchased from Vector Laboratories, Inc. (Burlingame, CA, USA). RealTime-Glo™ MT cell Viability Assay kit was purchased from Promega Corporation (Madison, WI, USA). Phospho-Smad1/ 5(S463/465)/ 9(S465/467) rabbit monoclonal antibody (#13820S), Smad1 (D5907) XP® rabbit monoclonal antibody (#6944), Phospho-Akt (Ser473) (D9E) XP® rabbit monoclonal antibody (#4060), Akt (pan) (C67E7) rabbit monoclonal antibody (#4691), and Cell lysis Buffer (10X) were obtained from Cell Signaling Technology (Danvers, MA, USA). The phospho-Smad 1/5/8 antibody, CU503AB rabbit polyclonal antibody was generously provided by the Thomas Jessell Laboratory; HHMI (Columbia University, NY, USA).

3.8 Cell culture maintenance – C2C12 cells

C2C12 cells were cryopreserved in liquid nitrogen in Freezing Medium (Gibco by Life Technologies, city, state, co). When required, cells were thawed and maintained in Complete Growth Media (CGM) which consists of DMEM/ 10% FBS/ 1X PSG in T-75 flasks, incubated at 37°C in 5% CO_2. C2C12 cells were sub-cultured every second day by the following protocol: a) cells were removed from the cell culture incubator and observed

under a microscope to note the confluency of cells and cellular structure; b) the growth medium was aspirated and the cells were washed with room temperature 1X PBS; c) Trypsin-EDTA (5 mL, 0.25%) was added to the flask, incubated for 3 minutes at 37°C to detach the cells and then the flask was examined under the microscope to ensure complete trypsinization of the cells; d) an equal volume of CGM was added to neutralize the trypsin; e) the cell suspension was collected, transferred to a 15 mL conical tube and the cells were pelleted at 1000 rpm for 3 minutes at room temperature; f) the supernatant was aspirated and the cell pellet was resuspended in CGM; g) the concentration of cells was determined using the Luna-FL™ Dual Fluorescence Cell Counter from Logos Biosystem (Annandale, VA, USA); and, finally, h) the cells were seeded at a 1:5 dilution into a fresh T-75 flask and incubated at 37°C in 5% CO_2.

3.9 Determination of cell concentration – C2C12 cells

At the time of the cell pellet resuspension (step (f)), a drop of the cell suspension was transferred to a fresh micro-centrifuge tube to serve as a representative sample. To determine the cell concentration a sample of the cells (18 µL) was mixed with 2 µL acridine orange/propidium iodide stain and 10 µL of this mixture was loaded onto a LUNA cell counting slide. The slide was inserted into the cell counter and the cell concentration and viability was recorded.

3.10 Determining cell viability using MT-Glo assay

C2C12 cells were seeded in a 96-well plate, 100 µL at 5 x 10^5 cells/mL, and incubated overnight in CGM to achieve 80-90% confluence. The medium was replaced with Serum Starvation Medium (SSM) containing DMEM/ 1X PS and the cultures were serum starved

for at least 16 h. The test compounds were prepared in DMEM/PS at the following concentrations: 1 mM, 100 μM, 10 μM, 1 μM, 0.1 μM, 0.01 μM. Cells incubated in the presence of DMEM/PS alone served as a positive control and treatment with 78 ppm Triton X-100 was used as negative control. Following the serum starvation period, the cells were treated with controls or test compounds for 24 h. Next, the MT Glo Cell Viability substrate and NanoLuc® enzyme were diluted in DMEM/PS according to manufacturer's protocol and added to the cells. The plate was then incubated for 30-40 minutes at 37°C, 5% CO_2. Cellular luminescence was measured using the FilterMax F5 Multi-mode Microplate Reader (Molecular Devices, San Jose, CA, USA). Cell viability from three independent experiments with individual experiments carried out in triplet was determined and reported as a percentage of control.

3.11 Treatment of C2C12 cells and preparation of whole cell lysates

C2C12 cells were seeded in 35 mm dishes at 7.5 x 10^4 cells/mL (3 mL) in CGM and incubated overnight at 37°C in 5% CO_2 to reach 70-80% confluence. Next, culture medium was replaced with SSM and incubated for 16-18 hours. After serum starvation, cells were treated with 50 ng/mL BMP7 (positive control) and the indicated concentrations of test compounds for 30 minutes. All samples were diluted in SSM. Following stimulation, the treatment medium was removed, and cultures were washed with ice cold 1X TBS for 2 minutes. The 1X TBS was replaced with 1X Lysis Buffer supplemented with 1vmM PMSF (phenylmethylsulfonyl fluoride) and incubated on ice for 10 minutes. The cells were scraped, collected into microcentrifuge tubes and incubated on ice for an additional 15 minutes to ensure complete cell lysis. The lysed cells were centrifuged at 15,000 rpm for

20 minutes at 4°C. The supernatant (whole cell lysate) was transferred to a fresh microcentrifuge tube and stored at -80°C.

3.12 Determination of Total Protein Concentration: Protein Assays

The Amido Schwarz TCA precipitation method was used to estimate the amount of total protein in the whole cell lysates. First, whole cell lysates were diluted 1:100 in dH_2O and total soluble protein was precipitated using 60% TCA (Trichloroacetic acid) and 1 M Tris/1% SDS. Precipitated protein was collected on nitrocellulose membranes (Millipore) and stained with Amido Black (Sigma) reagent. Stained protein was eluted from the membranes using Elution Buffer (1 M NaOH/0.5 M EDTA/Absolute ethanol). Absorbance of the eluted samples was measured at 630 nm using the Eppendorf BioSpectrometer (Lake Forest, CA, USA). The protein concentration in the whole cell lysates was determined using a BSA standard curve.

3.13 Western Blotting to determine Smad phosphorylation

The samples for Western blot analysis were prepared using 10 µg whole cell lysate in 1X Laemmli sample buffer. Samples were heated at 100°C for 5 minutes, immediately placed on ice for 5 minutes and centrifuged at 9500 rpm for 2 minutes at room temperature. The protein samples along with Precision Plus Protein Standard (5 µL) were loaded on 12% TGX Fast Cast Acrylamide gels. Protein was separated by SDS-PAGE using the Gel Electrophoresis System from Bio-Rad (Hercules, CA, USA) at 200 V. The nitrocellulose membrane (GE Healthcare Life Sciences, Pittsburgh, PA, USA) was pre-incubated in cold 1X Transfer Buffer (10 mM Tris, 2.5 mM glycine, 20% Methanol) for 30 minutes. Next, the separated proteins were transferred at 100 V onto the pre-equilibrated nitrocellulose

membranes. To ensure equal loading of proteins in every lane, the membrane was stained with Ponceau S and subsequently washed out with 1X TBS (3X). Non-specific binding sites were blocked by incubation of the membranes in BSA blocking buffer (5% BSA, 0.1% Tween 20, 1X TBS) for 30 minutes followed by incubation overnight at 4^{o}C with the desired primary antibody diluted in BSA blocking buffer. Next, the membranes were washed with 1X TBST (0.1% Tween 20/TBS) for 15 minutes (3X). Membranes were then probed with a HRP-conjugated secondary antibody diluted in milk blocking buffer (5% non-fat milk, 0.1% Tween20, 1X TBS) for 1 hour at room temperature. The blots were then washed again with 1X TBST for 15 minutes (3X). The blots were developed using Trident Pico Western HRP substrate solutions and analysed by capturing the chemiluminescent signal using the Omega Lum™ G Imaging System (San Francisco, CA, USA). Quantification of the western blots was carried out using ImageJ (Image Processing and Analysis in Java 1.8.0_112) developed at NIH.

CHAPTER IV. RESULTS AND DISCUSSION

4.1 *O*-(benzotriazole-1-yl)-*N*,*N*,*N'*,*N'*-tetramethyluronium hexafluorophosphate (HBTU) Promoted Synthesis of Benzimidazoles

Our goal is to develop a simple and functional group tolerant method to synthesize benzimidazoles. As the first step, we synthesized a valine derived amide precursor (**15**) to explore a suitable mild reaction condition for the synthesis of benzimidazoles. Compound **15** was synthesized using commercially available Boc-Val-OH and *o*-diaminobenzene via a standard peptide coupling protocol. Then, we proceeded to screen various mild conditions to perform a dehydrative cyclization of the amide **15** into the corresponding benzimidazole (**Table 4.1**). Our initial attempts to perform the dehydrative cyclization under a mild basic or acidic condition (**Table 4.1**, entry 2 – 4) failed to yield the desired product. We then realized that carbodiimides are known for their ability to promote oxidation or dehydration.[99,193] Based on this knowledge, we selected several commonly used carbodiimide-based coupling agents, including *N*,*N'*-diisopropylcarbodiimide (DIC), 1-ethyl-3-(3-dimethylaminopropyl) carbodiimide (EDCI), *O*-(1*H*-6-chlorobenzotriazole-1-yl)-1,1,3,3-tetramethyluronium hexafluorophosphate (HCTU) and HBTU to assess the dehydrative cyclization (**Table 4.1**, entry 5 – 9). We discovered that HBTU (1 equiv.) yielded the best conversion of **15** into the corresponding benzimidazole **15a** (**Table 4.1**, entry 7). As part of the exploration, we found that catalytic amount of HBTU (0.3 equiv.) is ineffective in providing the desired product in high yield. This finding suggests that HBTU is promoting the dehydrative cyclization and less likely to be acting as a catalyst. Although DIC, EDCI and HCTU are useful carbodiimide agents for amide formation, these

agents did not afford the desired product. This is perhaps due to the reduced reactivity of these coupling agents towards activating an amide bond.

Table 4.1. Optimization of conditions for the conversion of aryl-amide into benzimidazole.

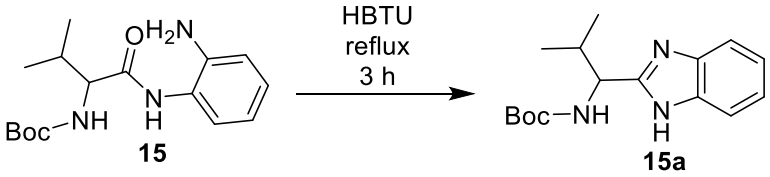

Entry	Reagent	Yield
1	No additives	No reaction
2	DIPEA	No reaction
3	DBU	No reaction
4	HCl	No reaction
5	DIC	No reaction
6	EDCI	No reaction
7	HBTU	94%
8	HCTU	5%
9	PyBOP	94%
10	DIPEA/HCl	No reaction
11	Tetramethylurea	No reaction

We also discovered that (benzotriazol-1-yloxy)-tripyrrolidinophosphonium hexafluorophosphate (PyBOP), a more reactive coupling agent compared to DIC and EDCI, indeed exhibited desirable reactivity towards the dehydrative cyclization. Phosphonium-based coupling agents are useful activating reagents for amide formation and cyclization of thioureas.[194]

4.1.1 One-pot, HBTU promoted strategy for the synthesis of benzimidazoles

With the successful discovery of HBTU as a suitable promotor of benzimidazole synthesis, we quickly realized that the amide precursor was synthesized *via* an HBTU activated process as well. Hence, we attempted a one-pot strategy to form the amide precursor from the parent carboxylic acid and perform the subsequent benzimidazole formation by using 2 equivalents of HBTU. This strategy worked extremely well as a simple one-pot process. Initial formation of aryl-amide occurred with high conversion within 4 hours at room temperature, and then a one-pot HBTU promoted cyclization yielded the desired product in less than 3 hours at refluxing temperature. The two-step, one-pot synthesis worked extremely well, yielding the products in 80 - 99% isolated yield (**Scheme 4.1**).

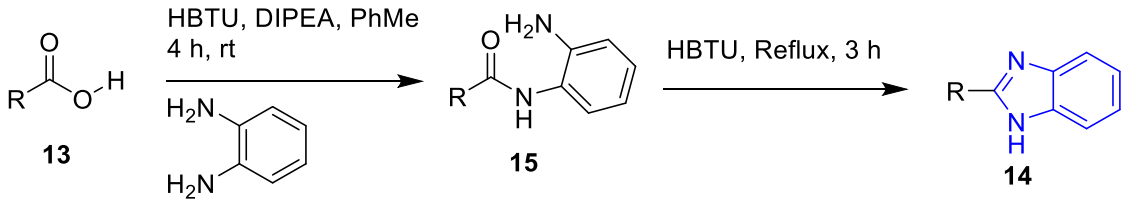

Scheme 4.1 Two-step, one-pot synthesis of benzimidazole derivative.

To further confirm the role of HBTU in this process, we performed a series of control reactions. We observed that none of the components that is part of the reaction mixture, either reagents or by-products from the amidation step promoted the benzimidazole synthesis (**Table 4.1**, entries 10 and 11). These observations led us to conclude that HBTU is in fact the promoter of benzimidazole synthesis, and it is presumably activating the amide bond.

To investigate the versatility of solvents, we performed the benzimidazole synthesis in 1,4-dioxane, dimethylformamide (DMF) or toluene. The coupling was performed in one of these solvents, and subsequently the crude reaction mixture was subjected to cyclization under refluxing temperature in the same solvent. Based on the high yield obtained, all three solvents were suitable for this operation, providing great flexibility with the choice of solvents.

4.1.2 Advantages of HBTU promoted approach in the synthesis of benzimidazoles

In comparison to reported methods for benzimidazole syntheses, HBTU promoted cyclization approach highlights several important improvements and advantages. First, the benzimidazole synthesis is a one pot process and high yielding, where current methods require isolation of the aryl-amide prior to dehydrative cyclization. Second, there is no need to perform the cyclization in the presence of an acid as a co-solvent, which greatly broadens the substrate scope and the functional group tolerability, including various protecting groups found in amino acids and peptides. Third, the reaction works extremely well in three different solvents enabling synthetic flexibility for substrates with limited solubility.

4.1.3 Substrate scope of our HBTU promoted approach

We proceeded to investigate the substrate scope using a small library of commercially available carboxylic acids (**Scheme 4.2**). Boc-Asp-OMe (**40b**) was successfully converted to the beta-benzimidazole derivative (**41b**) in 92% yield, providing a unique non-protein amino acid that is useful for medicinal chemistry. In addition, four different alkyl carboxylic acids (**40c**–**40f**) were converted into the corresponding benzimidazoles (**41c** – **41f**) in high yield. As peptide substrates are of prime interest to medicinal chemists, a Cbz-

protected dipeptide (**40g**) was successfully transformed into the C-terminal benzimidazole derivative (**41g**) in good yield as well. This demonstrates the utility of HBTU promoted method for the synthesis of peptide-based benzimidazoles for drug discovery.

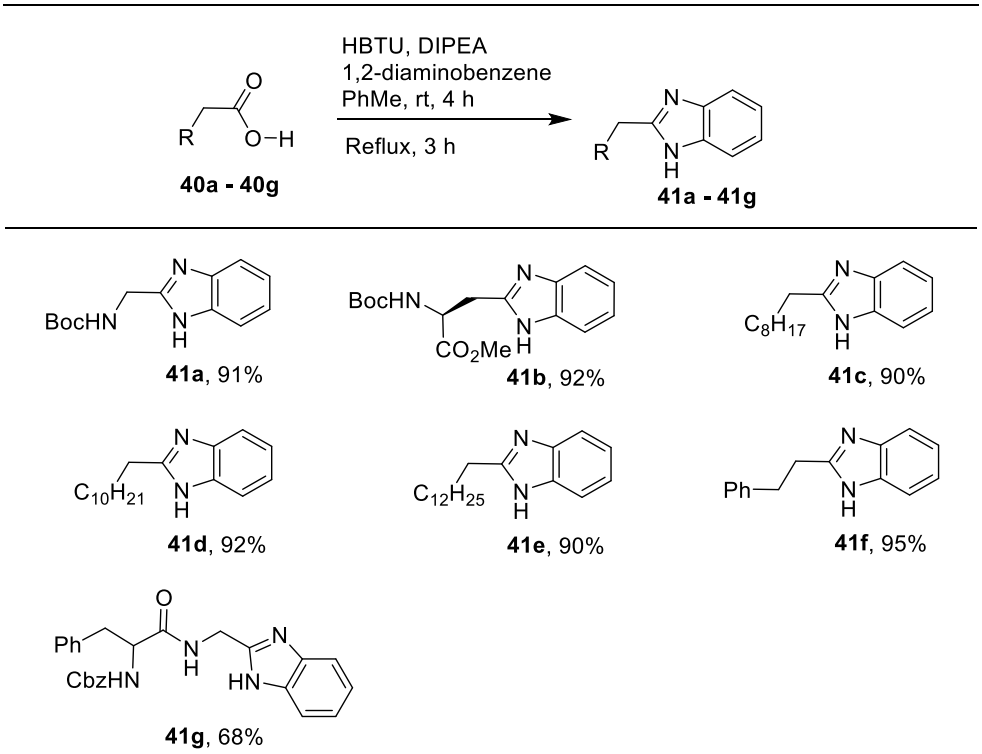

Scheme 4.2 Synthesis of alkyl benzimidazoles.

During our investigation, we realized that indole-2-carboxylic acid is a privileged motif and the corresponding benzimidazole is widely used in drug discovery efforts.[25,195] We successfully synthesized various indole-2-benzimidazoles (**43a**–**43f**), where the aryl ring of the benzimidazole is substituted with different functional groups (**Scheme 4.3**). We envisioned that having halogen substitution on the aryl-ring provides a useful chemical handle for further structure diversification *via* metal-catalyzed cross-coupling reactions. We also observed that electron rich 1,2-diaminobenzene derivatives yielded better yield

than those that are electron deficient. This may be due to change in nucleophilicity of the diaminobenzene.

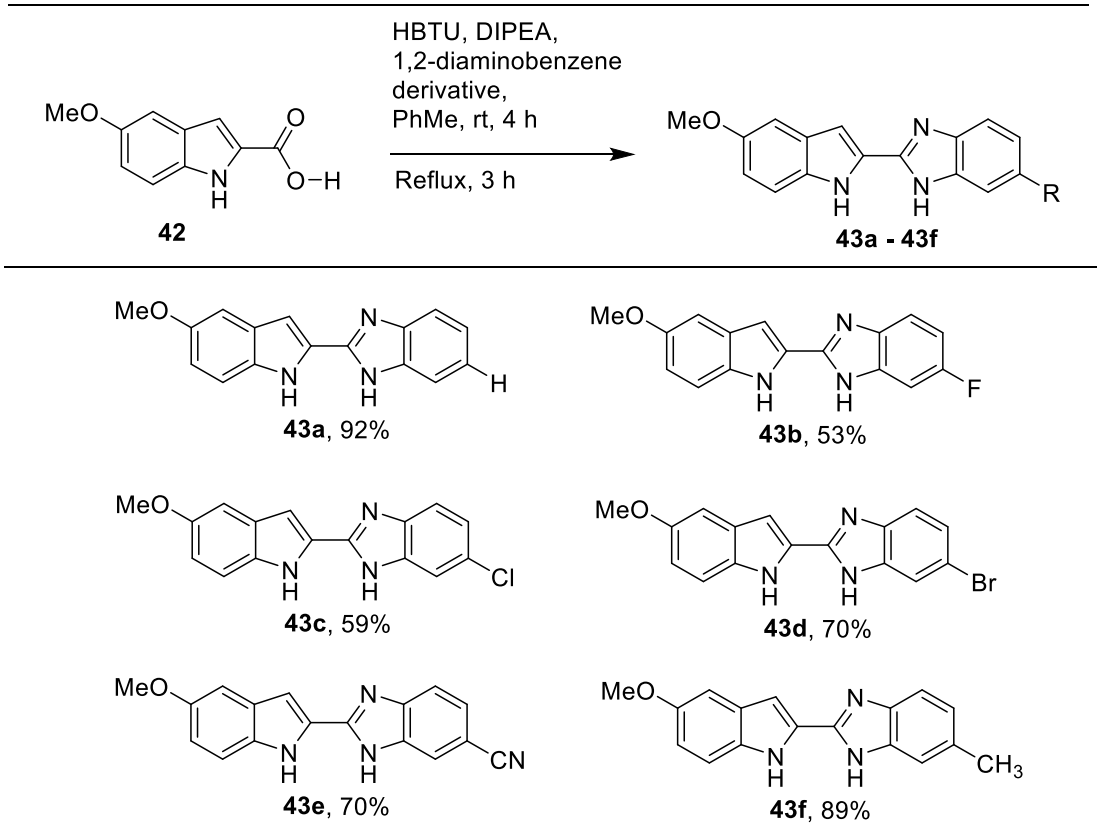

Scheme 4.3. Synthesis of indole-2-carboxylic acid derived benzimidazoles

To further validate the HBTU promoted method, we proceeded to synthesize an extensive library of alpha-amino acid derived benzimidazoles. There are two reasons for this endeavor: (i) we wanted to access a structurally diverse collection of alpha-amino benzimidazoles from commercially available amino acids with suitable protecting groups; and (ii) we envisioned accessing alpha-amino acids precursors for the synthesis of peptide-based benzimidazoles. This library includes thirteen Boc-protected amino acids (**44a** – **44n**,

Table 4.2) and three Cbz-protected amino acids (**48** – **50**, **Figure 4.1**). We reacted all Boc-amino acids with 1,2-diaminobenzene under optimized, one-pot reaction condition, and isolated the desired benzimidazoles (**45a** – **45n**) in excellent yield. We also learned that many side chains protecting groups, including benzyl ether, benzyl thioether, and benzyl esters are stable to the reaction condition. Additionally, the side chain of Boc-Asn-OH (**44l**) required no protecting group to generate the Boc-Asn derived benzimidazole **45l**. It is also interesting to note that compound **45d** is structurally similar to veliparib, a poly(ADP-ribose)polymerase (PARP) inhibitor that is in clinical trials.[138]

Table 4.2 Investigation of substrate scope for the synthesis of amino acid based benzimidazoles.

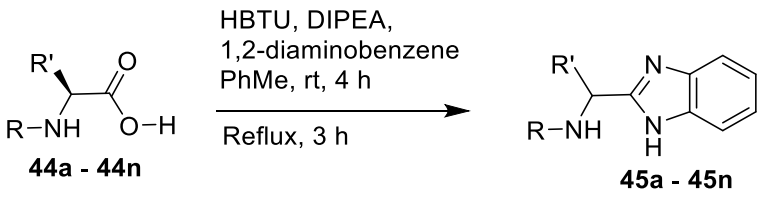

Entry	Amino acid	Product	Yield
1	Boc-Leu-OH (**44a**)	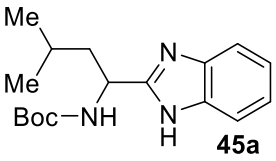	96%
2	Boc-Ileu-OH (**44b**)	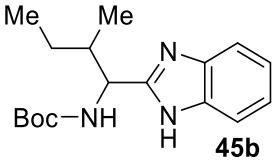	95%
3	Boc-Val-OH (**44c**)	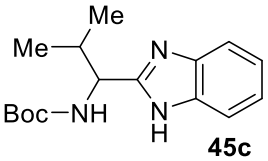	96%

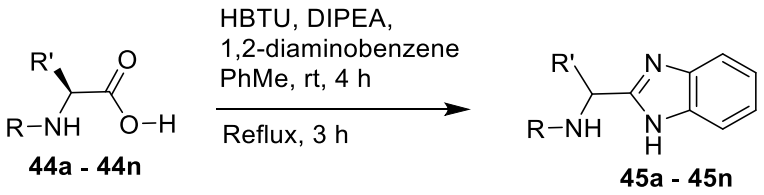

Entry	Amino acid	Product	Yield
4	Boc-Pro-OH (**44d**)	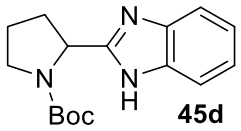 **45d**	99%
5	Boc-Tyr(OBn)-OH (**44e**)	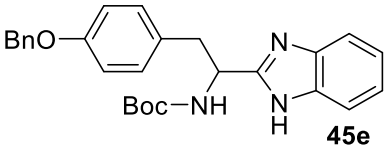 **45e**	84%
6	Boc-Ser(OBn)-OH (**44f**)	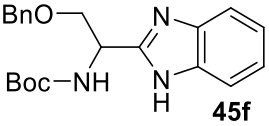 **45f**	84%
7	Boc-Cys(SBn)-OH (**44g**)	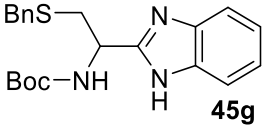 **45g**	99%
8	Boc-Thr(OBn)-OH (**44h**)	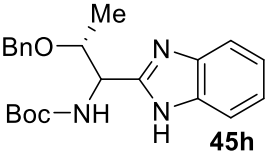 **45h**	94%
9	Boc-Lys(OBn)-OH (**44i**)	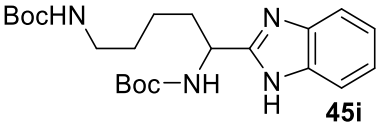 **45i**	99%

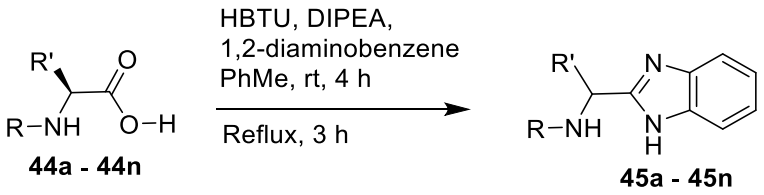

Entry	Amino acid	Product	Yield
10	Boc-Asp(OBn)-OH (**44j**)	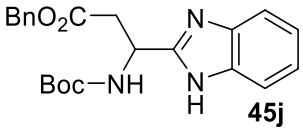 **45j**	90%
11	Boc-Glu(OBn)-OH (**44k**)	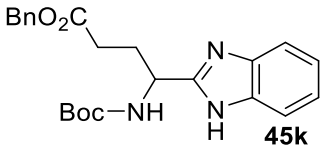 **45k**	80%
12	Boc-Asn-OH (**44l**)	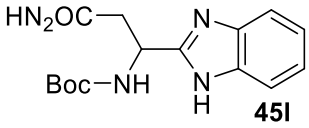 **45l**	96%
13	Boc-Gln-OH (**44m**)	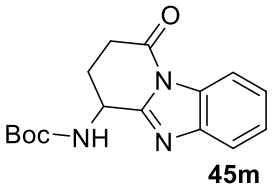 **45m**	96%
14	Boc-Phe-OH (**44n**)	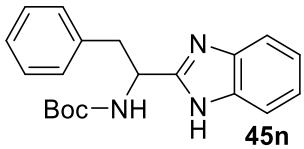 **45n**	99%

One interesting observation was made when Boc-Gln-OH (**44m**) was reacted to form the corresponding benzimidazole. Absence of protecting group on the side chain yielded an interesting tricyclic structure (**45m**). Based on a literature precedent,[196] we propose that the side chain amide underwent a transamidation reaction with the benzimidazole nitrogen,

generating the unique tricyclic product **45m**. Since compound **45m** has an amine handle, and a conformationally distinct tricyclic structure, it could be a useful synthon for medicinal chemistry efforts. We plan to explore the medicinal chemistry potential of benzimidazole **45m**.

We also utilized the HBTU promoted approach for the synthesis of two halogenated analogues of Boc-tyrosine derived benzimidazoles (**46** and **47**), and three *N*-Cbz protected amino acid derived benzimidazoles (**48** – **50**). Using these substrates, we demonstrated that both Boc and Cbz carbamates are tolerated. Additionally, having a halogen handle on the aryl ring of benzimidazole provides a new venue to diversify the benzimidazole core for medicinal chemistry purposes (**Figure 4.1**).

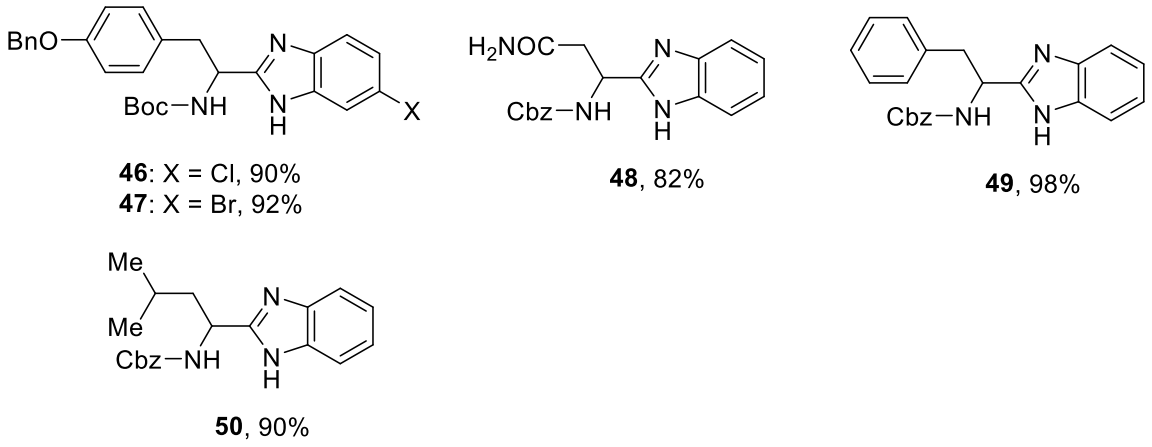

Figure 4.1 Structures of halogenated and *N*-Cbz protected amino acid based benzimidazoles.

It is reported that amino acid derived thiazoles have shown to be potent modulators of P-glycoprotein, which contributes to drug resistance in cancer cells.[197] Since the amino acid benzimidazoles we have generated, including **46**, **47**, **48** and **50** are isosteres of reported

thiazole derivatives, these compounds can be evaluated for potential P-glycoprotein binding affinity, and reversal of anti-cancer drug resistance. The proposed synthetic approach provides convenient entry to prepare and evaluate potentially bioactive P-glycoprotein modulators.

4.1.4 A plausible mechanism for the HBTU promoted synthesis of benzimidazoles

In addition to HBTU (**52**) being an effective coupling agent, we believe that HBTU is playing a very important role in the cyclization process. We propose a plausible mechanistic pathway, which may explain the HBTU-promoted formation of the benzimidazole (**Scheme 4.4**). The intermediate aryl-amide (**51**) is relatively stable, and for it to undergo dehydration, it needs to be activated. We propose that HBTU helps in the activation of amide, where the oxygen atom of the amide reacts with the carbodiimide motif first. Following the attack of the amide oxygen, a molecule of 1-hydroxybenzotriazole (HOBt, **55**) is lost from HBTU. In the subsequent step, the second aryl-amine motif (**54**) reacts to kick-out a molecule of tetramethylurea (**56**) and forms the desired benzimidazole (**14**). Based on LC-MS and ^{1}H-NMR analyses, we confirmed the formation of the key by-products, HOBt (**55**) and tetramethylurea (**56**) during the conversation of amide substrate into benzimidazole. This finding provides experimental support for this mechanistic proposal.

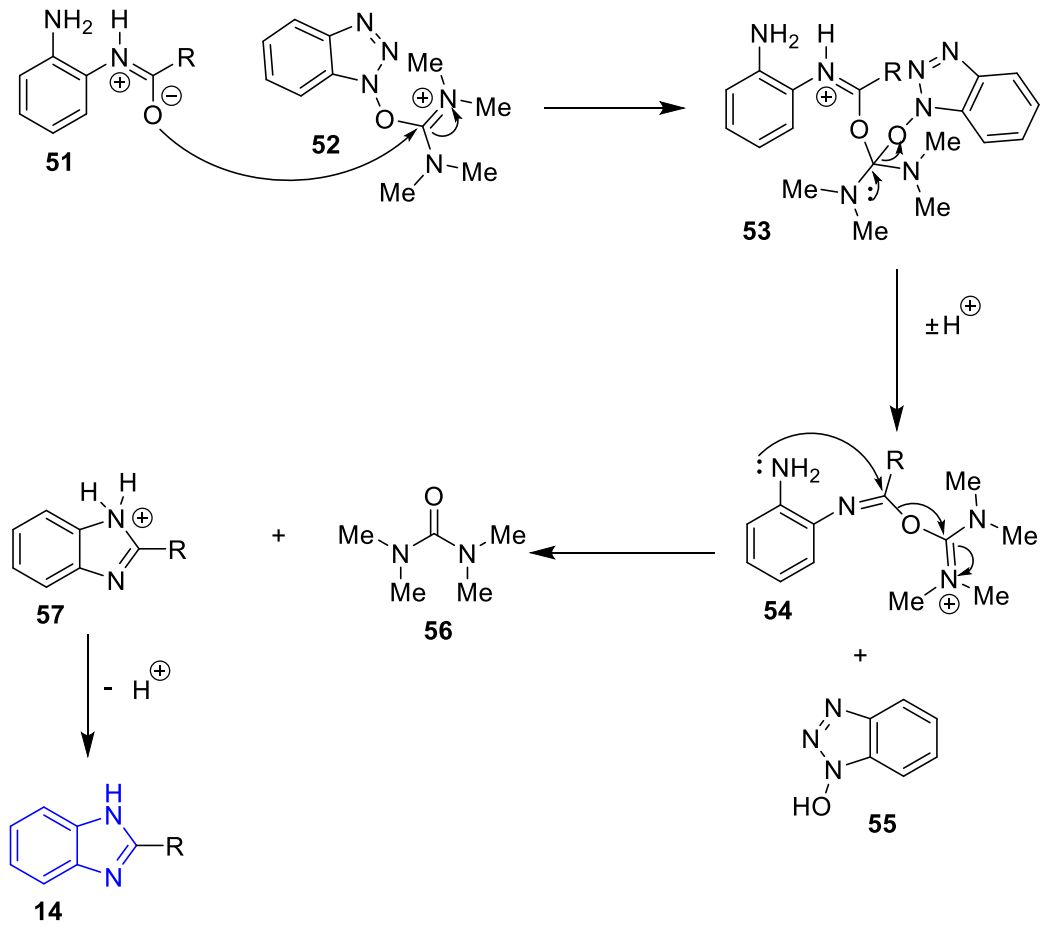

Scheme 4.4 Plausible mechanism of HBTU promoted cyclization.

4.2 A second library of aryl-benzimidazoles synthesized using the synthetic methodology developed in our lab

Using our new synthetic method, we synthesized a second library of benzimidazoles that are highly useful for our medicinal chemistry efforts. During this effort, we utilized the ability of HBTU to perform the dehydrative cyclization of the amide precursor to access the benzimidazoles. Using simple aryl carboxylic acid derived amide precursor **63a-63r** under an optimized condition, we successfully synthesized eighteen structurally distinct benzimidazoles **64a-64r** in high yields (**Figure 4.2**). The presence of electron withdrawing or electron donating groups on the aryl ring didn't have effect on the yield. Nowadays

much attention has been focused on substituted 2-aryl benzimidazoles as therapeutic agents,[198] and with the use of this synthetic methodology, this type of aryl benzimidazoles would be easily accessible.

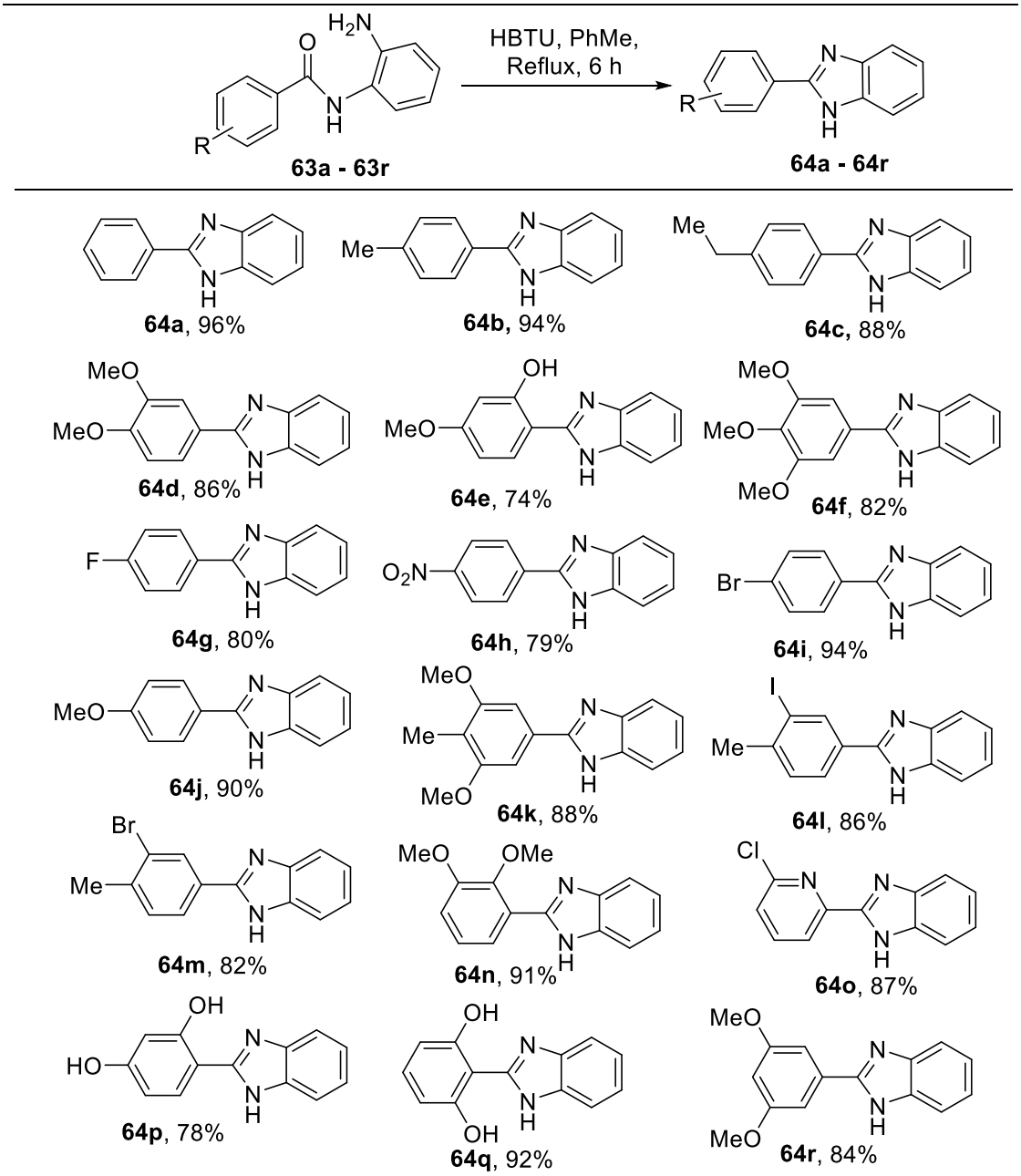

Figure 4.2 Synthesis of aryl-benzimidazoles.

Since indole based benzimidazoles is of great interest to medicinal chemists,[110,199,200] we proceeded to explore substrate scope for the synthesis of this motifs from indole amides. The synthesis of indole based benzimidazoles from indole amide *o*-phenylenediamine substrates (**Figure 4.3**) went on to afford excellent yields, **66a** – **66e**. The amide positions were varied on the indole core structure and these positions didn't influence the yields in the transformation of amide substrates to indole benzimidazoles.

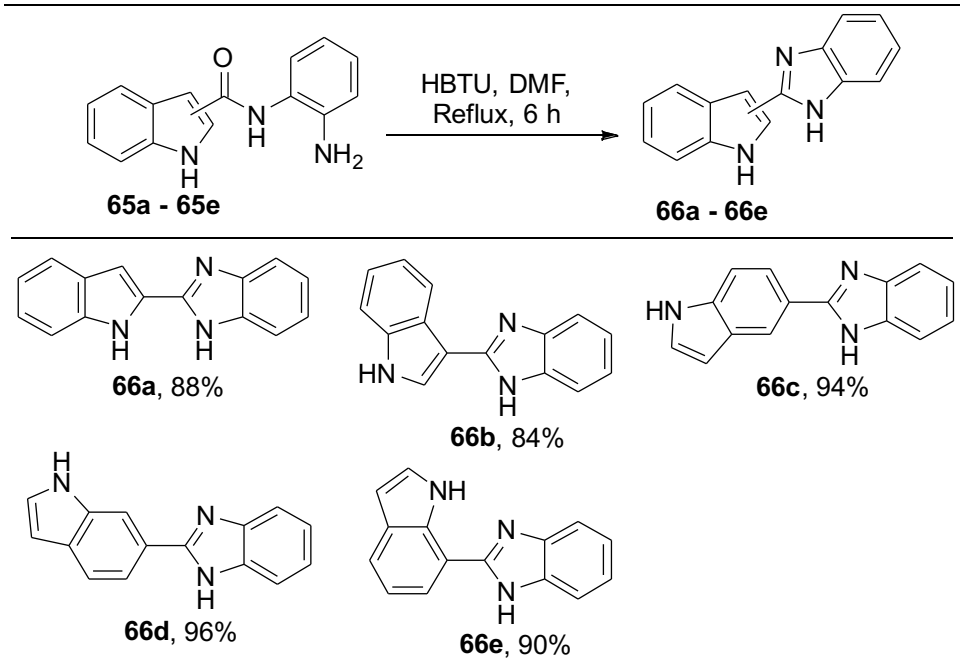

Figure 4.3 Synthesis of indole-based benzimidazoles.

2-substituted benzimidazoles are reported to be pharmacologically active, we investigated the substrate scope for alkyl carboxylic acid derived amide substrates (**Figure 4.4**). The conversion of these substrates to benzimidazoles afforded high yields (**68a** – **68k**). Alkyl chains with various substituents were explored with future investigation of the synthesized compounds as potential therapeutic leads.

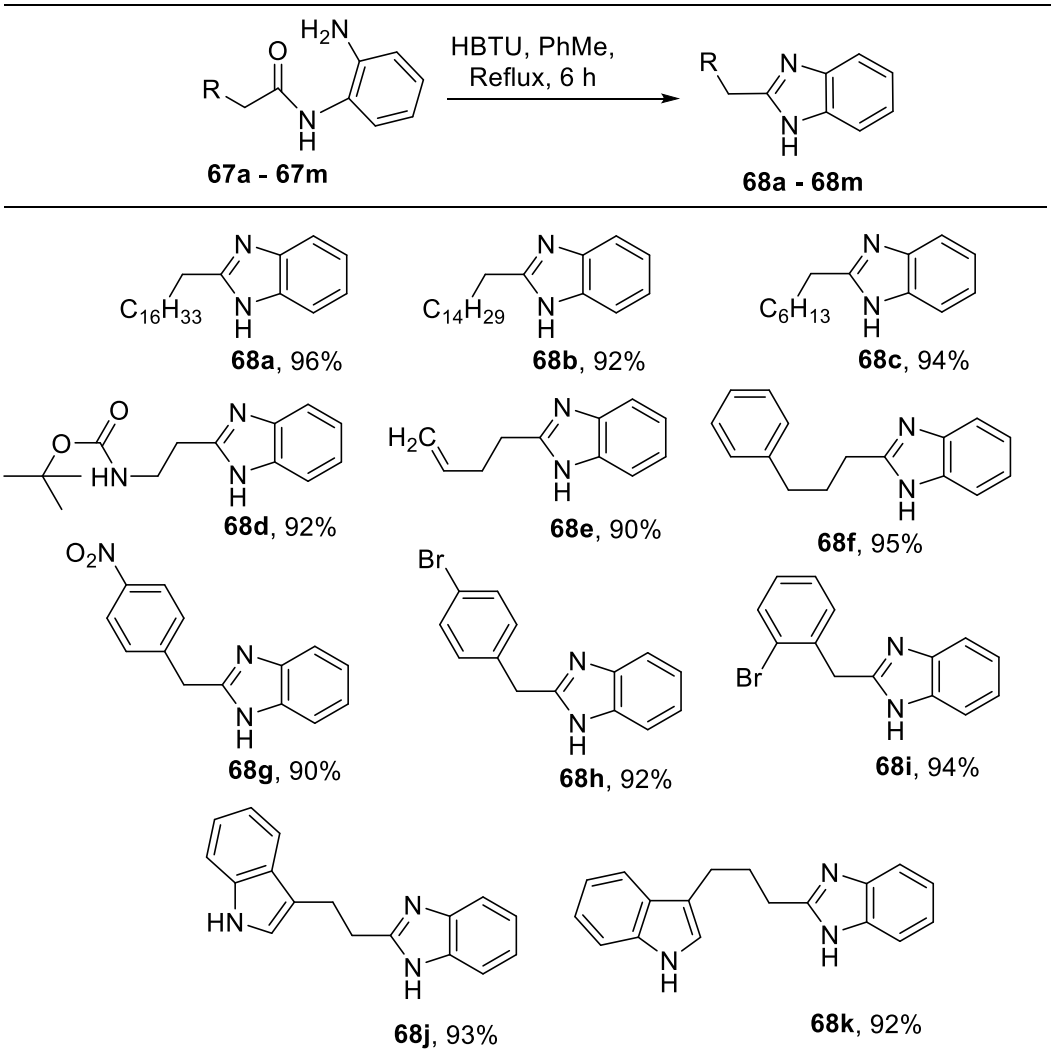

Figure 4.4 Synthesis of benzimidazoles from alkyl-amides.

4.3 A Mild *N*-Alkylation Methodology for the Structure Diversification of Indolyl-Benzimidazoles

We envisioned achieving selective reactivity for the *N*-alkylation based on the pKa differences between the indole and benzimidazole nitrogen in indole-benzimidazole hybrid molecule (**66a**). Our investigation began with identifying a suitable base for the alkylation process. *N*-benzylation was performed to determine the reactivity of 2-indolyl-benzimidazole **66a** (**Table 4.3**). We selected three commonly used organic bases (1,8-Diazabicyclo[5.4.0]undec-7-ene (DBU), triethylamine (TEA) and *N*,*N*-

Diisopropylethylamine (DIPEA)) and four commonly used inorganic bases (potassium carbonate (K_2CO_3), cesium carbonate (Cs_2CO_3), Sodium bicarbonate ($NaHCO_3$), and potassium bicarbonate ($KHCO_3$)) for our study. Our initial screening shows that all inorganic bases screened (**Table 4.3**, entries 5 – 8) are highly effective in selectively promoting the *N*-alkylation of indolyl-benzimidazoles. Under these conditions the alkylation occurred exclusively at the benzimidazole core. From the screening, we observed that all the organic bases (**Table 4.3**, entries 2 – 4) yielded no conversion to **71a**, perhaps due to their inability to deprotonate the benzimidazole or their reactivity towards benzyl bromide. As an additional component of screening, we also found that the reaction worked well in dimethylformamide (DMF) or acetonitrile (CH_3CN).

Table 4.3 Screening of different conditions for the *N*-alkylation.

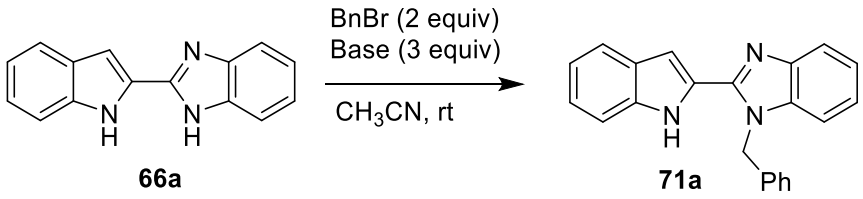

66a 71a

Entry	Base	Yield (%)
1	No base	No reaction
2	DBU	No reaction
3	TEA	No reaction
4	DIPEA	No reaction
5	K_2CO_3	90
6	Cs_2CO_3	92
7	$NaHCO_3$	86
8	$KHCO_3$	85

4.3.1 Substrate scope evaluation of selective *N*-alkylation strategy

Upon identifying a method to selectively alkylate the benzimidazole motif within the indolyl-benzimidazole scaffold, we evaluated the substrate scope of this selective *N*-alkylation strategy. Our initial exploration yielded a small library of *N*-benzyl benzimidazole derivatives (**Scheme 4.5**). Nine different commercially available benzyl bromides were reacted with indolyl-benzimidazole **66a** in the presence of K_2CO_3 (3 equiv.) in CH_3CN. Since a non-aqueous condition is used for this chemistry, we have used 3 equivalents of the base to ensure enough amount is dissolved in the reaction medium for the alkylation chemistry to proceed to completion. It is worthwhile to highlight that even with 3 equivalents of K_2CO_3, the alkylation is highly selective towards the benzimidazole motif, providing preferential reactivity. The benzyl bromides used in this study have either electron withdrawing or electron donating groups at the para-position. We were delighted to see that all benzyl bromides yielded the desired products (**71a** – **71j**) in very high yield (79-92%), and the electronic nature of the aryl ring had little effect on the reactivity.

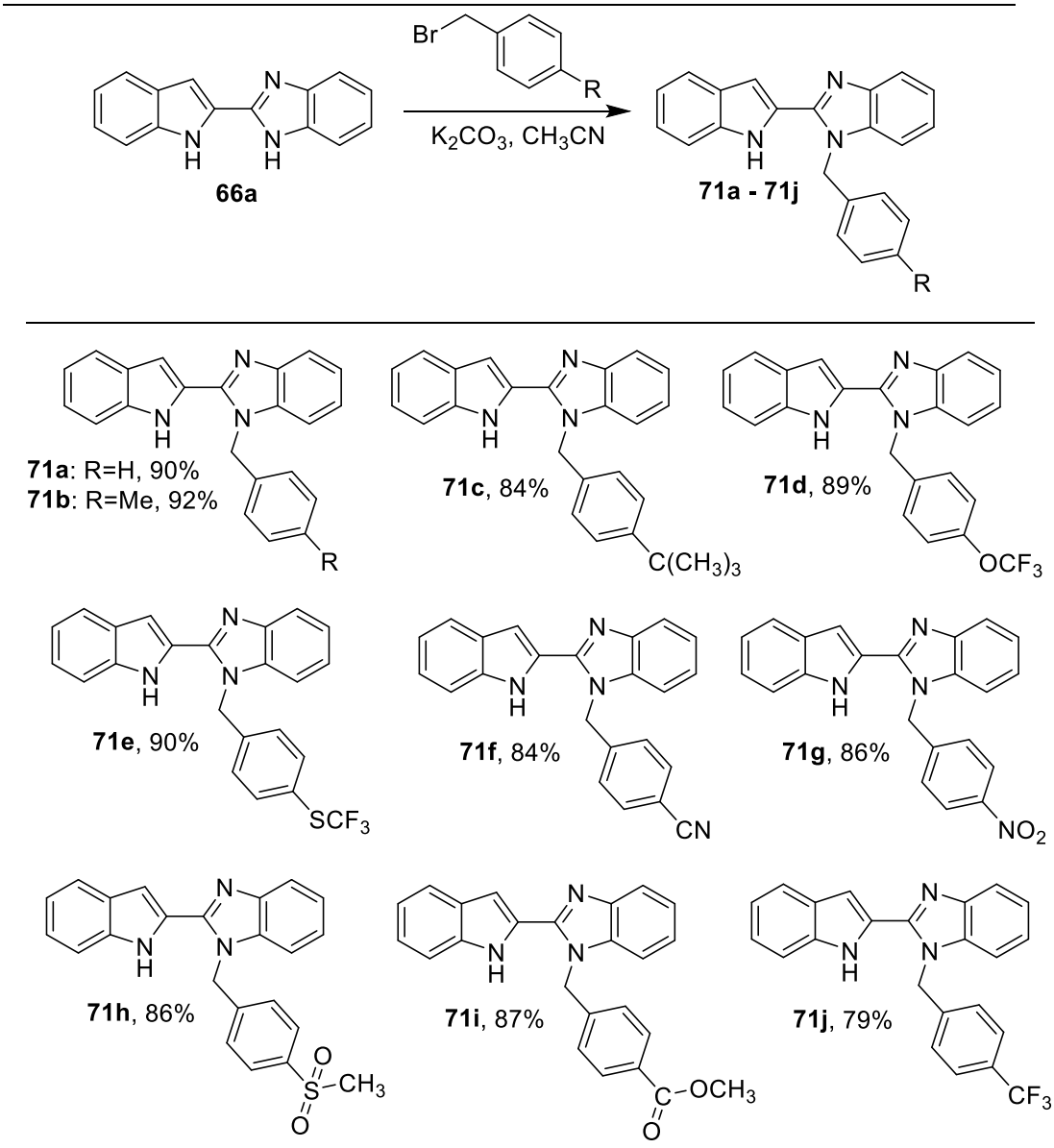

Scheme 4.5 Synthesis of *N*-benzylated derivatives of indolyl-benzimidazole using benzyl bromides.

As a next step, we further evaluated the utility of this method by alkylating **66a** with five different aliphatic bromides (**Scheme 4.6**). Despite their reduced reactivity compared to benzyl halides, we were pleasantly surprised that the alkylation reaction went smoothly to afford the desired products (**72a** – **72f**) in excellent yield (88% - 94%). The alkyl donors vary from a simple allyl group (**72d**) to structurally complex cycloalkyl groups (**72a**, **72b**

and **72c**) and a long aliphatic ether (**72f**). The allylated product (**72d**) is a useful synthon for further derivatization *via* olefin chemistry to generate new analogs for medicinal chemistry.

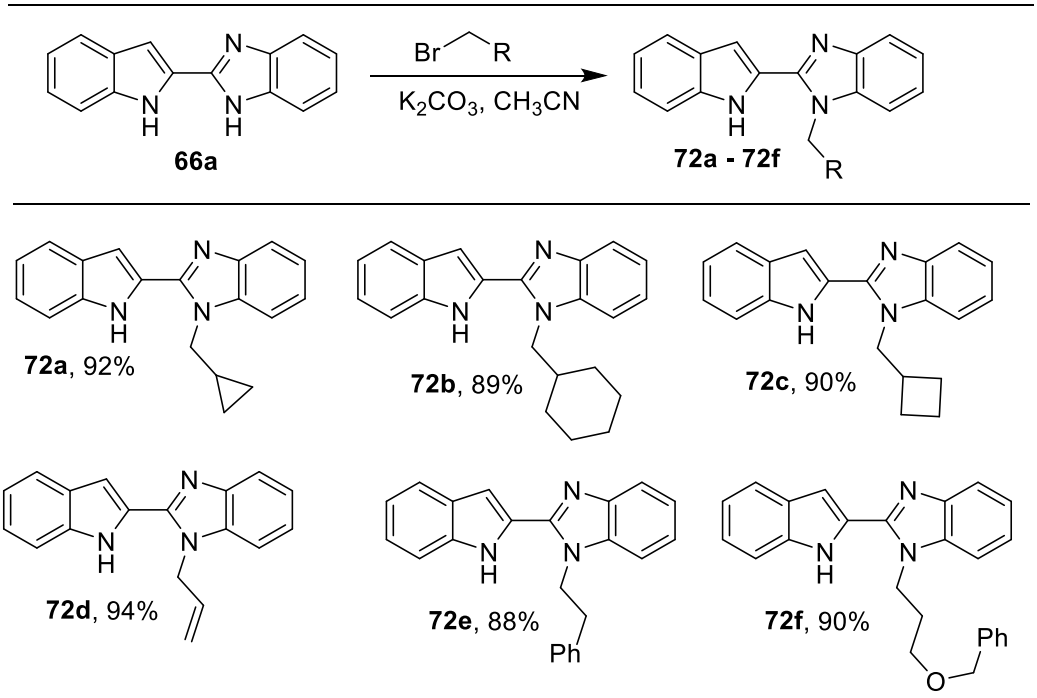

Scheme 4.6 Synthesis of *N*-alkylated derivatives indolyl-benzimidazole using aliphatic bromides.

To study the effect of substitution on the indole-motif, we synthesized a series of alkylated analogs using 5-methoxyindolylbenzimidazole (**43a**) as substrate (**Scheme 4.7**). Modification of the benzimidazole nitrogen of **43a** went smoothly under the optimized condition. Both benzyl-derivatives (**73a** and **73b**) and aliphatic derivatives (**73c**, **73d** and **73e**) afforded the desired product in excellent yield (78-96%). Although the 5-methoxyindole unit is electronically activated in comparison to the unsubstituted indole ring, we did not observe any trace of alkylation of the 5-methoxyindole nitrogen under the

reported condition. This further validates that K_2CO_3 is a very mild and highly selective base for the alkylation of the benzimidazole nitrogen.

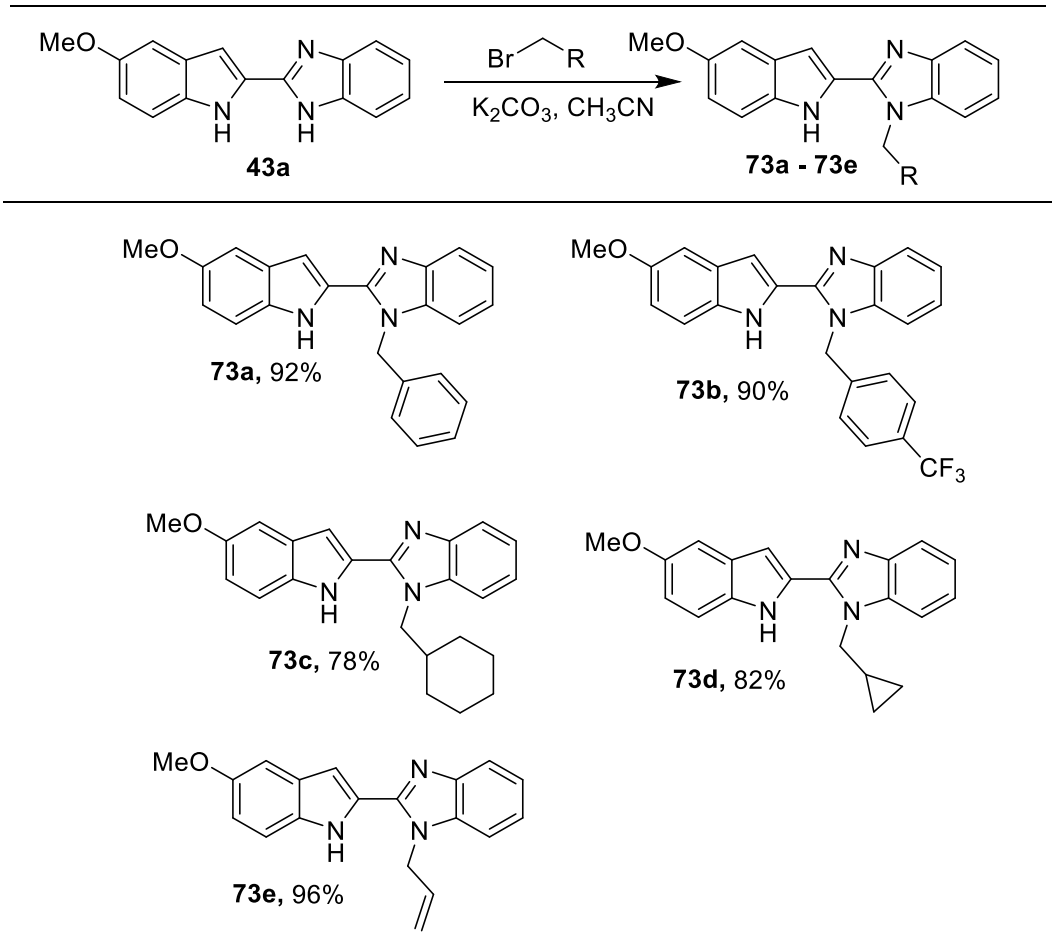

Scheme 4.7 Synthesis of *N*-alkylated derivatives of 5-methoxyindolylbenzimidazole.

4.3.2 Synthesis of symmetrical bis-*N,N*-alkylated 2-indolyl-benzimidazole

With the successful establishment of selective *N*-alkylation of indolyl-benzimidazole, we proceeded to explore a method to alkylate the indole nitrogen. We evaluated the ability of potassium hydroxide (KOH) to assist with the alkylation of **66a**. Since KOH is a relatively stronger base than the carbonate or bicarbonate, the benzylation of **66a** is tested at 0 ˚C to give us a mild reaction condition. With this modified protocol, we successfully alkylated

66a using KOH and alkyl donors in a stepwise fashion (**Scheme 4.8**), and obtained the symmetric, bis-alkylated indolylbenzimidazoles **75a**, **75b**, and **75c** in good yield (68-88%).

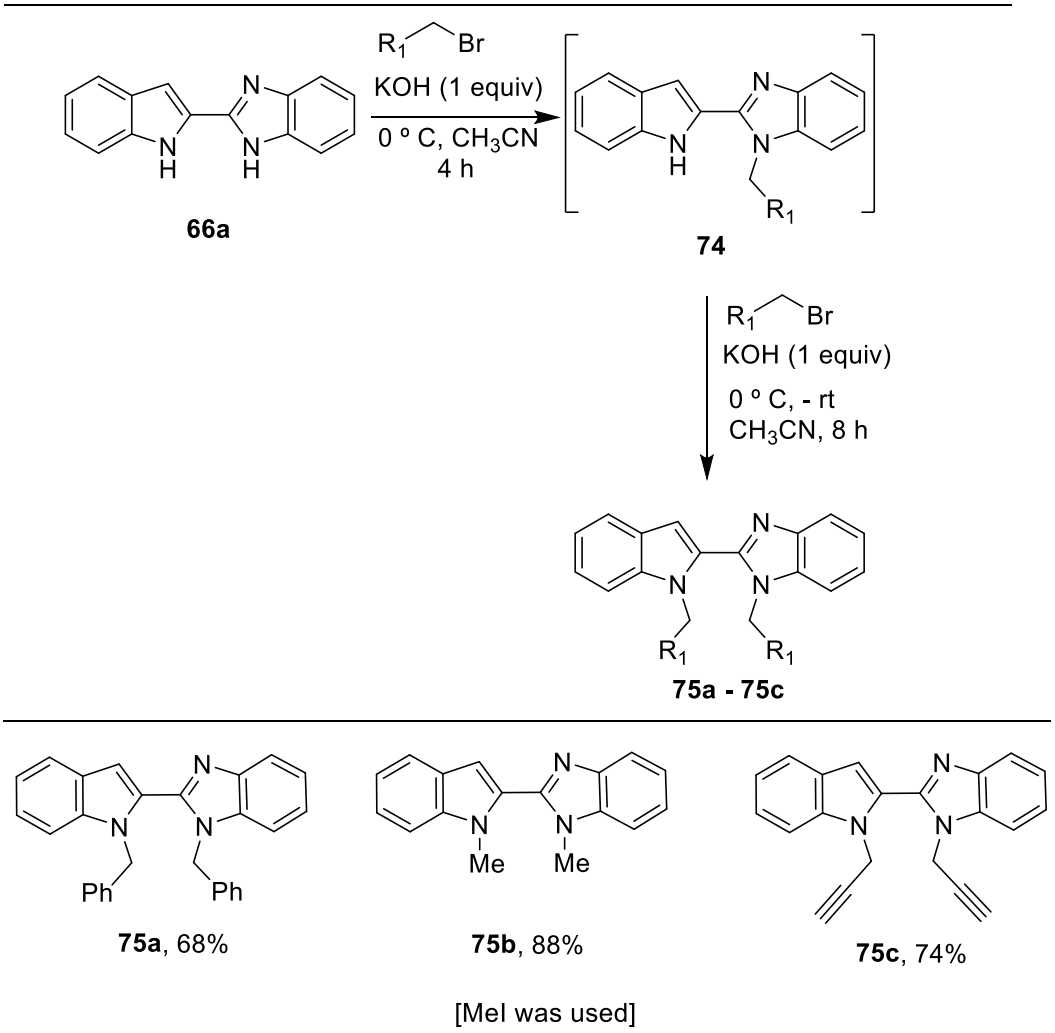

Scheme 4.8 Synthesis of a symmetrically bis-*N,N*-alkylated 2-indolylbenzimidazoles.

To advance the synthetic utility of this strategy, we developed a stepwise, one-pot, selective method to alkylate **66a** using two different alkyl bromide donors. The benzimidazole nitrogen in compound **66a** was successfully alkylated first with an alkyl bromide, and subsequently the indole nitrogen in **66a** was alkylated with a different alkyl bromide, in a

stepwise fashion and one-pot operation (**Scheme 4.9**). Using this strategy, we achieved the selectivity and synthesized asymmetrically alkylated 2-indolylbenzimidazoles **77a** – **77d**. From a medicinal chemistry stance, this approach enables one to quickly diversify the indolyl-benzimidazole core to generate novel analogs for drug discovery efforts.

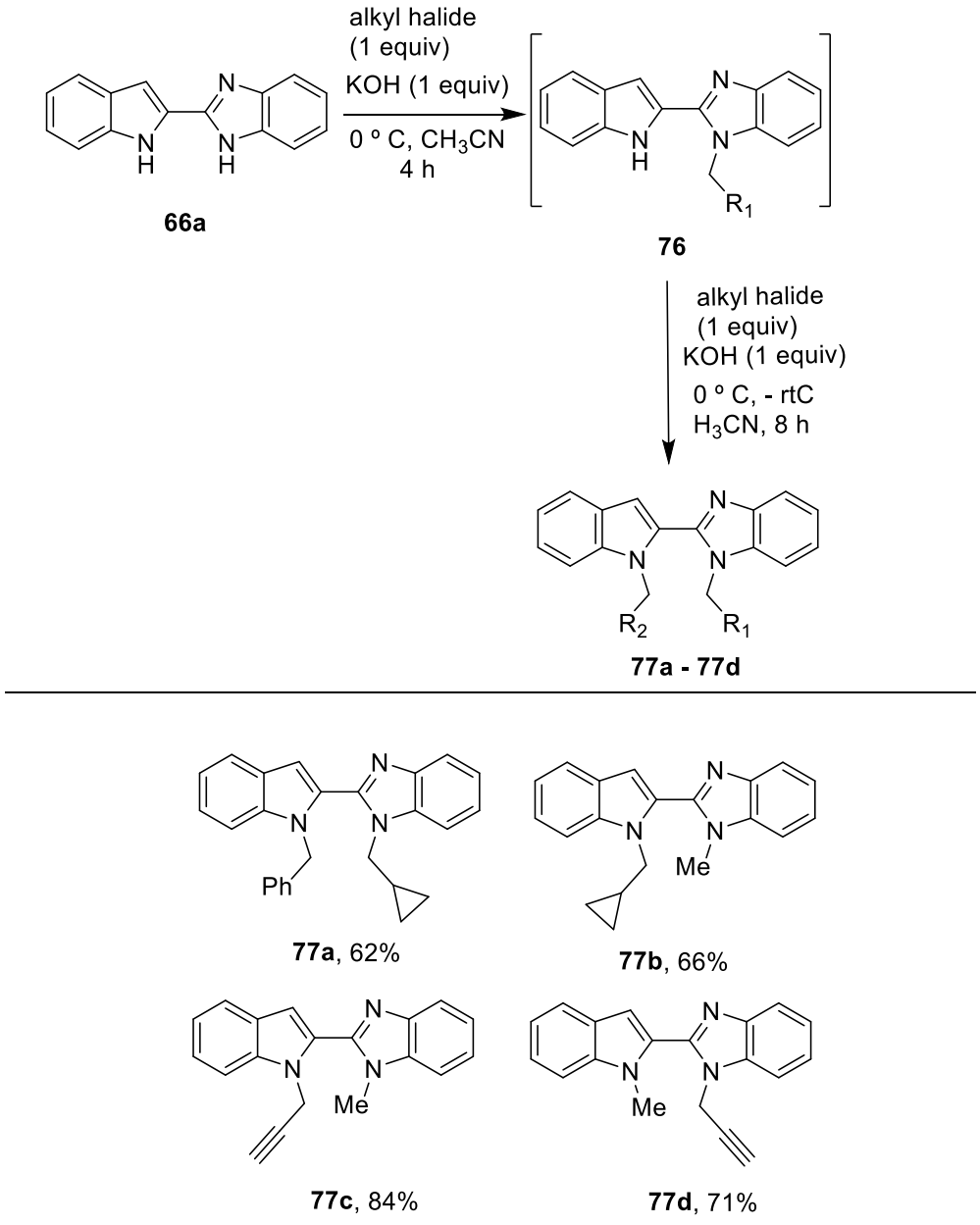

Scheme 4.9 Synthesis of asymmetrically bis-*N,N*-alkylated 2-indolylbenzimidazoles.

4.4 Synthesis of Bis-Benzimidazole derivatives

We used our reported HBTU promoted methodology to synthesize a series of bis-benzimidazoles (**Scheme 4.10**). We used commercially available bis-carboxylic acid containing substrate linkers (**78a** and **78b)** which underwent one pot synthesis to give the corresponding bis-benzimidazole products in good yields (85-93%).

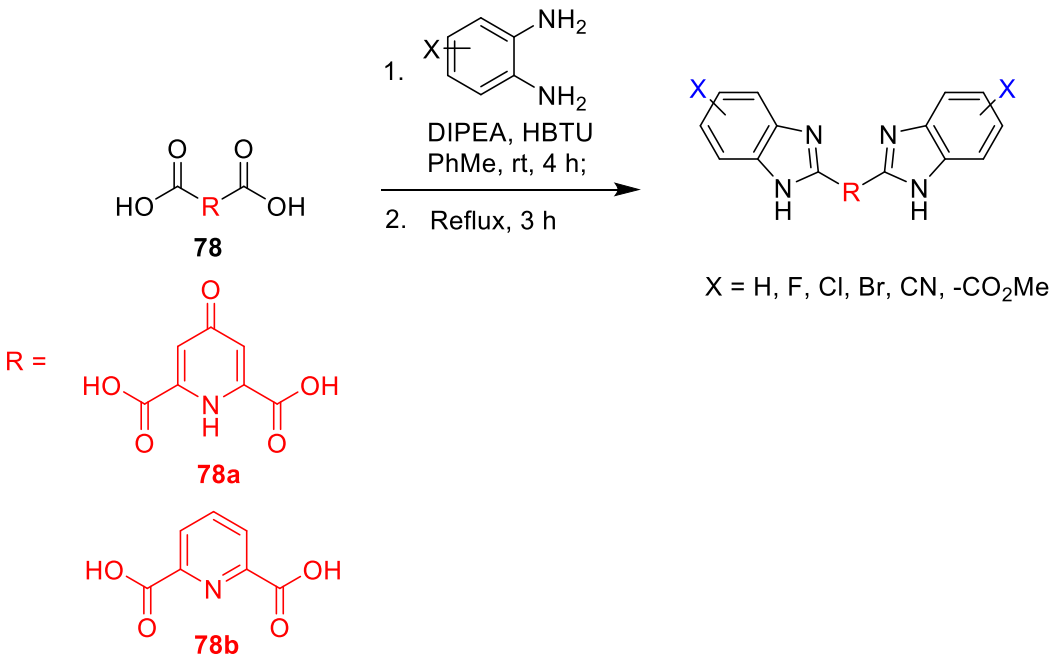

Scheme 4.10 Synthesis of bis-benzimidazole derivatives from different type of bis-dicarboxylic acid linkers and *o*-phenylenediamine derivatives.

We started our first strategy of synthesizing bis-benzimidazole derivatives by taking commercially available chelidamic acid monohydrate **78a** (**Scheme 4.10**), which underwent condensation-dehydration reaction with substituted *o*-phenylenediamine to yield the corresponding bis-benzimidazole derivatives **79a** - **79f** (**Figure 4.5**) in higher yields of 80 – 95%. Having substitution on the benzene rings was to help us in

understanding the effect of these diverse substituent groups in modulating the pharmacological properties of bis-benzimidazole derivatives. It is reported that having substitution on the benzene rings improves the pharmacological activities,[201] and in addition, the substituents used are potential handles for further modifications.

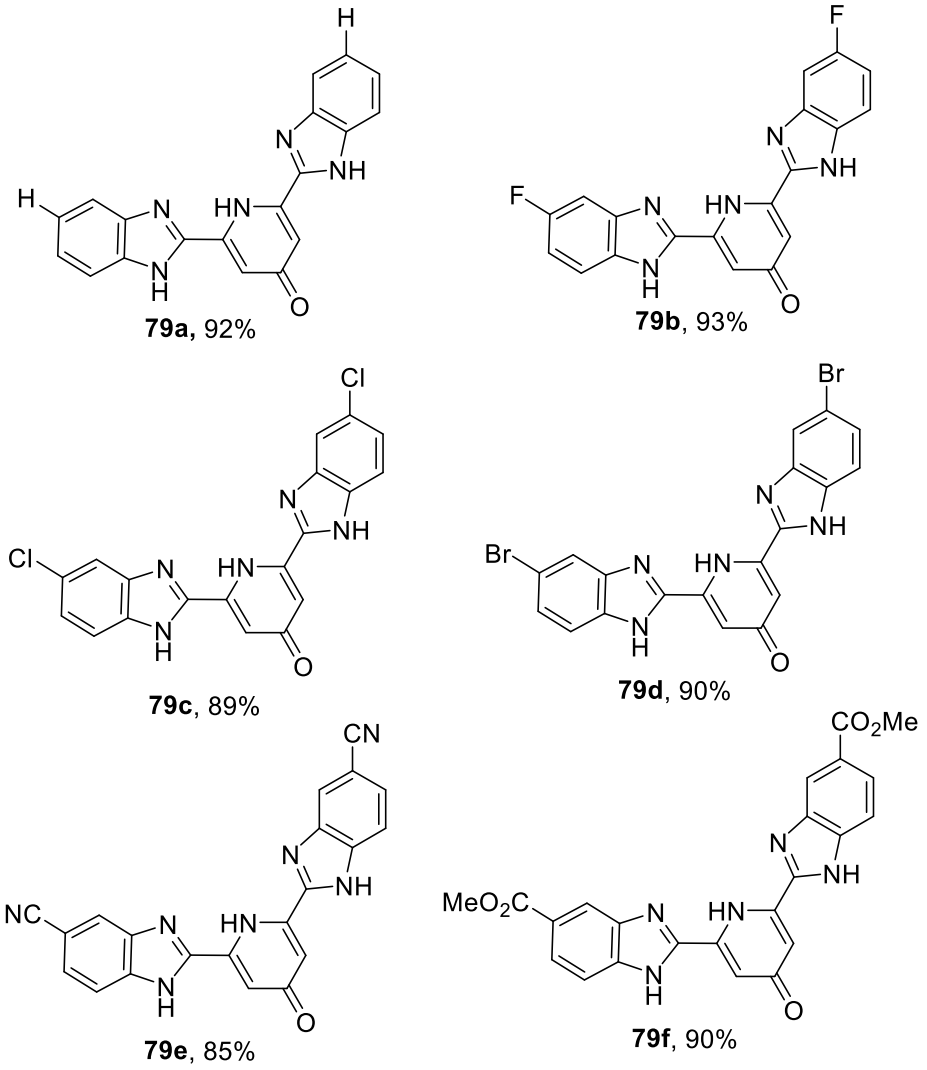

Figure 4.5 Synthesized bis-benzimidazole derivatives using chelidamic acid monohydrate linker.

We proceeded to carry out the second strategy by using 2,6-pyridine dicarboxylic acid **78b** (**Scheme 4.10**) to synthesize substituted bis-benzimidazole derivatives **80a** – **80f** (**Figure**

4.6). The only difference between the first and second strategy is the linker used and the aim was to evaluate the effect of the linkers in modulating physicochemical and pharmacological properties. In addition, the bis-benzimidazole derivatives **80a** – **80f** and their metal complexes are reported as potassium ion channel modulators[202], as light emitting materials,[203–205] pestivirus inhibitors,[206] and apoptosis inducers in cancer cell lines.[207,208]

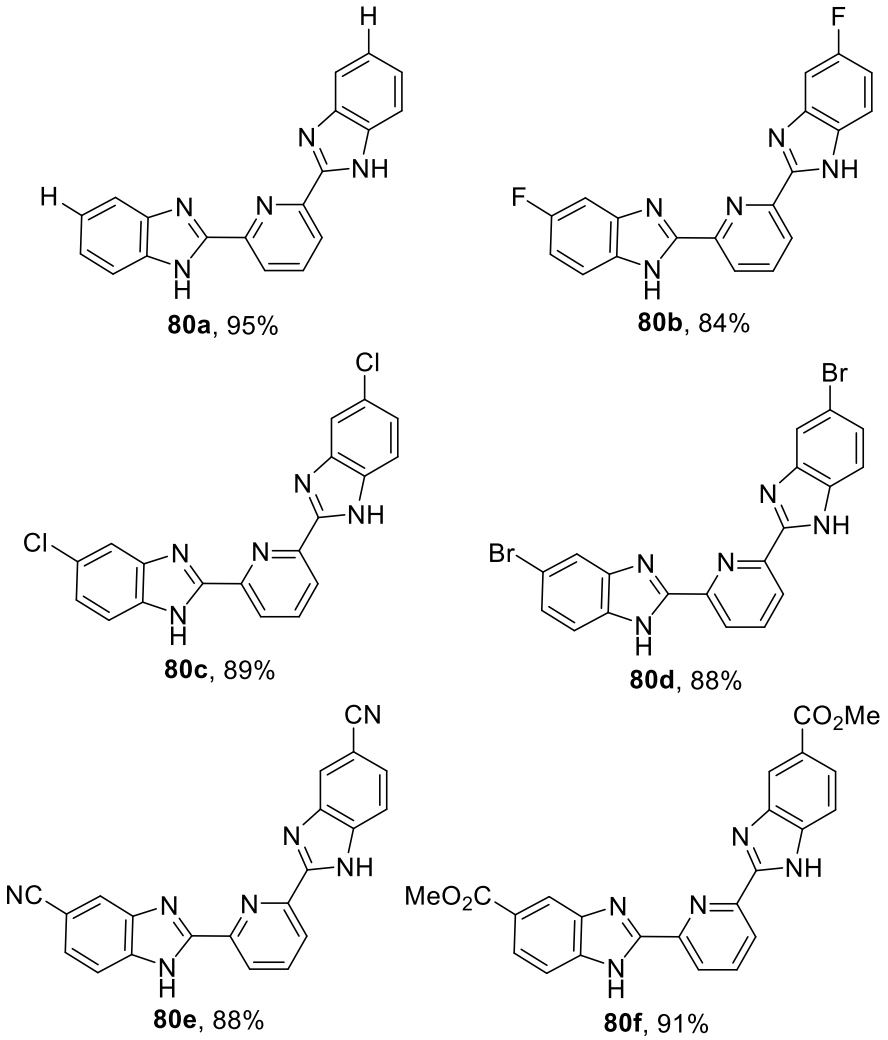

Figure 4.6 Synthesized bis-benzimidazole derivatives using 2,6-pyridine dicarboxylic acid linker.

4.5 Synthesis of substituted phenylbenzimidazoles

We used our reported HBTU promoted methodology to synthesize a library of substituted phenylbenzimidazoles (**Scheme 4.11** and **Scheme 4.12**). Commercially available benzoic acids with varying substitution patterns at 3, 4 and/or 5 positions were coupled with 1,2-diaminobenzene and cyclized to form substituted phenyl benzimidazoles.

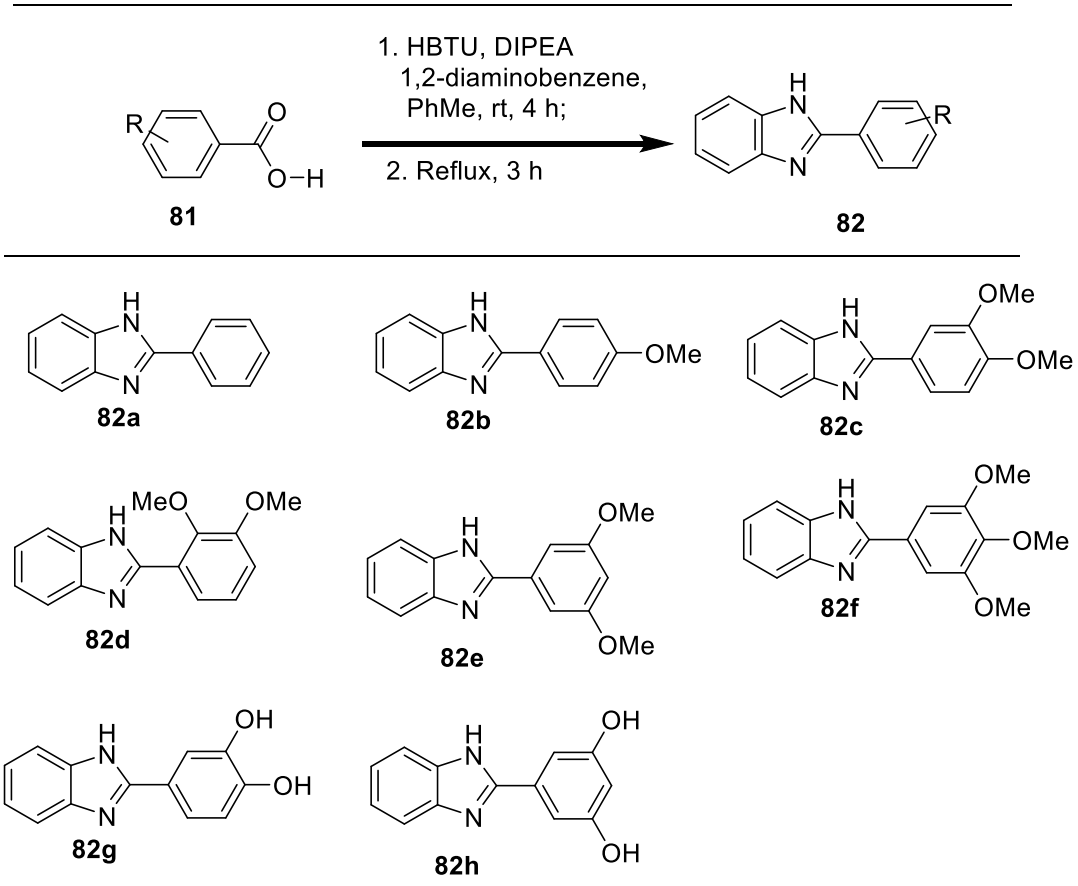

Scheme 4.11 Synthesis of substituted phenyl benzimidazoles

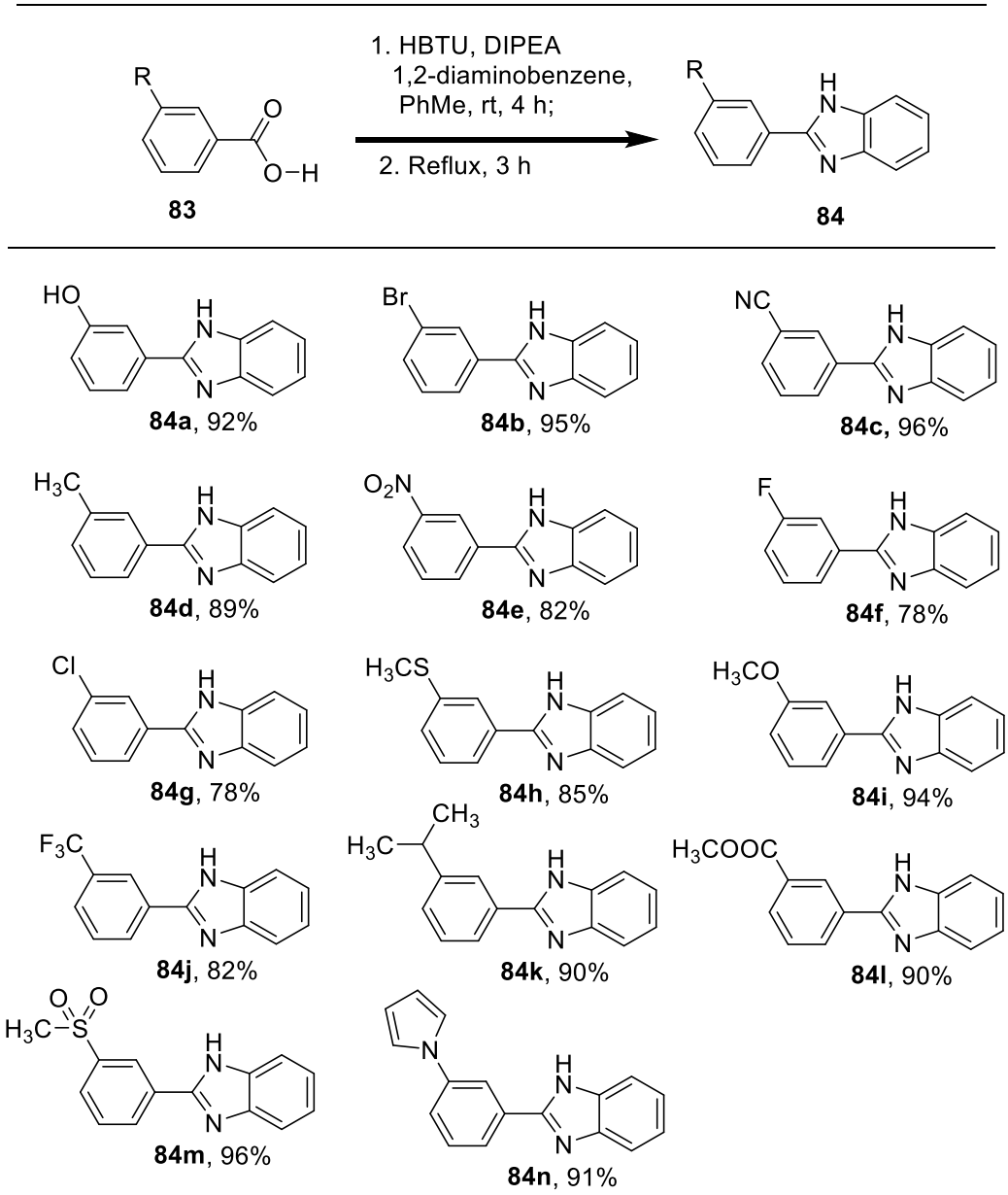

Scheme 4.12 Synthesis of 3-substituted phenyl benzimidazoles

4.6 Biological Evaluation of benzimidazoles

4.6.1 Evaluation of indole-based benzimidazoles for anti-cancer activity

MTT assay was done to evaluate the effect of selected indole-based benzimidazoles on cell viability. There has been limited exploration of 2-indolylbenzimidazole derivatives as potential chemotherapeutic leads. Our results indicate that **43a** (unsubstituted on the

benzimidazole ring), **43b**, **43c**, and **43d** (halogenated on the benzimidazole ring), and **43e** (cyano group on the benzimidazole ring) showed excellent cytotoxicity with IC_{50} values between 1.8 – 34 μM (**Table 4.4**). HepG2 cells are known to express drug metabolizing enzymes in high amount.[209] Thus, higher IC_{50} values observed for **43d**, **43e**, and **43f** in HepG2 cells could be explained by their metabolic sensitivity. Based on the IC_{50} values, all indolylbenzimidazoles showed slight selectivity towards the lung cancer cell line (A549), compared to other cell lines tested.

Table 4.4 Data of Inhibition of Cancer Cell Proliferation for 2-indolylbenzimidazole derivatives 43a – 43f.

		IC_{50} (μM)		
Compound	Structure	HeLa	A549	HepG2
43a	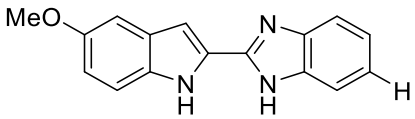	25.4 ± 6.1	3.8 ± 1.1	8.7 ± 3.4
43b	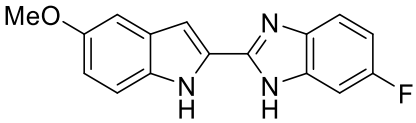	18.1 ± 4.6	15.6±4.6	23.8 ±5.7
43c	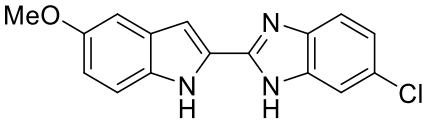	11.1 ± 2.0	4.0 ± 2.4	9.1 ± 1.0
43d	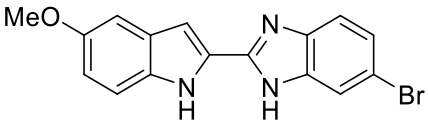	5.8 ± 0.9	1.8 ± 0.6	19.0 ±5.3
43e	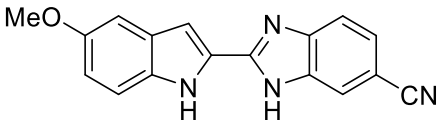	11.8 ± 4.5	5.9 ± 2.8	34.0±10.1
43f	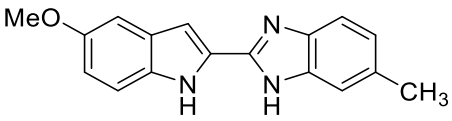	31.0±13.0	29.6±5.0	80.0±30.6

4.6.2 Evaluation of lipid-based benzimidazoles as potential anti-cancer agents

Addition of lipid motifs to drug leads improves their activity, hence we investigated different chain length containing lipid-based benzimidazoles.[210,211] Lipid-based benzimidazole derivatives **41c - 41e** were potent in cancer cells with the lowest IC_{50} value of 1.5 μM (**Table 4.5**). The results indicate that the long lipid motif increases the anti-cancer activity as compounds **41c** (C_{10}), **41d** (C_{12}), and **41e** (C_{14}) showed high anti-cancer activity whereas compound **68c** (C_8) was inactive. Compounds **68a** and **68b** were not tested because they were too hydrophobic and could not be solubilized in DMSO (**Table 4.5**).

Table 4.5 Data of Inhibition of Cancer Cell Proliferation for lipid-based benzimidazoles

		IC_{50} (μM)		
Compound	Structure	HeLa	A549	HepG2
41c	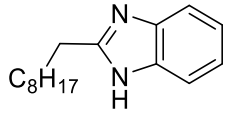	12.7 ± 2.5	6.5 ± 2.5	14.7 ± 2.7
41d	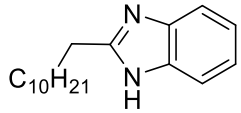	12.5 ± 2.9	1.5 ± 0.4	7.3 ± 1.1
41e	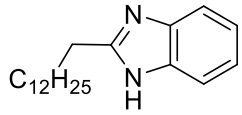	16.0 ± 5.7	1.7 ± 1.0	5.0 ± 1.7
68a	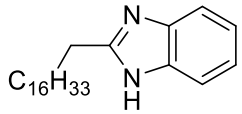	NT	NT	NT
68b	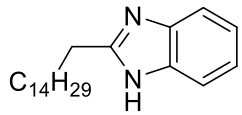	NT	NT	NT
68c	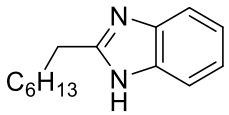	>100	>100	>100

4.6.3 HO-PI Assay

Based on the MTT cell viability assay results, experiments were performed to determine the cell death mechanism for selected compounds from our library, representing each class of synthesized benzimidazoles at their IC_{50} values such as indole based **43c, 43e**, and alkyl-based **68c, 41c**. Many anti-cancer drugs and experimental benzimidazole compounds are known to cause apoptosis.[212,213] Apoptosis was assayed using the double staining of Hoechst 33342 (HO) and propidium iodide (PI) dye and observation by fluorescence microscope. The blue fluorescent HO is a cell permeable nucleic acid dye that shows bright fluorescence in apoptotic cells due to chromatin condensation. The red-fluorescent propidium iodide is a cell impermeable DNA-binding dye, which can only stain the cells in situations where there is loss of plasma membrane integrity such as necrosis. Etoposide, an anticancer agent known to cause apoptosis, was used as a positive control in the assay [214]. The control cells appeared to be intact and the nuclei were stained with a less bright blue fluorescence, and the absence of red fluorescence also indicated regular, intact cells. Cells treated with select benzimidazole compounds exhibited bright blue fluorescence denoting apoptotic cells (white arrows, **Figure 4.7**). Necrotic cells show bright red nuclei. We found that most of the selected compounds induced apoptotic cell death from the HO-PI assay data (**Figure 4.7**). Compounds **43e, 68c,** and **41c** showed significant apoptosis which correlates to the cell viability assay. Thus, apoptosis was observed as a primary mechanism of cell death for the majority of benzimidazole compounds tested.

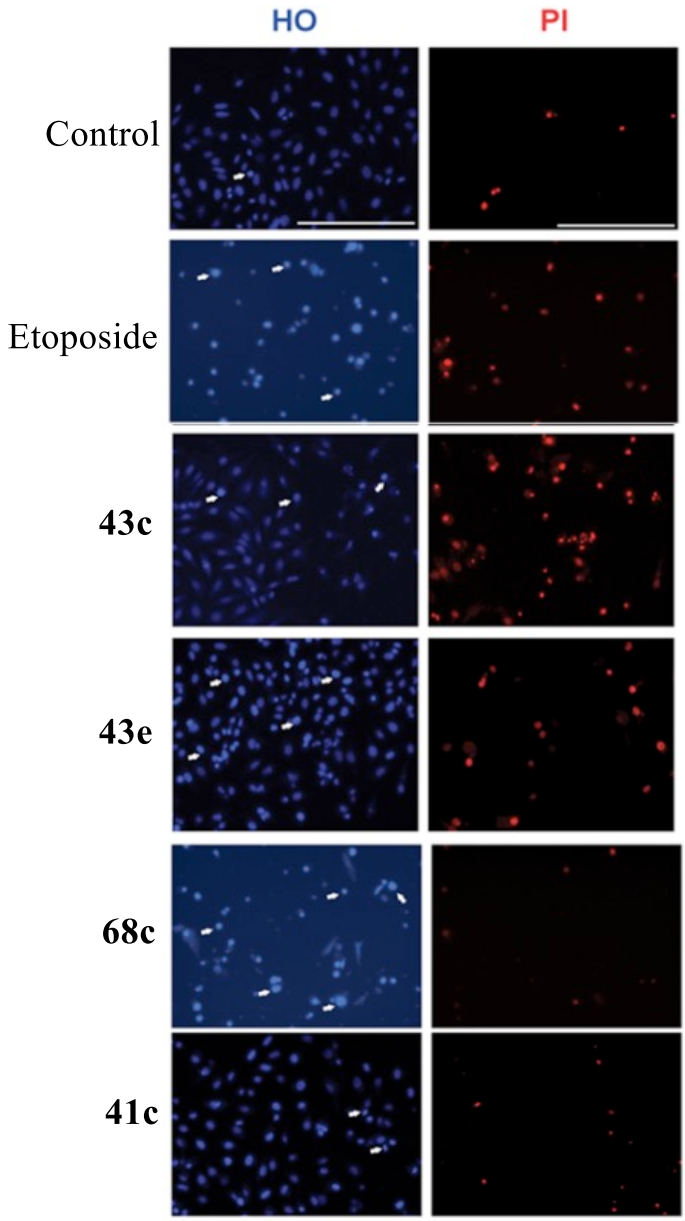

Figure 4.7 Apoptosis/necrosis assay using fluorescence microscopy. Representative images of HeLa cells stained with HO33342 and PI dyes after 24h of treatment with benzimidazole derivatives obtained by fluorescence microscopy (200X magnification). White arrows indicate bright blue apoptotic cells.

4.6.4 Evaluation of bis-benzimidazole derivatives for anti-cancer activity

The synthesized bis-benzimidazole derivatives **79a** – **79f** and **80a** – **80e** were evaluated for anti-cancer activity against HeLa, and MDA-MB231 cancer cell lines (**Table 4.6, Figure 4.8**) in order to determine their cytotoxicity. Doxorubicin was used as a positive control. Bis-benzimidazole **80e** was not tested since it was insoluble in DMSO. Overall the results indicated that bis-benzimidazole derivatives **79a – 79d**, and **80a** – **80d** were promising anti-proliferative agents with IC_{50} values between 2.72 – 28.53 μM (**Table 4.6**). Bis-benzimidazoles **79e, 79f** and **80f** were inactive which may be attributed to the effect of substituent groups on the benzene rings (**Table 4.6**). Compound **79a** had better activity compared to its analogs, **79b -79c**, implying that having substitution on the benzine rings has little effect in improving the activity, except for **79d** whose activity was within the range with **79a**. Having fluorine and chlorine substitution on **80a**, improves the activity. Compounds **80b** and **80c** showed improved activity against the cancer cell line tested compared to **80a**. Compound **80d** had comparable activity with **80a**, hence having bromine as a substituent on the benzene ring has little effect in improving the activity.

Table 4.6 Data of Inhibition of Cancer Cell Proliferation for bis-benzimidazole derivatives

	IC_{50} (μM)	
Compound	HeLa	MDA-MB231
79a	4.80 ± 0.98	6.38 ± 0.61
79b	28.53 ± 9.64	40.57 ± 3.07
79c	23.52 ± 3.48	17.44 ± 2.38
79d	8.89 ± 2.02	10.25 ± 2.52
79e	NA	NA
79f	NA	NA
80a	24.51 ± 3.54	18.74 ± 4.70
80b	2.72 ± 0.50	4.62 ± 0.91
80c	6.97 ± 0.87	8.84 ± 0.36
80d	18.80 ± 2.53	24.66 ± 3.21
80f	NA	NA
Doxorubicin	0.08 ± 0.01	0.11 ± 0.02

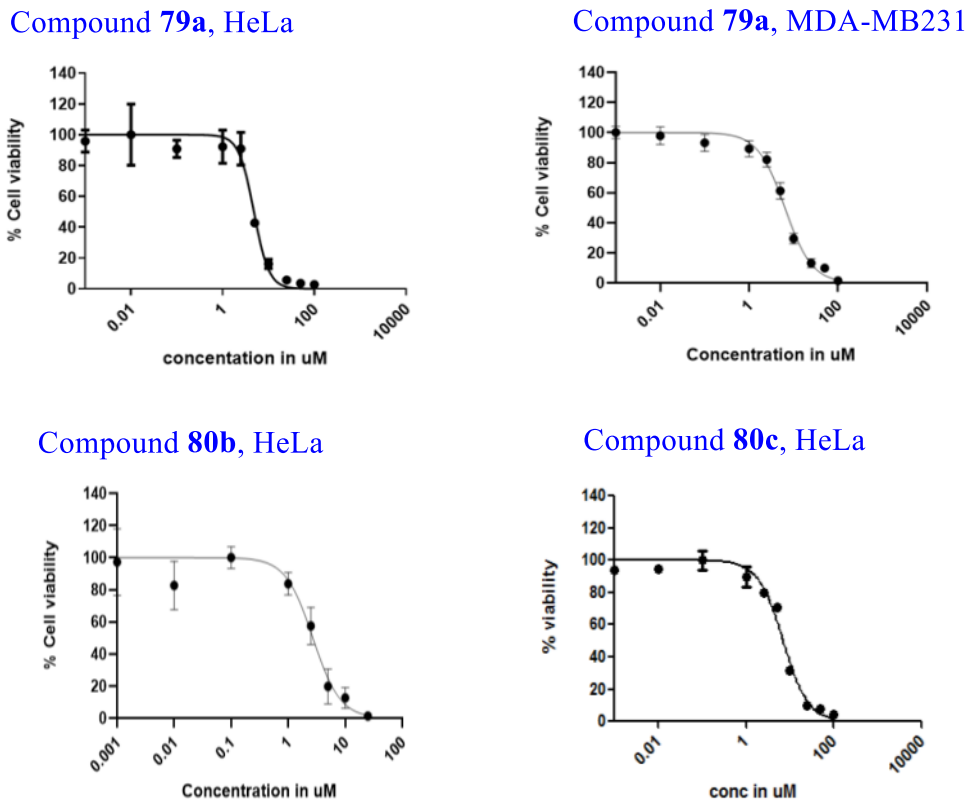

Figure 4.8 Cell viability graphs of 79a, 80b and 80c against HeLa and MDA-MB231 tumor cell lines.

4.6.5 Evaluation of bis-benzimidazole derivatives as topoisomerase II inhibitors

Human DNA topoisomerases has been recognized as an attractive target for developing anti-cancer drugs.[188] Two types of topoisomerase exist, namely, type I topoisomerase (Topo I) and type II topoisomerase (Topo II).[215] Topo I, introduces single-strand breaks in DNA, whereas Topo II introduces double-strand breaks and requires ATP for full activity.[188] Both isomers are nuclear enzymes that are crucial in resolving topological challenges that occur during DNA transcription, replication, and chromosome segregation.[216]

Topo II is the specific target of some of the most active anti-cancer drugs such as etoposide, doxorubicin, mitoxantrone, amonafide, and amsacrine.[217] However, Topo II inhibitors have some therapeutic limitations because of their serious side effects during cancer chemotherapy.[218] Thus, development of new anti-cancer Topo II inhibitors is necessary for improving cancer treatment.[187] Several benzimidazole derivatives are reported as novel Topo II inhibitors.[188,189] Topo II-mediated DNA relaxation assay was performed for bis-benzimidazole **79a**. The work is done in collaboration with the Low lab and performed with the assistance of Shilpa. To determine Topo II inhibitory activity of bis-benzimidazole **79a**, doxorubicin was used as a positive control and the assay done at different concentration of 10, 20 and 30 μM for both bis-benzimidazole **79a** (**Figure 4.9A** and **4.9B**) and doxorubicin.

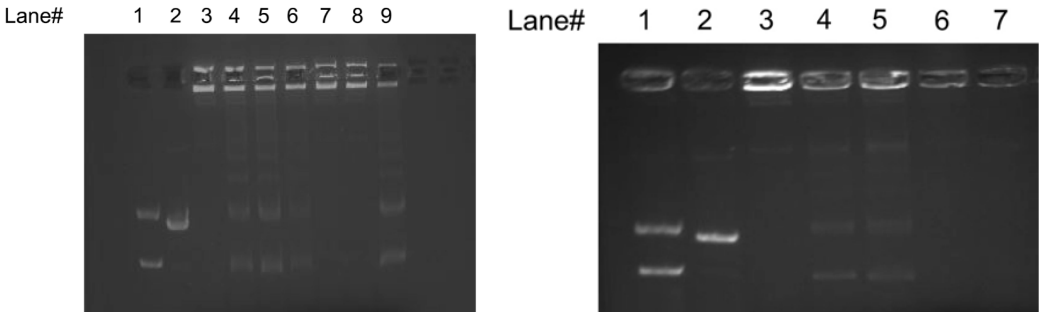

Figure 4.9A Topo II agarose gel assay results. Lane 1 is decatenated DNA (control), Lane 2 is Linear DNA (control), Lane 3 is kinetoplast DNA (kDNA-control), Lane 4 is kDNA with Topo II enzyme, Lane 5 is kDNA with enzyme and DMSO (negative control), Lane 6 is kDNA with enzyme and doxorubicin (10 μM) positive control, Lane 7 corresponds to kDNA with enzyme and bis-benzimidazole 79a (30 μM), Lane 8 corresponds to kDNA with enzyme and bis-benzimidazole 79a (20 μM) and Lane 9 corresponds to kDNA with enzyme and bis-benzimidazole 79a (10 μM). **Figure 4.9B** Topo II agarose gel assay results for bis-benzimidazole 79a and doxorubicin at 20 μM. Lane 1 is decatenated DNA (control), lane 2 is linear DNA (control), lane 3 is kinetoplast DNA (kDNA-control), lane 4 is kDNA with Topo II enzyme, lane 5 is kDNA with enzyme and DMSO (negative control), lane 6 is kDNA with enzyme and doxorubicin (20 μM)-positive control and lane 7 corresponds to kDNA with enzyme and bis-benzimidazole 79a (20 μM).

After performing Topo II assay, at 10 μM, there was slight inhibition by doxorubicin but not bis-benzimidazole **79a**. At 20 μM, there was complete inhibition for both bis-benzimidazole **79a** and doxorubicin (**Figure 4.9A** and **4.9B**). Top II assay was repeated at 20 μM to ascertain the results (**Figure 4.9B**). We hypothesize that since bis-benzimidazole derivatives **79d, 80b** and **80c** are analogs of compound **79a**, have similar Topo II inhibition potential properties. Bis-benzimidazole derivatives are reported to mediate Topo I and II activity[219,220,220–228] and their ability to interact with DNA,[229,230] have made them an effective precursors for a wide range of drugs targeting DNA and DNA related processes. Bis-benzimidazole derivative **80a** is reported to have a wide range of properties such as binding to DNA,[231–234] an efficient anion receptor,[235] as a luminescent complex ligand,[203,236] a receptor for urea recognition[237,238], a chemo-sensor for ions,[239–241] a coordinating ligand,[204,242–247] induces cancer cell apoptosis,[207,248] detects toxic benzene metabolites,[249] as a potent and selective inhibitor of small conductance calcium-activated potassium channels (SK),[202] and as a potent transmembrane anion transporter.[250]

4.6.6 Evaluation of aryl benzimidazoles as BMPs agonists.

4.6.6.1 MT-Glo Assay

The synthesized aryl benzimidazole derivatives (**Scheme 4.11** and **4.12**) were evaluated for cell cytotoxicity using MT-Glo assay in C2C12 cell lines (**Table 4.7** and **Table 4.8**). Compounds targeting BMPs pathways are supposed to be non-toxic to the cells and this explains why carrying out cell cytotoxicity test is important. MT-Glo assay results indicates that majority of the compounds were non-toxic to cells. Compounds **84l** and **84n** (**Table 4.8**) were cytotoxic to the cells and there deemed not good to be evaluated for further BMP

tests. Compounds **82c**, **84a**, **84h**, and **84i** had IC_{50} values in the range of 29 – 40 μM (**Table 4.7** and **Table 4.8**), not too toxic to prevent them from further BMP testing.

Table 4.7 MT-Glo analysis for cell cytotoxicity of the screened compounds against C2C12 cell lines

Compound	Structure	IC_{50} (μM)
82a	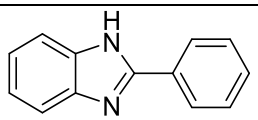	>100
82b	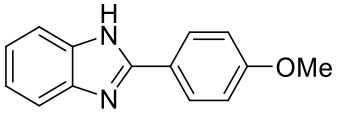	>100
82c	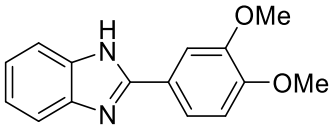	29.24
82d	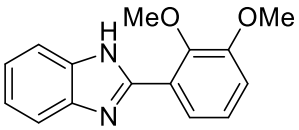	>100
82e	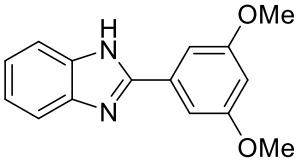	70.2
82f	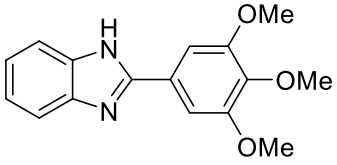	>100
82g	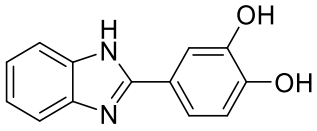	66.85
82h	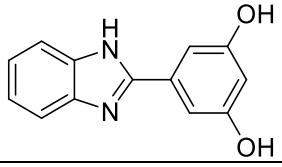	>100

Table 4.8 MT Glo cell cytotoxicity test for 3-substituted phenyl benzimidazoles

Compound	Structure	IC_{50} (μM)
84a	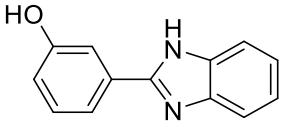	40.14
84b	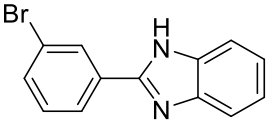	93.29
84c	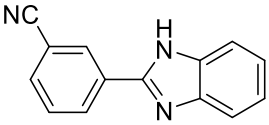	>500
84d	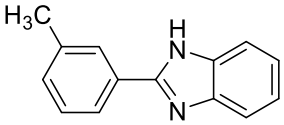	>500
84e	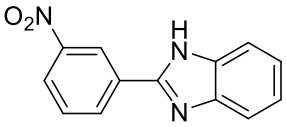	34.58
84f	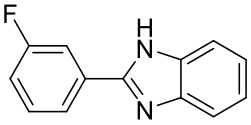	>500
84g	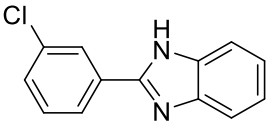	>1000

Compound	Structure	IC_{50} (μM)
84h	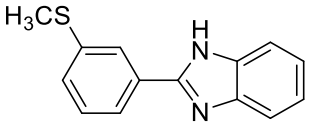	36.53
84i	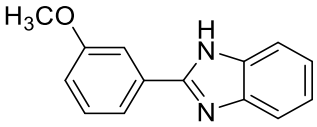	38.09
84j	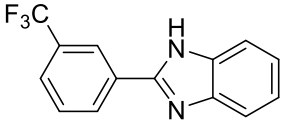	>100
84k	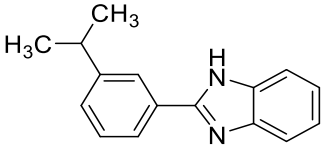	>500
84l	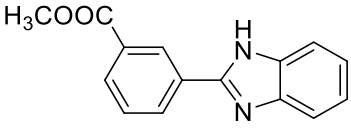	4.38
84m	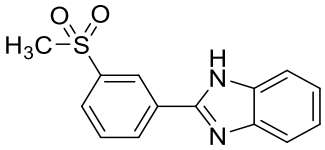	>100
84n	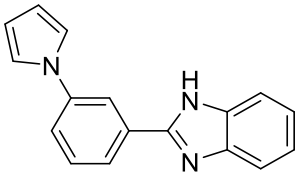	13.23

4.6.6.2 Smad-Phosphorylation Assay

After performing cell cytotoxicity assay, compounds were selected for smad-phosphorylation experiments to determine their contribution to BMPs signaling pathways. The expression of smads were assessed using Immunofluorescent labelling and Western blotting experiments. The work is done in collaboration with the Perron lab and performed

by Dr. Perron. BMP7 was used as a positive control. Treatments of **82c, 82e, 84a,** and **84h** in the immunofluorescence labelling assay (**Figure 4.10** and **Figure 4.11**) caused translocation of pSmads into the nucleus. Compounds **82c** and compounds **82e** showed the most increased Smads phosphorylation compared to the positive control BMP7 (**Figure 4.11**). Among the 3-substituted phenyl benzimidazoles, **82g**, **82h**, **84a**, **84b** and **84i**, only compounds **82h** and **84a** showed to some extend Smad phosphorylation but lower than that of compounds **82c** and **82e** (**Figure 4.10**). Compound **82a** had no substitution (**Scheme 4.11**) and didn't cause phosphorylation of Smads. Likewise, compound **82b** with a substitution at para position (**Scheme 4.11**) didn't cause phosphorylation of smads (**Figure 4.10**). Di-substitution methoxy's (**82c** and **82e**) on aryl ring at positions 3 and 4 or at 3 and 5 is crucial for pSmad activity than mono-substitution (**82b** and **84i**, **Scheme 4.11**). We took one of the most active compounds, **82e**, and performed western blot analysis. Compound **82e** increased the expression of pSmad in a concentration dependent manner and the results validates immunoblotting observations. Overall our results suggest that di-methoxy-benzimidazoles **82c** and **82e** from a library of small molecules aryl benzimidazoles were identified as promising compounds for further evaluation.

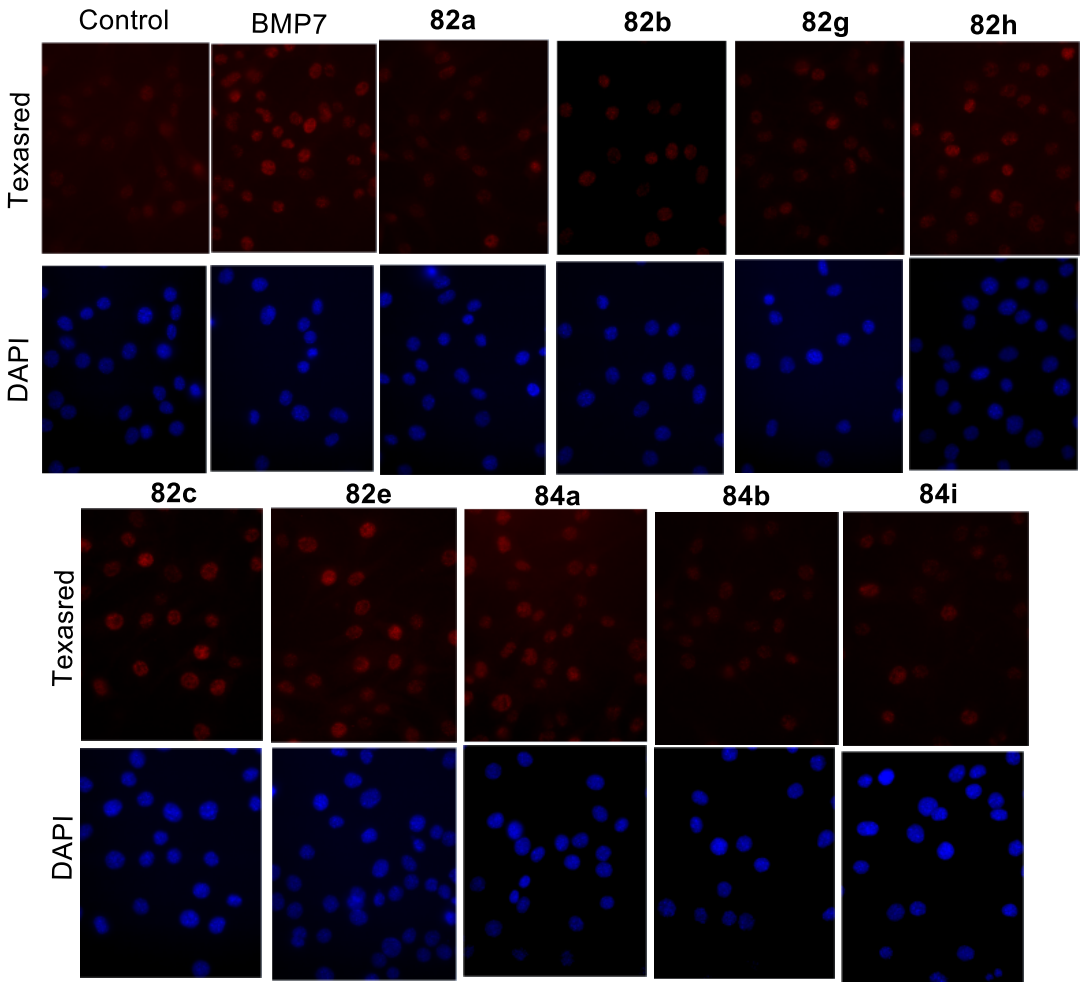

Figure 4.10 Fluorescence Imaging Immunoblotting Assay. Treatment of 82a, 82b, 82c, 82e, 82h, 82g, 84a, 84b, and 84i in C2C12 cells.

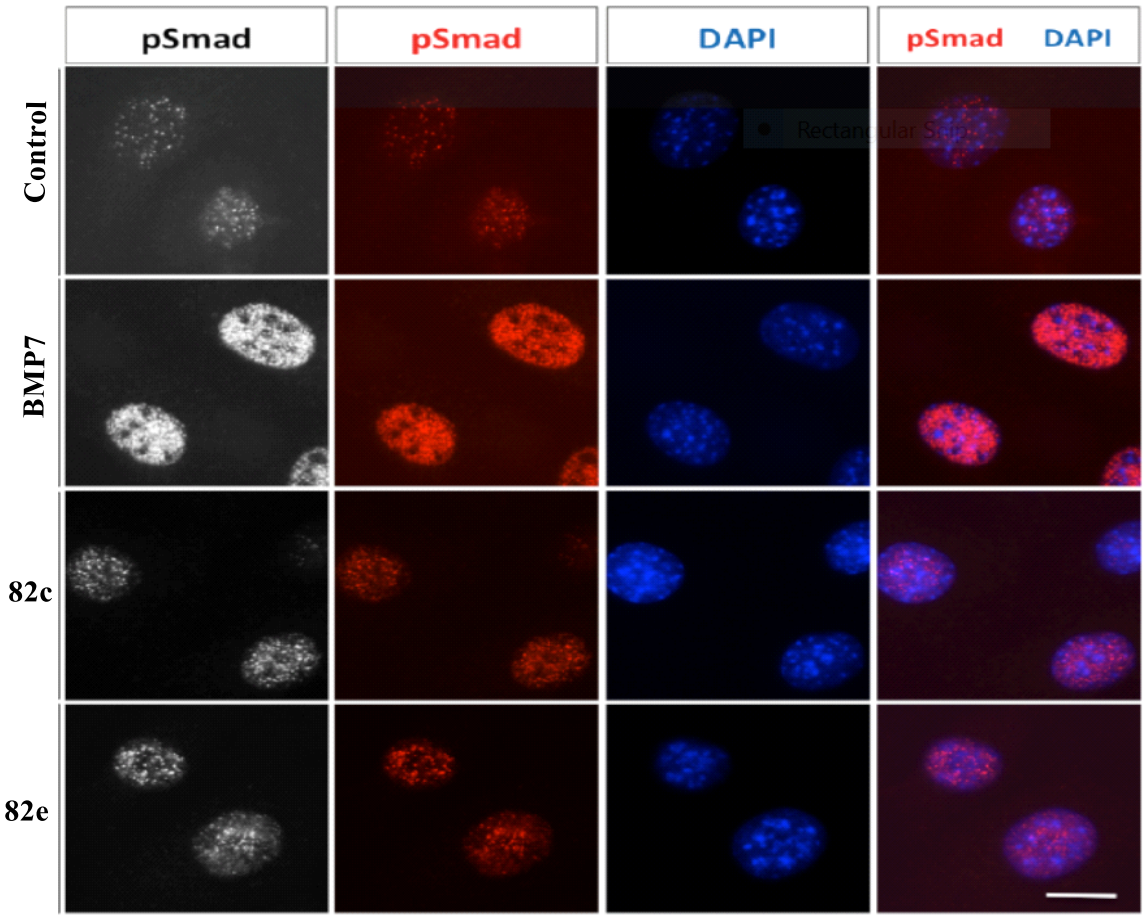

Figure 4.11 Fluorescence imaging. Treatment of 82c and 82e in C2C12 cells caused translocation of pSmad into the nucleus.

CONCLUSIONS

Benzimidazole is a privileged, and routinely used pharmacophore lead in the drug discovery process. We have reported two convenient and mild methodologies for the synthesis of benzimidazoles: (a) a dehydrative cyclization strategy for the synthesis of benzimidazoles using HBTU promoted approach from aryl/alkyl amide substrates and (b) an efficient one-pot conversion of carboxylic acids into benzimidazoles using HBTU promoted approach. These synthetic approaches are high yielding, acid free and tolerates various common functional groups. We have also reported a simple and highly effective synthetic method to chemo-selectively alkylate the indolyl-benzimidazole scaffold using a wide range of benzyl and alkyl aliphatic bromides. These reported methods are more convenient for the synthesis and structural diversification of benzimidazole derivatives and will enable medicinal chemists to explore the SAR of benzimidazole-based drug leads.

We successfully used the reported synthetic methodologies to synthesize different classes of benzimidazoles and selected a representative of each class for bioassay evaluation. Indole-based and lipid-based benzimidazoles were tested for cell viability and results revealed that they are potential anticancer agents. The primary mechanism for cancer cell death induced by the tested compounds is apoptosis. Bis-benzimidazole derivatives were also evaluated for anti-cancer and topoisomerase II inhibition properties. Bis-benzimidazoles **79a**, **79b**, **80a**, and **80c** showed promising anti-cancer activities against the cell line tested. Compound **79a** is a potential Topo II inhibitor.

We also tested aryl benzimidazoles against bone morphogenetic proteins (BMPs) signaling pathways. Our results suggest that bis disubstituted methoxy compounds **82c** and **82e** from

a library of small molecules aryl benzimidazoles are promising BMP receptor agonist where they stimulated downstream cascade canonical pSmad-signaling pathways in C2C12 cells. The reported benzimidazole derivatives possess anti-cancer and bone morphogenetic protein (BMPs) agonist properties. Our findings suggest that further development of these scaffolds could provide drug leads towards new chemotherapeutics and agonists for BMP signaling pathway.

REFERENCES

(1) Walsh, C. T. Nature Loves Nitrogen Heterocycles. *Tetrahedron Lett*. **2015**, *56* (23), 3075–3081.

(2) Kaur, N. Review on the Synthesis of Six-Membered *N,N*-Heterocycles by Microwave Irradiation. *Synth*. *Commun*. **2015**, *45* (10), 1145–1182.

(3) Asif, M. A Mini Review: Biological Significances of Nitrogen Hetero Atom Containing Heterocyclic Compounds. *Int. J. Bioorg. Chem*. **2017**, *2* (3), 146 -152.

(4) Garuti, L.; Roberti, M.; Pizzirani, D. Nitrogen-Containing Heterocyclic Quinones: A Class of Potential Selective Antitumor Agents. *Mini Rev. Med. Chem.* **2007**, *7* (5), 481 - 489.

(5) Kaur, N. Multiple Nitrogen-Containing Heterocycles: Metal and Non-Metal Assisted Synthesis. *Synth*. *Commun*. **2019**, *49* (13), 1633–1658.

(6) Thansandote, P.; Lautens, M. Construction of Nitrogen-Containing Heterocycles by C-H Bond Functionalization. *Chem*. *Eur*. *J*. **2009**, *15* (24), 5874–5883.

(7) Vitaku, E.; Smith, D. T.; Njardarson, J. T. Analysis of the Structural Diversity, Substitution Patterns, and Frequency of Nitrogen Heterocycles among U.S. FDA Approved Pharmaceuticals: Miniperspective. *J*. *Med*. *Chem*. **2014**, *57* (24), 10257–10274.

(8) Zhang, B.; Studer, A. Recent Advances in the Synthesis of Nitrogen Heterocycles via Radical Cascade Reactions Using Isonitriles as Radical Acceptors. *Chem*. *Soc*. *Rev*. **2015**, *44* (11), 3505–3521.

(9) Morgenthaler, M.; Schweizer, E.; Hoffmann-Röder, A.; Benini, F.; Martin, R. E.; Jaeschke, G.; Wagner, B.; Fischer, H.; Bendels, S.; Zimmerli, D.; Schneider, J.;

Diederich, F.; Kansy, M.; Müller, K. Predicting and Tuning Physicochemical Properties in Lead Optimization: Amine Basicities. *ChemMedChem* **2007**, *2* (8), 1100–1115.

(10) Anand, K.; Wakode, S. Development of Drugs Based on Benzimidazole Heterocycle: Recent Advancement and Insights. *Int. J. Chem. Stud.* ***2017, 5*** (2), 350 - 362.

(11) Sun, X.; Lv, X.-H.; Ye, L.-M.; Hu, Y.; Chen, Y.-Y.; Zhang, X.-J.; Yan, M. Synthesis of Benzimidazoles via Iridium-Catalyzed Acceptorless Dehydrogenative Coupling. *Org. Biomol. Chem.* **2015**, *13* (27), 7381–7383.

(12) Bhattacharya, S.; Chaudhuri, P. Medical Implications of Benzimidazole Derivatives as Drugs Designed for Targeting DNA and DNA Associated Processes. *Curr. Med. Chem.* **2008**, *15* (18), 1762 - 1777.

(13) Hirashima, S.; Suzuki, T.; Ishida, T.; Noji, S.; Yata, S.; Ando, I.; Komatsu, M.; Ikeda, S.; Hashimoto, H. Benzimidazole Derivatives Bearing Substituted Biphenyls as Hepatitis C Virus NS5B RNA-Dependent RNA Polymerase Inhibitors: Structure−Activity Relationship Studies and Identification of a Potent and Highly Selective Inhibitor JTK-109. *J. Med. Chem.* **2006**, *49* (15), 4721–4736.

(14) Chu, B.; Liu, F.; Li, L.; Ding, C.; Chen, K.; Sun, Q.; Shen, Z.; Tan, Y.; Tan, C.; Jiang, Y. A Benzimidazole Derivative Exhibiting Antitumor Activity Blocks EGFR and HER2 Activity and Upregulates DR5 in Breast Cancer Cells. *Cell Death Dis.* **2015**, *6* (3), e1686–e1686.

(15) Cevik, U. A.; Saglik, B. N.; Ozkay, Y.; Canturk, Z.; Bueno, J.; Demirci, F.; Koparal, A. S. Synthesis of New Fluoro-Benzimidazole Derivatives as an Approach towards

the Discovery of Novel Intestinal Antiseptic Drug Candidates. *Curr. Pharm. Des.* **2017**, *23* (15), 2276 - 2286.

(16) Yadav, G.; Ganguly, S. Structure Activity Relationship (SAR) Study of Benzimidazole Scaffold for Different Biological Activities: A Mini-Review. *Eur. J. Med. Chem.* **2015**, *97*, 419–443.

(17) Galal, S. A.; Abdelsamie, A. S.; Shouman, S. A.; Attia, Y. M.; Ali, H. I.; Tabll, A.; El-Shenawy, R.; El Abd, Y. S.; Ali, M. M.; Mahmoud, A. E.; Abdel-Halim, A. H.; Fyiad, A. A.; Girgis, A. S.; El-Diwani, H. I. Part I: Design, Synthesis and Biological Evaluation of Novel Pyrazole-Benzimidazole Conjugates as Checkpoint Kinase 2 (Chk2) Inhibitors with Studying Their Activities Alone and in Combination with Genotoxic Drugs. *Eur. J. Med. Chem.* **2017**, *134*, 392–405.

(18) Adegboye, A. A.; Khan, K. M.; Salar, U.; Aboaba, S. A.; Kanwal; Chigurupati, S.; Fatima, I.; Taha, M.; Wadood, A.; Mohammad, J. I.; Khan, H.; Perveen, S. 2-Aryl Benzimidazoles: Synthesis, In Vitro α-Amylase Inhibitory Activity, and Molecular Docking Study. *Eur. J. Med. Chem.* **2018**, *150*, 248–260.

(19) Shin, Y.; Suchomel, J.; Cardozo, M.; Duquette, J.; He, X.; Henne, K.; Hu, Y.-L.; Kelly, R. C.; McCarter, J.; McGee, L. R.; Medina, J. C.; Metz, D.; San Miguel, T.; Mohn, D.; Tran, T.; Vissinga, C.; Wong, S.; Wannberg, S.; Whittington, D. A.; Whoriskey, J.; Yu, G.; Zalameda, L.; Zhang, X.; Cushing, T. D. Discovery, Optimization, and in Vivo Evaluation of Benzimidazole Derivatives AM-8508 and AM-9635 as Potent and Selective PI3Kδ Inhibitors. *J. Med. Chem.* **2016**, *59* (1), 431–447.

(20) Tatani, K.; Hiratochi, M.; Kikuchi, N.; Kuramochi, Y.; Watanabe, S.; Yamauchi, Y.; Itoh, F.; Isaji, M.; Shuto, S. Identification of Adenine and Benzimidazole Nucleosides as Potent Human Concentrative Nucleoside Transporter 2 Inhibitors: Potential Treatment for Hyperuricemia and Gout. *J. Med. Chem.* **2016**, *59* (8), 3719–3731.

(21) Lapierre, J. M.; Eathiraj, S.; Vensel, D.; Liu, Y.; Bull, C. O.; Cornell-Kennon, S.; Iimura, S.; Kelleher, E. W.; Kizer, D. E.; Koerner, S.; Makhija, S.; Matsuda, A.; Moussa, M.; Namdev, N.; Savage, R. E.; Szwaya, J.; Volckova, E.; Westlund, N.; Wu, H.; Schwartz, B. Discovery of 3-(3-(4-(1-Aminocyclobutyl)Phenyl)-5-Phenyl-3 *H* -Imidazo[4,5- *b*]Pyridin-2-Yl)Pyridin-2-Amine (ARQ 092): An Orally Bioavailable, Selective, and Potent Allosteric AKT Inhibitor. *J. Med. Chem.* **2016**, *59* (13), 6455–6469.

(22) Muth, A.; Subramanian, V.; Beaumont, E.; Nagar, M.; Kerry, P.; McEwan, P.; Srinath, H.; Clancy, K.; Parelkar, S.; Thompson, P. R. Development of a Selective Inhibitor of Protein Arginine Deiminase 2. *J. Med. Chem.* **2017**, *60* (7), 3198–3211.

(23) Hoyt, S. B.; Park, M. K.; London, C.; Xiong, Y.; Tata, J.; Bennett, D. J.; Cooke, A.; Cai, J.; Carswell, E.; Robinson, J.; MacLean, J.; Brown, L.; Belshaw, S.; Clarkson, T. R.; Liu, K.; Liang, G.-B.; Struthers, M.; Cully, D.; Wisniewski, T.; Ren, N.; Bopp, C.; Sok, A.; Cai, T.-Q.; Stribling, S.; Pai, L.-Y.; Ma, X.; Metzger, J.; Verras, A.; McMasters, D.; Chen, Q.; Tung, E.; Tang, W.; Salituro, G.; Buist, N.; Kuethe, J.; Rivera, N.; Clemas, J.; Zhou, G.; Gibson, J.; Maxwell, C. A.; Lassman, M.; McLaughlin, T.; Castro-Perez, J.; Szeto, D.; Forrest, G.; Hajdu, R.; Rosenbach, M.; Ali, A. Discovery of Benzimidazole CYP11B2 Inhibitors with *in Vivo* Activity in Rhesus Monkeys. *ACS Med. Chem. Lett.* **2015**, *6* (5), 573–578.

(24) Parks, D. J.; Parsons, W. H.; Colburn, R. W.; Meegalla, S. K.; Ballentine, S. K.; Illig, C. R.; Qin, N.; Liu, Y.; Hutchinson, T. L.; Lubin, M. L.; Stone, D. J.; Baker, J. F.; Schneider, C. R.; Ma, J.; Damiano, B. P.; Flores, C. M.; Player, M. R. Design and Optimization of Benzimidazole-Containing Transient Receptor Potential Melastatin 8 (TRPM8) Antagonists. *J. Med. Chem.* **2011**, *54* (1), 233–247.

(25) Venable, J. D.; Cai, H.; Chai, W.; Dvorak, C. A.; Grice, C. A.; Jablonowski, J. A.; Shah, C. R.; Kwok, A. K.; Ly, K. S.; Pio, B.; Wei, J.; Desai, P. J.; Jiang, W.; Nguyen, S.; Ling, P.; Wilson, S. J.; Dunford, P. J.; Thurmond, R. L.; Lovenberg, T. W.; Karlsson, L.; Carruthers, N. I.; Edwards, J. P. Preparation and Biological Evaluation of Indole, Benzimidazole, and Thienopyrrole Piperazine Carboxamides: Potent Human Histamine H_4 Antagonists. *J. Med. Chem.* **2005**, *48* (26), 8289–8298.

(26) Sørensen, U. S.; Strøbæk, D.; Christophersen, P.; Hougaard, C.; Jensen, M. L.; Nielsen, E. Ø.; Peters, D.; Teuber, L. Synthesis and Structure–Activity Relationship Studies of 2-(N-Substituted)-Aminobenzimidazoles as Potent Negative Gating Modulators of Small Conductance Ca^{2+} -Activated K^+ Channels. *J. Med. Chem.* **2008**, *51* (23), 7625–7634.

(27) Balboni, G.; Trapella, C.; Sasaki, Y.; Ambo, A.; Marczak, E. D.; Lazarus, L. H.; Salvadori, S. Influence of the Side Chain Next to C-Terminal Benzimidazole in Opioid Pseudopeptides Containing the Dmt-Tic Pharmacophore. *J. Med. Chem.* **2009**, *52* (17), 5556–5559.

(28) Kishore Babu, P. N.; Ramadevi, B.; Poornachandra, Y.; Ganesh Kumar, C. Synthesis, Antimicrobial, and Anticancer Evaluation of Novel 2-(3-

Methylindolyl)Benzimidazole Derivatives. *Med. Chem. Res.* **2014**, *23* (9), 3970–3978.

(29) Ramanjulu, J. M.; Pesiridis, G. S.; Yang, J.; Concha, N.; Singhaus, R.; Zhang, S.-Y.; Tran, J.-L.; Moore, P.; Lehmann, S.; Eberl, H. C.; Muelbaier, M.; Schneck, J. L.; Clemens, J.; Adam, M.; Mehlmann, J.; Romano, J.; Morales, A.; Kang, J.; Leister, L.; Graybill, T. L.; Charnley, A. K.; Ye, G.; Nevins, N.; Behnia, K.; Wolf, A. I.; Kasparcova, V.; Nurse, K.; Wang, L.; Puhl, A. C.; Li, Y.; Klein, M.; Hopson, C. B.; Guss, J.; Bantscheff, M.; Bergamini, G.; Reilly, M. A.; Lian, Y.; Duffy, K. J.; Adams, J.; Foley, K. P.; Gough, P. J.; Marquis, R. W.; Smothers, J.; Hoos, A.; Bertin, J. Design of Amidobenzimidazole STING Receptor Agonists with Systemic Activity. *Nature* **2018**, *564* (7736), 439–443.

(30) Dokla, E. M. E.; Abutaleb, N. S.; Milik, S. N.; Li, D.; El-Baz, K.; Shalaby, M.-A. W.; Al-Karaki, R.; Nasr, M.; Klein, C. D.; Abouzid, K. A. M.; Seleem, M. N. Development of Benzimidazole-Based Derivatives as Antimicrobial Agents and Their Synergistic Effect with Colistin against Gram-Negative Bacteria. *Eur. J. Med. Chem.* **2020**, *186*, 111850.

(31) Jeyakkumar, P.; Liu, H. B.; Gopala, L.; Cheng, Y.; Peng, X. M.; Geng, R. X.; Zhou, C. H. Novel Benzimidazolyl Tetrahydroprotoberberines: Design, Synthesis, Antimicrobial Evaluation and Multi-Targeting Exploration. *Bioorg. Med. Chem. Lett.* **2017**, *27* (8), 1737–1743.

(32) El-Gohary, N. S.; Shaaban, M. I. Synthesis, Antimicrobial, Antiquorum-Sensing and Antitumor Activities of New Benzimidazole Analogs. *Eur. J. Med. Chem.* **2017**, *137*, 439–449.

(33) Agh-Atabay, N. Synthesis and Investigation of Antimicrobial Activity of Some Bisbenzimidazole-Derived Chelating Agents. *Eur. J. Med. Chem.* **2003**, *38* (10), 875–881.

(34) Göker, H.; Özden, S.; Yıldız, S.; Boykin, D. W. Synthesis and Potent Antibacterial Activity against MRSA of Some Novel 1,2-Disubstituted-1H-Benzimidazole-N-Alkylated-5-Carboxamidines. *Eur. J. Med. Chem.* **2005**, *40* (10), 1062–1069.

(35) Ramprasad, J.; Nayak, N.; Dalimba, U.; Yogeeswari, P.; Sriram, D.; Peethambar, S. K.; Achur, R.; Kumar, H. S. S. Synthesis and Biological Evaluation of New Imidazo[2,1-b][1,3,4]Thiadiazole-Benzimidazole Derivatives. *Eur. J. Med. Chem.* **2015**, *95*, 49–63.

(36) Zhang, H. Z.; He, S. C.; Peng, Y. J.; Zhang, H. J.; Gopala, L.; Tangadanchu, V. K. R.; Gan, L.-L.; Zhou, C.-H. Design, Synthesis and Antimicrobial Evaluation of Novel Benzimidazole-Incorporated Sulfonamide Analogues. *Eur. J. Med. Chem.* **2017**, *136*, 165–183.

(37) Abraham, R.; Prakash, P.; Mahendran, K.; Ramanathan, M. A Novel Series of N-Acyl Substituted Indole-Linked Benzimidazoles and Naphthoimidazoles as Potential Anti Inflammatory, Anti Biofilm and Anti Microbial Agents. *Microb. Pathog.* **2018**, *114*, 409–413.

(38) Song, D.; Ma, S. Recent Development of Benzimidazole-Containing Antibacterial Agents. *ChemMedChem* **2016**, *11* (7), 646–659.

(39) Janupally, R.; Jeankumar, V. U.; Bobesh, K. A.; Soni, V.; Devi, P. B.; Pulla, V. K.; Suryadevara, P.; Chennubhotla, K. S.; Kulkarni, P.; Yogeeswari, P.; Sriram, D. Structure-Guided Design and Development of Novel Benzimidazole Class of

Compounds Targeting DNA GyraseB Enzyme of Staphylococcus Aureus. *Bioorg. Med. Chem.* **2014**, *22* (21), 5970–5987.

(40) Picconi, P.; Hind, C.; Jamshidi, S.; Nahar, K.; Clifford, M.; Wand, M. E.; Sutton, J. M.; Rahman, K. M. Triaryl Benzimidazoles as a New Class of Antibacterial Agents against Resistant Pathogenic Microorganisms. *J. Med. Chem.* **2017**, *60* (14), 6045–6059.

(41) Monforte, A. M.; Ferro, S.; De Luca, L.; Lo Surdo, G.; Morreale, F.; Pannecouque, C.; Balzarini, J.; Chimirri, A. Design and Synthesis of N1-Aryl-Benzimidazoles 2-Substituted as Novel HIV-1 Non-Nucleoside Reverse Transcriptase Inhibitors. *Bioorg. Med. Chem.* **2014**, *22* (4), 1459–1467.

(42) Miao, T. T.; Tao, X. B.; Li, D. D.; Chen, H.; Jin, X. Y.; Geng, Y.; Wang, S. F.; Gu, W. Synthesis and Biological Evaluation of 2-Aryl-Benzimidazole Derivatives of Dehydroabietic Acid as Novel Tubulin Polymerization Inhibitors. *RSC Adv.* **2018**, *8* (31), 17511–17526.

(43) Li, P.; Zhang, W.; Jiang, H.; Li, Y.; Dong, C.; Chen, H.; Zhang, K.; Du, Z. Design, Synthesis and Biological Evaluation of Benzimidazole–Rhodanine Conjugates as Potent Topoisomerase II Inhibitors. *Med. Chem. Commun.* **2018**, *9* (7), 1194–1205.

(44) Hegde, M.; Sharath Kumar, K. S.; Thomas, E.; Ananda, H.; Raghavan, S. C.; Rangappa, K. S. A Novel Benzimidazole Derivative Binds to the DNA Minor Groove and Induces Apoptosis in Leukemic Cells. *RSC Adv.* **2015**, *5* (113), 93194–93208.

(45) Alpan, A. S.; Zencir, S.; Zupkó, I.; Coban, G.; Réthy, B.; Gunes, H. S.; Topcu, Z. Biological Activity of Bis-Benzimidazole Derivatives on DNA Topoisomerase I and HeLa, MCF7 and A431 Cells. *J. Enzyme Inhib. Med. Chem.* **2009**, *24* (3), 844–849.

(46) Alkahtani, H. M.; Abbas, A. Y.; Wang, S. Synthesis and Biological Evaluation of Benzo[d]Imidazole Derivatives as Potential Anti-Cancer Agents. *Bioorg. Med. Chem. Lett.* **2012**, *22* (3), 1317–1321.

(47) Nayak, V. L.; Nagesh, N.; Ravikumar, A.; Bagul, C.; Vishnuvardhan, M. V. P. S.; Srinivasulu, V.; Kamal, A. 2-Aryl Benzimidazole Conjugate Induced Apoptosis in Human Breast Cancer MCF-7 Cells through Caspase Independent Pathway. *Apoptosis* **2017**, *22* (1), 118–134.

(48) Darwish, S. A.; Elbayaa, R. Y.; Ashour, H. M.; Khalil, M. A.; Badawey, E. A. Potential Anticancer Agents: Design, Synthesis of New Pyrido[1,2-a]Benzimidazoles and Related Derivatives Linked to Alkylating Fragments. *Med. chem.* **2018**, *08* (04).

(49) Rashedy, A.; Aboul-Enein, H. Benzimidazole Derivatives as Potential Chemotherapeutic Agents. *Curr. Drug Ther.* **2013**, *8* (1), 1-14.

(50) Refaat, H. M. Synthesis and Anticancer Activity of Some Novel 2-Substituted Benzimidazole Derivatives. *Eur. J. Med. Chem.* **2010**, *45* (7), 2949–2956.

(51) Oksuzoglu, E.; Tekiner-Gulbas, B.; Alper, S.; Temiz-Arpaci, O.; Ertan, T.; Yildiz, I.; Diril, N.; Sener-Aki, E.; Yalcin, I. Some Benzoxazoles and Benzimidazoles as DNA Topoisomerase I and II Inhibitors. *J. Enzyme Inhib. Med. Chem.* **2008**, *23* (1), 37–42.

(52) Chahrour, O.; Abdalla, A.; Lam, F.; Midgley, C.; Wang, S. Synthesis and Biological Evaluation of Benzyl Styrylsulfonyl Derivatives as Potent Anticancer Mitotic Inhibitors. *Bioorg. Med. Chem. Lett.* **2011**, *21* (10), 3066–3069.

(53) Wang, Z.; Deng, X.; Xiong, S.; Xiong, R.; Liu, J.; Zou, L.; Lei, X.; Cao, X.; Xie, Z.; Chen, Y.; Liu, Y.; Zheng, X.; Tang, G. Design, Synthesis and Biological Evaluation

of Chrysin Benzimidazole Derivatives as Potential Anticancer Agents. *Nat. Prod. Res.* **2018**, *32* (24), 2900–2909.

(54) Yadav, S.; Narasimhan, B.; kaur, H. Perspectives of Benzimidazole Derivatives as Anticancer Agents in the New Era. *Anti-Cancer Agents Med. Chem.* **2016**, *16* (11), 1403 - 1425.

(55) Gaba, M.; Gaba, P.; Uppal, D.; Dhingra, N.; Bahia, M. S.; Silakari, O.; Mohan, C. Benzimidazole Derivatives: Search for GI-Friendly Anti-Inflammatory Analgesic Agents. *Acta Pharm. Sin. B* **2015**, *5* (4), 337–342.

(56) Achar, K. C. S.; Hosamani, K. M.; Seetharamareddy, H. R. In-Vivo Analgesic and Anti-Inflammatory Activities of Newly Synthesized Benzimidazole Derivatives. *Eur. J. Med. Chem.* **2010**, *45* (5), 2048–2054.

(57) Ganie, A. M.; Dar, A. M.; Dar*, F. A. K. and B. A. Benzimidazole Derivatives as Potential Antimicrobial and Antiulcer Agents: *A Mini-Rev. Med. Chem.* **2019**, *19* (16), 1292 - 1297.

(58) Alpan, A. S.; Parlar, S.; Carlino, L.; Tarikogullari, A. H.; Alptüzün, V.; Güneş, H. S. Synthesis, Biological Activity and Molecular Modeling Studies on 1H-Benzimidazole Derivatives as Acetylcholinesterase Inhibitors. *Bioorg. Med. Chem.* **2013**, *21* (17), 4928–4937.

(59) Desai, N. C.; Shihory, N. R.; Kotadiya, G. M.; Desai, P. Synthesis, Antibacterial and Antitubercular Activities of Benzimidazole Bearing Substituted 2-Pyridone Motifs. *Eur. J. Med. Chem.* **2014**, *82*, 480–489.

(60) Starčević, K.; Kralj, M.; Ester, K.; Sabol, I.; Grce, M.; Pavelić, K.; Karminski-Zamola, G. Synthesis, Antiviral and Antitumor Activity of 2-Substituted-5-Amidino-Benzimidazoles. *Bioorg. Med. Chem.* **2007**, *15* (13), 4419–4426.

(61) Valdez, J.; Cedillo, R.; Hernández-Campos, A.; Yépez, L.; Hernández-Luis, F.; Navarrete-Vázquez, G.; Tapia, A.; Cortés, R.; Hernández, M.; Castillo, R. Synthesis and Antiparasitic Activity of 1H-Benzimidazole Derivatives. *Bioorg. Med. Chem. Lett.* **2002**, *12* (16), 2221–2224.

(62) Mayence, A.; Pietka, A.; Collins, M. S.; Cushion, M. T.; Tekwani, B. L.; Huang, T. L.; Vanden Eynde, J. J. Novel Bisbenzimidazoles with Antileishmanial Effectiveness. *Bioorg. Med. Chem. Lett.* **2008**, *18* (8), 2658–2661.

(63) Farahat, A. A.; Ismail, M. A.; Kumar, A.; Wenzler, T.; Brun, R.; Paul, A.; Wilson, W. D.; Boykin, D. W. Indole and Benzimidazole Bichalcophenes: Synthesis, DNA Binding and Antiparasitic Activity. *Eur. J. Med. Chem.* **2018**, *143*, 1590–1596.

(64) Townsend, L. B.; Wise, D. S. The Synthesis and Chemistry of Certain Anthelmintic Benzimidazoles. *Parasitol. Today* **1990**, *6* (4), 107–112.

(65) Salahuddin; Shaharyar, M.; Mazumder, A. Benzimidazoles: A Biologically Active Compounds. *Arabian J. Chem.* **2017**, *10*, S157–S173.

(66) Kumar, J. R.; Jawahar L., J.; Pathak, D. P. Synthesis of Benzimidazole Derivatives: As Anti-Hypertensive Agents. *E-J. Chem.* **2006**, *3* (4), 278–285.

(67) Baumann, M.; Baxendale, I. R.; Ley, S. V.; Nikbin, N. An Overview of the Key Routes to the Best Selling 5-Membered Ring Heterocyclic Pharmaceuticals. *Beilstein J. Org. Chem.* **2011**, *7*, 442–495.

(68) LaBarbera, D. V.; Skibo, E. B. Synthesis of Imidazo[1,5,4-de]Quinoxalin-9-Ones, Benzimidazole Analogues of Pyrroloiminoquinone Marine Natural Products. *Bioorg. Med. Chem.* **2005**, *13* (2), 387–395.

(69) Martins, P.; Jesus, J.; Santos, S.; Raposo, L. R.; Roma-Rodrigues, C.; Baptista, P. V.; Fernandes, A. R. Heterocyclic Anticancer Compounds: Recent Advances and the Paradigm Shift towards the Use of Nanomedicine's Tool Box. *Molecules* **2015**, *20* (9), 16852–16891.

(70) Rajam, S.; Ranjith, R. The Chemistry and Biological Significance of Imidazole, Benzimidazole, Benzoxazole, Tetrazole and Quinazolinone Nucleus. *J. Chem. Pharm. res.* **2016**, 8 (5), 505 - 526.

(71) Gandhi, P.; Schmitt, E. K.; Chen, C.-W.; Samantray, S.; Venishetty, V. K.; Hughes, D. Triclabendazole in the Treatment of Human Fascioliasis: A Review. *Trans. R. Soc. Trop. Med. Hyg.* **2019**, *113* (12), 797 - 804.

(72) Alaqeel, S. I. Synthetic Approaches to Benzimidazoles from O-Phenylenediamine: A Literature Review. *J. Saudi Chem. Soc.* **2017**, *21* (2), 229–237.

(73) Mazurov, A. Traceless Synthesis of Benzimidazoles on Solid Supporty. *Bioorg. Med. Chem. Lett.* **2000**, 4.

(74) Kilburn, J. P.; Lau, J.; Jones, R. C. F. Solid-Phase Synthesis of Substituted 2-Aminomethylbenzimidazoles. *Tetrahedron Lett.* **2000**, *41* (28), 5419–5421.

(75) Vaidyanathan, S.; Surber, B. W. Microwave Mediated Hydrogen Deuterium Exchange: A Rapid Synthesis of 2H-Substituted Benzimidazole. *Tetrahedron Lett.* **2005**, *46* (31), 5195–5197.

(76) Wang, Y.; Sarris, K.; Sauer, D. R.; Djuric, S. W. A Simple and Efficient One Step Synthesis of Benzoxazoles and Benzimidazoles from Carboxylic Acids. *Tetrahedron Lett*. **2006**, *47* (28), 4823–4826.

(77) Das, B.; Holla, H.; Srinivas, Y. Efficient (Bromodimethyl)Sulfonium Bromide Mediated Synthesis of Benzimidazoles. *Tetrahedron Lett*. **2007**, *48* (1), 61–64.

(78) Perkins, J. J.; Zartman, A. E.; Meissner, R. S. Synthesis of 2-(Alkylamino)Benzimidazoles. *Tetrahedron Lett*. **1999**, *40* (6), 1103–1106.

(79) Singhal, S.; Khanna, P.; Panda, S. S.; Khanna, L. Recent Trends in the Synthesis of Benzimidazoles From *o* -Phenylenediamine *via* Nanoparticles and Green Strategies Using Transition Metal Catalysts. *J. Heterocyclic. Chem*. **2019**, *56* (10), 2702–2729.

(80) Rithe, S. R.; Jagtap, R. S.; Ubarhande, S. S. One Pot synthesis of Substituted Benzimidazole Derivatives and their Characterization. *Rasayan J. Chem*. **2015**, *8* (2), 213 - 217.

(81) Samanta, D.; Rana, A.; Bats, J. W.; Schmittel, M. A One-Pot Multistep Cyclization Yielding Thiadiazoloimidazole Derivatives. *Beilstein J. Org. Chem*. **2014**, *10*, 2989–2996.

(82) Herrera Cano, N.; Uranga, J. G.; Nardi, M.; Procopio, A.; Wunderlin, D. A.; Santiago, A. N. Selective and Eco-Friendly Procedures for the Synthesis of Benzimidazole Derivatives. The Role of the $Er(OTf)_3$ Catalyst in the Reaction Selectivity. *Beilstein J. Org. Chem*. **2016**, *12*, 2410–2419.

(83) Venkateswarlu, Y.; Kumar, S.; Leelavathi, P. Facile and Efficient One-Pot Synthesis of Benzimidazoles Using Lanthanum Chloride. *Org. Med. Chem. Lett*. **2013**, *3* (1), 7.

(84) Lai, T. T.; Xie, D.; Zhou, C. H.; Cai, G. X. Copper-Catalyzed Inter/Intramolecular *N* -Alkenylation of Benzimidazoles via Tandem Processes Involving Selectively Mild Iodination of Sp ^{3} C–H Bond at α-Position of Ester. *J. Org. Chem.* **2016**, *81* (19), 8806–8815.

(85) Zhang, R.; Qin, Y.; Zhang, L.; Luo, S. Oxidative Synthesis of Benzimidazoles, Quinoxalines, and Benzoxazoles from Primary Amines by *Ortho* -Quinone Catalysis. *Org. Lett.* **2017**, *19* (20), 5629–5632.

(86) Adharvana Chari, M.; Shobha, D.; Sasaki, T. Room Temperature Synthesis of Benzimidazole Derivatives Using Reusable Cobalt Hydroxide (II) and Cobalt Oxide (II) as Efficient Solid Catalysts. *Tetrahedron Lett.* **2011**, *52* (43), 5575–5580.

(87) Cimarelli, C.; Di Nicola, M.; Diomedi, S.; Giovannini, R.; Hamprecht, D.; Properzi, R.; Sorana, F.; Marcantoni, E. An Efficient One-Pot Two Catalyst System in the Construction of 2-Substituted Benzimidazoles: Synthesis of Benzimidazo[1,2-c]Quinazolines. *Org. Biomol. Chem.* **2015**, *13* (48), 11687–11695.

(88) Carvalho, L. C. R.; Fernandes, E.; Marques, M. M. B. Developments Towards Regioselective Synthesis of 1,2-Disubstituted Benzimidazoles. *Chem. Eur. J.* **2011**, *17* (45), 12544–12555.

(89) Chen, L. H.; Chang, C. M.; Salunke, D. B.; Sun, C. M. Divergent Synthesis of Unsymmetrical Annulated Biheterocyclic Compound Libraries: Benzimidazole Linked Indolo-Benzodiazepines/Quinoxaline. *ACS Comb. Sci.* **2011**, *13* (4), 391–398.

(90) Bahrami, K.; Khodaei, M. M.; Naali, F. Mild and Highly Efficient Method for the Synthesis of 2-Arylbenzimidazoles and 2-Arylbenzothiazoles. *J. Org. Chem.* **2008**, *73* (17), 6835–6837.

(91) Bahrami, K.; Khodaei, M. M.; Nejati, A. Synthesis of 1,2-Disubstituted Benzimidazoles, 2-Substituted Benzimidazoles and 2-Substituted Benzothiazoles in SDS Micelles. *Green Chem*. **2010**, *12* (7), 1237.

(92) Bastug, G.; Eviolitte, C.; Markó, I. E. Functionalized Orthoesters as Powerful Building Blocks for the Efficient Preparation of Heteroaromatic Bicycles. *Org*. *Lett*. **2012**, *14* (13), 3502–3505.

(93) Phillips-Ladenburg Benzimidazole Synthesis. In *Comprehensive Organic Name Reactions and Reagents*; John Wiley & Sons, Inc.: Hoboken, NJ, USA, **2010**; p conrr496.

(94) Lin, S.; Yang, L. A Simple and Efficient Procedure for the Synthesis of Benzimidazoles Using Air as the Oxidant. *Tetrahedron Lett*. **2005**, *46* (25), 4315–4319.

(95) Aggarwal, T.; Kumar, S.; Verma, A. K. Iodine-Mediated Synthesis of Heterocycles via Electrophilic Cyclization of Alkynes. *Org*. *Biomol*. *Chem*. **2016**, *14* (32), 7639–7653.

(96) Mamedov, V. A. Recent Advances in the Synthesis of Benzimidazol(on)Es via Rearrangements of Quinoxalin(on)Es. *RSC Adv*. **2016**, *6* (48), 42132–42172.

(97) Wright, J. B. The Chemistry of the Benzimidazoles. *Chem*. *Rev*. **1951**, *48* (3), 397–541.

(98) Sontakke, V. A.; Ghosh, S.; Lawande, P. P.; Chopade, B. A.; Shinde, V. S. A Simple, Efficient Synthesis of 2-Aryl Benzimidazoles Using Silica Supported Periodic Acid Catalyst and Evaluation of Anticancer Activity. *ISRN Org*. *Chem*. **2013**, *2013*, 1–7.

(99) Pfitzner, K. E.; Moffatt, J. G. A New and Selective Oxidation of Alcohols. *J. Am. Chem. Soc.* **1963**, *85* (19), 3027–3028.

(100) Peng, J.; Ye, M.; Zong, C.; Hu, F.; Feng, L.; Wang, X.; Wang, Y.; Chen, C. Copper-Catalyzed Intramolecular C–N Bond Formation: A Straightforward Synthesis of Benzimidazole Derivatives in Water. *J. Org. Chem.* **2011**, *76* (2), 716–719.

(101) Diao, X.; Wang, Y.; Jiang, Y.; Ma, D. Assembly of Substituted 1 *H* -Benzimidazoles and 1,3-Dihydrobenzimidazol-2-Ones via CuI/ L -Proline Catalyzed Coupling of Aqueous Ammonia with 2-Iodoacetanilides and 2-Iodophenylcarbamates. *J. Org. Chem.* **2009**, *74* (20), 7974–7977.

(102) Chen, C.; Chen, C.; Li, B.; Tao, J.; Peng, J. Aqueous Synthesis of 1-H-2-Substituted Benzimidazoles via Transition-Metal-Free Intramolecular Amination of Aryl Iodides. *Molecules* **2012**, *17* (11), 12506–12520.

(103) Moorthy, J. N.; Neogi, I. IBX-Mediated One-Pot Synthesis of Benzimidazoles from Primary Alcohols and Arylmethyl Bromides. *Tetrahedron Lett.* **2011**, *52* (30), 3868–3871.

(104) Wray, B. C.; Stambuli, J. P. Synthesis of *N* -Arylindazoles and Benzimidazoles from a Common Intermediate. *Organic Lett.* **2010**, *12* (20), 4576–4579.

(105) Wang, Q.; Schreiber, S. L. Copper-Mediated Amidation of Heterocyclic and Aromatic C–H Bonds. *Org. Lett.* **2009**, *11* (22), 5178–5180.

(106) Cui, W.; Kargbo, R. B.; Sajjadi-Hashemi, Z.; Ahmed, F.; Gauuan, J. F. Efficient One-Pot Synthesis of 2-Substituted Benzimidazoles from Triacyloxyborane Intermediates. *Synlett.* **2012**, *2012* (02), 247–250.

(107) Trivedi, R.; De, S. K.; Gibbs, R. A. A Convenient One-Pot Synthesis of 2-Substituted Benzimidazoles. *J. Mol. Catal. A Chem.* **2006**, *245* (1–2), 8 - 11.

(108) Zhang, Z. H.; Yin, L.; Wang, Y. M. An Expeditious Synthesis of Benzimidazole Derivatives Catalyzed by Lewis Acids. *Catal. Commun.* **2007**, *8* (7), 1126–1131.

(109) Cescon, L. A.; Day, A. R. Preparation of Some Benzimidazolylamino Acids. Reactions of Amino Acids with o-Phenylenediamines. *J. Org. Chem.* **1962**, *27* (2), 581–586.

(110) Singla, R.; Gupta, K. B.; Upadhyay, S.; Dhiman, M.; Jaitak, V. Design, Synthesis and Biological Evaluation of Novel Indole-Benzimidazole Hybrids Targeting Estrogen Receptor Alpha (ER-α). *Eur. J. Med. Chem.* **2018**, *146*, 206–219.

(111) Mondal, S.; Thompson, P. R. Protein Arginine Deiminases (PADs): Biochemistry and Chemical Biology of Protein Citrullination. *Acc. Chem. Res.* **2019**, *52* (3), 818–832.

(112) Lewis, H. D.; Liddle, J.; Coote, J. E.; Atkinson, S. J.; Barker, M. D.; Bax, B. D.; Bicker, K. L.; Bingham, R. P.; Campbell, M.; Chen, Y. H.; Chung, C.; Craggs, P. D.; Davis, R. P.; Eberhard, D.; Joberty, G.; Lind, K. E.; Locke, K.; Maller, C.; Martinod, K.; Patten, C.; Polyakova, O.; Rise, C. E.; Rüdiger, M.; Sheppard, R. J.; Slade, D. J.; Thomas, P.; Thorpe, J.; Yao, G.; Drewes, G.; Wagner, D. D.; Thompson, P. R.; Prinjha, R. K.; Wilson, D. M. Inhibition of PAD4 Activity Is Sufficient to Disrupt Mouse and Human NET Formation. *Nat. Chem. Biol.* **2015**, *11*, 189.

(113) Fuhrmann, J.; Thompson, P. R. Protein Arginine Methylation and Citrullination in Epigenetic Regulation. *ACS Chem. Biol.* **2016**, *11* (3), 654–668.

(114) Kenner, G. W.; McCombie, S. W.; Smith, K. M. Pyrroles and Related Compounds. Part XXIV. Separation and Oxidative Degradation of Chlorophyll Derivatives. *J. Chem. Soc., Perkin Trans. 1* **1973**, 2517.

(115) Chakraborty, A.; Debnath, S.; Ghosh, T.; Maiti, D. K.; Majumdar, S. An Efficient Strategy for N-Alkylation of Benzimidazoles/Imidazoles in SDS-Aqueous Basic Medium and N-Alkylation Induced Ring Opening of Benzimidazoles. *Tetrahedron* **2018**, *74* (40), 5932–5941.

(116) Karchava, A. V.; Melkonyan, F. S.; Yurovskaya, M. A. New Strategies for the Synthesis of N-Alkylated Indoles (Review). *Chem. Heterocycl. Comp.* **2012**, *48* (3), 391–407.

(117) Earle, M. J.; McCormac, P. B.; Seddon, K. R. Regioselective Alkylation in Ionic Liquids. *Chem. Commun.* **1998**, No. 20, 2245–2246.

(118) Le, Z.-G.; Chen, Z.-C.; Hu, Y.; Zheng, Q.-G. Organic Reactions in Ionic Liquids: A Simple and Highly Regioselective N-Substitution of Pyrrole. *Synth.* **2004**, *2004* (12), 1951–1954.

(119) Siegel, R. L.; Miller, K. D.; Jemal, A. Cancer Statistics, 2019. *CA. A Cancer J. Clin.* **2019**, *69* (1), 7 – 34.

(120) Street, W. Cancer Facts & Figures 2020. **1930**, 76.

(121) Siegel, R. L.; Miller, K. D.; Jemal, A. Cancer Statistics, 2017. *CA: A Cancer J. Clin.* **2017**, *67* (1), 7 – 30.

(122) Types of Cancer Treatment https://www.cancer.gov/about-cancer/treatment/types.

(123) Liang, X. J.; Chen, C.; Zhao, Y.; Wang, P. C. Circumventing Tumor Resistance to Chemotherapy by Nanotechnology. In *Multi-Drug Resist. Cancer*. **2010**, *596*, 467 - 488.

(124) Holohan, C.; Van Schaeybroeck, S.; Longley, D. B.; Johnston, P. G. Cancer Drug Resistance: An Evolving Paradigm. *Nat. Rev. Cancer* **2013**, *13* (10), 714 - 726.

(125) Markman, J. L.; Rekechenetskiy, A.; Holler, E.; Ljubimova, J. Y. Nanomedicine Therapeutic Approaches to Overcome Cancer Drug Resistance. *Adv. Drug Deliv. Rev.* **2013**, *65* (13–14), 1866 - 1879.

(126) Krzyszczyk, P.; Acevedo, A.; Davidoff, E. J.; Timmins, L. M.; Marrero-Berrios, I.; Patel, M.; White, C.; Lowe, C.; Sherba, J. J.; Hartmanshenn, C.; O'Neill, K. M.; Balter, M. L.; Fritz, Z. R.; Androulakis, I. P.; Schloss, R. S.; Yarmush, M. L. The Growing Role of Precision and Personalized Medicine for Cancer Treatment. *Technology* **2018**, *06* (03n04), 79–100.

(127) Mokhtari, R. B.; Homayouni, T. S.; Baluch, N.; Morgatskaya, E.; Kumar, S.; Das, B.; Yeger, H. Combination Therapy in Combating Cancer. *Oncotarget* **2017**, *8* (23).

(128) Reese, M. J.; Knapp, D. W.; Anderson, K. M.; Mund, J. A.; Case, J.; Jones, D. R.; Packer, R. A. In Vitro Effect of Chlorambucil on Human Glioma Cell Lines (SF767 and U87-MG), and Human Microvascular Endothelial Cell (HMVEC) and Endothelial Progenitor Cells (ECFCs), in the Context of Plasma Chlorambucil Concentrations in Tumor-Bearing Dogs. *PLoS ONE* **2018**, *13* (9), e0203517.

(129) Di Antonio, M.; McLuckie, K. I. E.; Balasubramanian, S. Reprogramming the Mechanism of Action of Chlorambucil by Coupling to a G-Quadruplex Ligand. *J. Am. Chem. Soc.* **2014**, *136* (16), 5860–5863.

(130) Panasci, L.; Paiement, J.-P.; Christodoulopoulos, G.; Belenkov, A.; Malapetsa, A.; Aloyz, R. Chlorambucil Drug Resistance in Chronic Lymphocytic Leukemia: The Emerging Role of DNA Repair. *Clin. Cancer Res*. **2001**, *7*(3),454-461.

(131) Longley, D. B.; Harkin, D. P.; Johnston, P. G. 5-Fluorouracil: Mechanisms of Action and Clinical Strategies. *Nat. Rev. Cancer* **2003**, *3* (5), 330–338.

(132) Mader, R. M.; Müller, M.; Steger, G. G. Resistance to 5-Fluorouracil. *General Pharmacology: The Vascular System* **1998**, *31* (5), 661–666.

(133) Pommier, Y.; Leo, E.; Zhang, H.; Marchand, C. DNA Topoisomerases and Their Poisoning by Anticancer and Antibacterial Drugs. *Chem. Bio*. **2010**, *17* (5), 421–433.

(134) Helmbach, H.; Kern, M. A.; Rossmann, E.; Renz, K.; Kissel, C.; Gschwendt, B.; Schadendorf, D. Drug Resistance Towards Etoposide and Cisplatin in Human Melanoma Cells Is Associated with Drug-Dependent Apoptosis Deficiency. *J. Investi. Derma.* **2002**, *118* (6), 923 – 932.

(135) Kanwal, A.; Saddique, F. A.; Aslam, S.; Ahmad, M.; Zahoor, A. F.; Mohsin, N.-A. Benzimidazole Ring System as a Privileged Template for Anticancer Agents. *Pharm. Chem. J*. **2018**, *51* (12), 1068–1077.

(136) Purushottamachar, P.; Ramalingam, S.; C.O. Njar, V. Development of Benzimidazole Compounds for Cancer Therapy. In *Chemistry and Applications of Benzimidazole and its Derivatives*; Marinescu, M., Ed.; IntechOpen, **2019**.

(137) Hoy, S. M. Bendamustine: A Review of Its Use in the Management of Chronic Lymphocytic Leukaemia, Rituximab-Refractory Indolent Non-Hodgkin's Lymphoma and Multiple Myeloma. *Drugs* **2012**, *72* (14), 1929–1950.

(138) Wagner, L. Profile of Veliparib and Its Potential in the Treatment of Solid Tumors. *Onco Targets Ther.* **2015**, 1931.

(139) Decaudin, D.; El Botty, R.; Diallo, B.; Massonnet, G.; Fleury, J.; Naguez, A.; Raymondie, C.; Davies, E.; Smith, A.; Wilson, J.; Howes, C.; Smith, P. D.; Cassoux, N.; Piperno-Neumann, S.; Roman-Roman, S.; Némati, F. Selumetinib-Based Therapy in Uveal Melanoma Patient-Derived Xenografts. *Oncotarget* **2018**, *9* (31), 21674–21686.

(140) McClurg, U. L.; Azizyan, M.; Dransfield, D. T.; Namdev, N.; Chit, N. C. T. H.; Nakjang, S.; Robson, C. N. The Novel Anti-Androgen Candidate Galeterone Targets Deubiquitinating Enzymes, USP12 and USP46, to Control Prostate Cancer Growth and Survival. *Oncotarget* **2018**, *9* (38), 24992–25007.

(141) Eilers, U.; Klumperman, J.; Hauri, H. P. Nocodazole, a Microtubule-Active Drug, Interferes with Apical Protein Delivery in Cultured Intestinal Epithelial Cells (Caco-2). *J. Cell Bio.* **1989**, *108* (1), 13–22.

(142) Hranjec, M.; Kralj, M.; Piantanida, I.; Sedić, M.; Šuman, L.; Pavelić, K.; Karminski-Zamola, G. Novel Cyano- and Amidino-Substituted Derivatives of Styryl-2-Benzimidazoles and Benzimidazo[1,2-a]Quinolines. Synthesis, Photochemical Synthesis, DNA Binding, and Antitumor Evaluation, Part 3. *J. Med. Chem.* **2007**, *50* (23), 5696–5711.

(143) Bansal, Y.; Silakari, O. The Therapeutic Journey of Benzimidazoles: A Review. *Bioorg. Med. Chem.* **2012**, *20* (21), 6208–6236.

(144) Carreira, A. C.; Alves, G. G.; Zambuzzi, W. F.; Sogayar, M. C.; Granjeiro, J. M. Bone Morphogenetic Proteins: Structure, Biological Function and Therapeutic Applications. *Arch. Biochem. Biophys.* **2014**, *561*, 64 - 73.

(145) Wang, R. N.; Green, J.; Wang, Z.; Deng, Y.; Qiao, M.; Peabody, M.; Zhang, Q.; Ye, J.; Yan, Z.; Denduluri, S.; Idowu, O.; Li, M.; Shen, C.; Hu, A.; Haydon, R. C.; Kang, R.; Mok, J.; Lee, M. J.; Luu, H. L.; Shi, L. L. Bone Morphogenetic Protein (BMP) Signaling in Development and Human Diseases. *Genes & Diseases* **2014**, *1* (1), 87–105.

(146) Prakash, C. A.; Parthiban, J.; Balakrishnan, R.; Anandh, B.; Lokesh, B. Bone Morphogenetic Proteins-An Update. *Biomed. Pharmacol. J.* **2015**, *8*, 329–333.

(147) Genthe, J. R.; Min, J.; Farmer, D. M.; Shelat, A. A.; Grenet, J. A.; Lin, W.; Finkelstein, D.; Vrijens, K.; Chen, T.; Guy, R. K.; Clements, W. K.; Roussel, M. F. Ventromorphins: A New Class of Small Molecule Activators of the Canonical BMP Signaling Pathway. *ACS Chem. Biol.* **2017**, *12* (9), 2436–2447.

(148) Katagiri, T.; Watabe, T. Bone Morphogenetic Proteins. *Cold Spring Harb. Perspect. Biol.* **2016**, *8* (6), a021899.

(149) Chen, D.; Zhao, M.; Mundy, G. R. Bone Morphogenetic Proteins. *Growth Factors* **2004**, *22* (4), 233–241.

(150) Grinspan, J. B. Bone Morphogenetic Proteins. *Vitam. Horm.* **2015**, 99, 195 - 222.

(151) Bradford, S. T. J.; Ranghini, E. J.; Grimley, E.; Lee, P. H.; Dressler, G. R. High-Throughput Screens for Agonists of Bone Morphogenetic Protein (BMP) Signaling Identify Potent Benzoxazole Compounds. *J. Biol. Chem.* **2019**, *294* (9), 3125–3136.

(152) Xiao, Y. T.; Xiang, L. X.; Shao, J. Z. Bone Morphogenetic Protein. *Biochem. Biophys. Re. Commun.* **2007**, *362* (3), 550 - 553.

(153) Chenard, K. E.; Teven, C. M.; He, T. C.; Reid, R. R. Bone Morphogenetic Proteins in Craniofacial Surgery: Current Techniques, Clinical Experiences, and the Future of Personalized Stem Cell Therapy. *J. Biomed. Biotechnol.* **2012**, *2012*, 1 - 14.

(154) Peng, J.; Li, Q.; Wigglesworth, K.; Rangarajan, A.; Kattamuri, C.; Peterson, R. T.; Eppig, J. J.; Thompson, T. B.; Matzuk, M. M. Growth Differentiation Factor 9: Bone Morphogenetic Protein 15 Heterodimers Are Potent Regulators of Ovarian Functions. *Proc. Natl. Acad. Sci.* **2013**, *110* (8), E776 - E785.

(155) Rengachary, S. S. Bone Morphogenetic Proteins: Basic Concepts. Neurosurg. Focus **2002**, *13* (6), 1–6.

(156) Miyazono, K. Signal Transduction by Bone Morphogenetic Protein Receptors: Functional Roles of Smad Proteins. *Bone* **1999**, *25* (1), 91–93.

(157) Cecchi, S.; Bennet, S. J.; Arora, M. Bone Morphogenetic Protein-7: Review of Signalling and Efficacy in Fracture Healing. *J. Orthop. Translat.* **2016**, *4*, 28 - 34.

(158) Oryan, A.; Alidadi, S.; Moshiri, A.; Bigham-Sadegh, A. Bone Morphogenetic Proteins: A Powerful Osteoinductive Compound with Non-Negligible Side Effects and Limitations: Bone Morphogenetic Proteins in Bone Healing. *BioFactors* **2014**, *40* (5), 459–481.

(159) Heldin, C.-H.; Moustakas, A. Signaling Receptors for TGF-β Family Members. *Cold Spring Harb. Perspect. Biol.* **2016**, *8* (8), a022053.

(160) Chen, G.; Deng, C.; Li, Y.-P. TGF-β and BMP Signaling in Osteoblast Differentiation and Bone Formation. *Int. J. Biol. Sci.* **2012**, *8* (2), 272–288.

(161) Chan, C. K. Y.; Mason, A.; Cooper, C.; Dennison, E. Novel Advances in the Treatment of Osteoporosis. **2016**, *119*, 13.

(162) Wang, N.; Zhao, G.; Zhang, Y.; Wang, X.; Zhao, L.; Xu, P.; Shou, D. A Network Pharmacology Approach to Determine the Active Components and Potential Targets of Curculigo Orchioides in the Treatment of Osteoporosis. *Med. Sci. Monit.* **2017**, *23*, 5113–5122.

(163) Diwan, A. D.; Leong, A.; Appleyard, R.; Bhargav, D.; Fang, Z. M.; Wei, A. Bone Morphogenetic Protein-7 Accelerates Fracture Healing in Osteoporotic Rats. *Indian J. Orthop.* **2013**, *47* (6), 540–546.

(164) Varanasi, S. S.; Tuck, S. P.; Mastana, S. S.; Dennison, E.; Cooper, C.; Vila, J.; Francis, R. M.; Datta, H. K. Lack of Association of Bone Morphogenetic Protein 2 Gene Haplotypes with Bone Mineral Density, Bone Loss, or Risk of Fractures in Men. *J. Osteoporos* **2011**, *2011*.

(165) Odén, A.; McCloskey, E. V.; Kanis, J. A.; Harvey, N. C.; Johansson, H. Burden of High Fracture Probability Worldwide: Secular Increases 2010-2040. *Osteoporos Int.* **2015**, *26* (9), 2243–2248.

(166) Yp, Z.; Ry, X.; B, Z.; F, Z.; Xs, Z.; Ll, Z.; H, L. Gender Differences on Osteoporosis Health Beliefs and Related Behaviors in Non-Academic Community Chinese. *J Community Health* **2014**, *39* (3), 545–551.

(167) Khosla, S.; Hofbauer, L. C. Osteoporosis Treatment: Recent Developments and Ongoing Challenges. *The Lancet Diabetes & Endocrinology* **2017**, *5* (11), 898–907.

(168) Zhao, B.; Xing, G.; Wang, A. The BMP Signaling Pathway Enhances the Osteoblastic Differentiation of Bone Marrow Mesenchymal Stem Cells in Rats with Osteoporosis. *J. Orthop. Surg. Res.* **2019**, *14* (1), 462.

(169) Kanakaris, N. K.; Petsatodis, G.; Tagil, M.; Giannoudis, P. V. Is There a Role for Bone Morphogenetic Proteins in Osteoporotic Fractures? *Injury* **2009**, *40*, S21–S26.

(170) Khosla, S.; Westendorf, J. J.; Oursler, M. J. Building Bone to Reverse Osteoporosis and Repair Fractures. *J. Clin. Invest.* **2008**, *118* (2), 421–428.

(171) Yang, J. Bone Morphogenetic Proteins: Relationship between Molecular Structure and Their Osteogenic Activity. *Food Science and Human Wellness* **2014**, 9.

(172) Dumic-Cule, I.; Peric, M.; Kucko, L.; Grgurevic, L.; Pecina, M.; Vukicevic, S. Bone Morphogenetic Proteins in Fracture Repair. *International Orthopaedics (SICOT)* **2018**, *42* (11), 2619–2626.

(173) Feng, L.; Cook, B.; Tsai, S.-Y.; Zhou, T.; LaFlamme, B.; Evans, T.; Chen, S. Discovery of a Small-Molecule BMP Sensitizer for Human Embryonic Stem Cell Differentiation. *Cell Rep.* **2016**, *15* (9), 2063–2075.

(174) Vrijens, K.; Lin, W.; Cui, J.; Farmer, D.; Low, J.; Pronier, E.; Zeng, F.-Y.; Shelat, A. A.; Guy, K.; Taylor, M. R.; Chen, T.; Roussel, M. F. Identification of Small Molecule Activators of BMP Signaling. *PLoS ONE* **2013**, *8* (3), e59045.

(175) Yu, P. B.; Hong, C. C.; Sachidanandan, C.; Babitt, J. L.; Deng, D. Y.; Hoyng, S. A.; Lin, H. Y.; Bloch, K. D.; Peterson, R. T. Dorsomorphin Inhibits BMP Signals Required for Embryogenesis and Iron Metabolism. *Nat. Chem. Biol.* **2008**, *4* (1), 33–41.

(176) Pigeon, C.; Ilyin, G.; Courselaud, B.; Leroyer, P.; Turlin, B.; Brissot, P. A New Mouse Liver-Specific Gene, Encoding a Protein Homologous to Human Antimicrobial Peptide Hepcidin, Is Overexpressed during Iron Overload. 10.

(177) Fraenkel, P. G.; Traver, D.; Donovan, A.; Zahrieh, D.; Zon, L. I. Ferroportin1 Is Required for Normal Iron Cycling in Zebrafish. *J. Clin. Invest.* **2005**, *115* (6), 1532–1541.

(178) Silvestri, L.; Nai, A.; Dulja, A.; Pagani, A. Hepcidin and the BMP-SMAD Pathway: An Unexpected Liaison. In *Vitamins and Hormones*; Elsevier, 2019; Vol. 110, pp 71–99.

(179) Nemeth, E. Hepcidin Regulates Cellular Iron Efflux by Binding to Ferroportin and Inducing Its Internalization. *Science* **2004**, *306* (5704), 2090–2093.

(180) Anderson, G. J.; Darshan, D. Small-Molecule Dissection of BMP Signaling. *Nat. Chem. Biol.* **2008**, *4* (1), 15–16.

(181) Cuny, G. D.; Yu, P. B.; Laha, J. K.; Xing, X.; Liu, J.-F.; Lai, C. S.; Deng, D. Y.; Sachidanandan, C.; Bloch, K. D.; Peterson, R. T. Structure–Activity Relationship Study of Bone Morphogenetic Protein (BMP) Signaling Inhibitors. *Bioorg. Med. Chem. Lett.* **2008**, *18* (15), 4388–4392.

(182) Hong, C. C.; Yu, P. B. Applications of Small Molecule BMP Inhibitors in Physiology and Disease. *Cytokine & Growth Factor Reviews* **2009**, *20* (5–6), 409–418.

(183) Baek, S.; Choi, S.-W.; Park, S.-J.; Lee, S.-H.; Chun, H.-S.; Kim, S. H. Quinoline Compound KM11073 Enhances BMP-2-Dependent Osteogenic Differentiation of

C2C12 Cells via Activation of P38 Signaling and Exhibits In Vivo Bone Forming Activity. *PLoS ONE* **2015**, *10* (3), e0120150.

(184) Cao, Y.; Wang, C.; Zhang, X.; Xing, G.; Lu, K.; Gu, Y.; He, F.; Zhang, L. Selective Small Molecule Compounds Increase BMP-2 Responsiveness by Inhibiting Smurf1-Mediated Smad1/5 Degradation. *Sci. Rep.* **2015**, *4* (1), 4965.

(185) Beaulieu, P. L.; Gillard, J.; Jolicoeur, E.; Duan, J.; Garneau, M.; Kukolj, G.; Poupart, M.-A. From Benzimidazole to Indole-5-Carboxamide Thumb Pocket I Inhibitors of HCV NS5B Polymerase. Part 1: Indole C-2 SAR and Discovery of Diamide Derivatives with Nanomolar Potency in Cell-Based Subgenomic Replicons. *Bioorg. Med. Chem. Lett.* **2011**, *21* (12), 3658–3663.

(186) Brands, M.; Ergüden, J.-K.; Hashimoto, K.; Heimbach, D.; Schröder, C.; Siegel, S.; Stasch, J.-P.; Weigand, S. Novel, Selective Indole-Based ECE Inhibitors: Lead Optimization via Solid-Phase and Classical Synthesis. *Bioorg. Med. Chem. Lett.* **2005**, *15* (19), 4201–4205.

(187) Zhuo, S.-T.; Li, C.-Y.; Hu, M.-H.; Chen, S.-B.; Yao, P.-F.; Huang, S.-L.; Ou, T.-M.; Tan, J.-H.; An, L.-K.; Li, D.; Gu, L.-Q.; Huang, Z.-S. Synthesis and Biological Evaluation of Benzo[a]Phenazine Derivatives as a Dual Inhibitor of Topoisomerase I and II. *Org. Biomol. Chem.* **2013**, *11* (24), 3989.

(188) Li, P.-H.; Zeng, P.; Chen, S.-B.; Yao, P.-F.; Mai, Y.-W.; Tan, J.-H.; Ou, T.-M.; Huang, S.-L.; Li, D.; Gu, L.-Q.; Huang, Z.-S. Synthesis and Mechanism Studies of 1,3-Benzoazolyl Substituted Pyrrolo[2,3- *b*]Pyrazine Derivatives as Nonintercalative Topoisomerase II Catalytic Inhibitors. *J. Med. Chem.* **2016**, *59* (1), 238–252.

(189) Li, P.; Zhang, W.; Jiang, H.; Li, Y.; Dong, C.; Chen, H.; Zhang, K.; Du, Z. Design, Synthesis and Biological Evaluation of Benzimidazole–Rhodanine Conjugates as Potent Topoisomerase II Inhibitors. *MedChemComm* **2018**, *9* (7), 1194–1205.

(190) Mosmann, T. Rapid Colorimetric Assay for Cellular Growth and Survival: Application to Proliferation and Cytotoxicity Assays. *J. Immunol. Methods* **1983**, *65* (1–2), 55–63.

(191) Refaat, H. M. Synthesis and Anticancer Activity of Some Novel 2-Substituted Benzimidazole Derivatives. *Eur. J. Med. Chem.* **2010**, *45* (7), 2949–2956.

(192) Ozden, S.; Karataş, H.; Yildiz, S.; Göker, H. Synthesis and Potent Antimicrobial Activity of Some Novel 4-(5, 6-Dichloro-1H-Benzimidazol-2-Yl)-N-Substituted Benzamides. *Arch. Pharm. (Weinheim)* **2004**, *337* (10), 556–562.

(193) Stevens, C. L.; Singhal, G. H.; Ash, A. B. Carbodiimides. Dehydration of Ureas. *J. Org. Chem.* **1967**, *32* (9), 2895–2895.

(194) Wan, Z.-K.; Ousman, E. F.; Papaioannou, N.; Saiah, E. Phosphonium-Mediated Cyclization of N-(2-Aminophenyl)Thioureas: Efficient Synthesis of 2-Aminobenzimidazoles. *Tetrahedron Lett.* **2011**, *52* (32), 4149–4152.

(195) Kaushik, N. K.; Kaushik, N.; Attri, P.; Kumar, N.; Kim, C. H.; Verma, A. K.; Choi, E. H. Biomedical Importance of Indoles. *Molecules* **2013**, *18* (6), 6620–6662.

(196) Maekawa, K.; Ohtani, J. Synthesis of 1,2,3,4-Tetrahydro-1-Oxo-Pyrido[1,2-a]Benzimidazole. *Agric. Bio. Chem.* **1978**, *42* (2), 483 – 484.

(197) Singh, S.; Prasad, N. R.; Chufan, E. E.; Patel, B. A.; Wang, Y.-J.; Chen, Z.-S.; Ambudkar, S. V.; Talele, T. T. Design and Synthesis of Human ABCB1 (P-Glycoprotein) Inhibitors by Peptide Coupling of Diverse Chemical Scaffolds on

Carboxyl and Amino Termini of (*S*)-Valine-Derived Thiazole Amino Acid. *J. Med. Chem.* **2014**, *57* (10), 4058–4072.

(198) Akhtar, W.; Khan, M. F.; Verma, G.; Shaquiquzzaman, M.; Rizvi, M. A.; Mehdi, S. H.; Akhter, M.; Alam, M. M. Therapeutic Evolution of Benzimidazole Derivatives in the Last Quinquennial Period. *Eur. J. Med. Chem.* **2017**, *126*, 705–753.

(199) Ateş-Alagöz, Z.; Kuş, C.; Çoban, T. Synthesis and Antioxidant Properties of Novel Benzimidazoles Containing Substituted Indole or 1,1,4,4-Tetramethyl-1,2,3,4-Tetrahydro-Naphthalene Fragments. *J. Enzyme Inhib. Med. Chem.* **2005**, *20* (4), 325–331.

(200) Lee, Y. T.; Chiu, F. Y.; Barve, I. J.; Sun, C. M. Microwave-Assisted Synthesis of Benzimidazole-Linked Indoline and Indole Hybrids from C-2 Linked (*o* -Aminobenzyl)Benzimidazoles. *Adv. Synth. Catal.* **2018**, *360* (3), 502–512.

(201) Yu, X. H.; Hong, X. Q.; Chen, W. H. Fluorinated Bisbenzimidazoles: A New Class of Drug-like Anion Transporters with Chloride-Mediated, Cell Apoptosis-Inducing Activity. *Org. Biomol. Chem.* **2019**, *17* (6), 1558–1571.

(202) Simó-Vicens, R.; Bomholtz, S. H.; Sørensen, U. S.; Bentzen, B. H. 2,6-Bis(2-Benzimidazolyl)Pyridine (BBP) Is a Potent and Selective Inhibitor of Small Conductance Calcium-Activated Potassium (SK) Channels. *Front. Pharmacol.* **2018**, *9*, 1409.

(203) Petoud, S.; Bünzli, J. C. G.; Schenk, K. J.; Piguet, C. Luminescent Properties of Lanthanide Nitrato Complexes with Substituted Bis(Benzimidazolyl)Pyridines. *Inorg. Chem.* **1997**, *36* (7), 1345–1353.

(204) Wei, S. Y.; Wang, J. L.; Zhang, C. S.; Xu, X. T.; Zhang, X. X.; Wang, J. X.; Xing, Y.-H. D ^{7} /d ^{8} Metal Complexes Constructed from 2,6-Bis(2-Benzimidazolyl)Pyridyl or 2,6-Di-(Pyrazol-3-Yl)Pyridine Derivatives: Synthesis, Structure, Characterization, and Photocatalytic Activity. *ChemPlusChem* **2015**, *80* (3), 549–558.

(205) Tam, A. Y.-Y.; Lam, W. H.; Wong, K. M.-C.; Zhu, N.; Yam, V. W.-W. Luminescent Alkynylplatinum(II) Complexes of 2,6-Bis(N-Alkylbenzimidazol-2′-Yl)Pyridine-Type Ligands with Ready Tunability of the Nature of the Emissive States by Solvent and Electronic Property Modulation. *Chem. Eur. J.* **2008**, *14* (15), 4562–4576.

(206) Musiu, S.; Pürstinger, G.; Stallinger, S.; Vrancken, R.; Haegeman, A.; Koenen, F.; Leyssen, P.; Froeyen, M.; Neyts, J.; Paeshuyse, J. Substituted 2,6-Bis(Benzimidazol-2-Yl)Pyridines: A Novel Chemical Class of Pestivirus Inhibitors That Targets a Hot Spot for Inhibition of Pestivirus Replication in the RNA-Dependent RNA Polymerase. *Antiviral Research* **2014**, *106*, 71–79.

(207) Li, L.; Cao, W.; Zheng, W.; Fan, C.; Chen, T. Ruthenium Complexes Containing 2,6-Bis(Benzimidazolyl)Pyridine Derivatives Induce Cancer Cell Apoptosis by Triggering DNA Damage-Mediated P53 Phosphorylation. *Dalton Trans.* **2012**, *41* (41), 12766.

(208) Liu, S.; Cao, W.; Yu, L.; Zheng, W.; Li, L.; Fan, C.; Chen, T. Zinc(Ii) Complexes Containing Bis-Benzimidazole Derivatives as a New Class of Apoptosis Inducers That Trigger DNA Damage-Mediated P53 Phosphorylation in Cancer Cells. *Dalton Trans.* **2013**, *42* (16), 5932.

(209) Hewitt, N. J.; Hewitt, P. Phase I and II Enzyme Characterization of Two Sources of HepG2 Cell Lines. *Xenobiotica* **2004**, *34* (3), 243–256.

(210) Yarlagadda, V.; Akkapeddi, P.; Manjunath, G. B.; Haldar, J. Membrane Active Vancomycin Analogues: A Strategy to Combat Bacterial Resistance. *J. Med. Chem.* **2014**, *57* (11), 4558–4568.

(211) Yoganathan, S.; Miller, S. J. Structure Diversification of Vancomycin through Peptide-Catalyzed, Site-Selective Lipidation: A Catalysis-Based Approach To Combat Glycopeptide-Resistant Pathogens. *J. Med. Chem.* **2015**, *58* (5), 2367–2377.

(212) Yadav, S.; Narasimhan, B.; Kaur, H. Perspectives of Benzimidazole Derivatives as Anticancer Agents in the New Era. *Anti-cancer Agents Med. Chem.* **2016**, *16* (11), 1403–1425.

(213) El Rashedy, A. A.; Aboul-Enein, H. Y. Benzimidazole Derivatives as Potential Anticancer Agents. *Mini Rev. Med. Chem.* **2013**, *13* (3), 399–407.

(214) Willmore, E.; Frank, A. J.; Padget, K.; Tilby, M. J.; Austin, C. A. Etoposide Targets Topoisomerase IIalpha and IIbeta in Leukemic Cells: Isoform-Specific Cleavable Complexes Visualized and Quantified in Situ by a Novel Immunofluorescence Technique. *Mol. Pharmacol.* **1998**, *54* (1), 78–85.

(215) Shrestha, A.; Jo, H.; Kwon, Y.; Lee, E.-S. Design, Synthesis, and Structure-Activity Relationships of New Benzofuro[3,2-b]Pyridin-7-Ols as DNA Topoisomerase II Inhibitors. *Bioorg. Med. Chem. Lett.* **2018**, *28* (4), 566–571.

(216) Vos, S. M.; Tretter, E. M.; Schmidt, B. H.; Berger, J. M. All Tangled up: How Cells Direct, Manage and Exploit Topoisomerase Function. *Nat. Rev. Mol. Cell Biol.* **2011**, *12* (12), 827–841.

(217) Atwell, G. J.; Rewcastle, G. W.; Baguley, B. C.; Denny, W. A. Potential Antitumor Agents. 50. In Vivo Solid-Tumor Activity of Derivatives of N-[2-(Dimethylamino)Ethyl]Acridine-4-Carboxamide. *J. Med. Chem.* **1987**, *30* (4), 664–669.

(218) Ortega, J. A.; Riccardi, L.; Minniti, E.; Borgogno, M.; Arencibia, J. M.; Greco, M. L.; Minarini, A.; Sissi, C.; De Vivo, M. Pharmacophore Hybridization To Discover Novel Topoisomerase II Poisons with Promising Antiproliferative Activity. *J. Med. Chem.* **2018**, *61* (3), 1375–1379.

(219) Beerman, T. A.; McHugh, M. M.; Sigmund, R.; Lown, J. W.; Rao, K. E.; Bathini, Y. Effects of Analogs of the DNA Minor Groove Binder Hoechst 33258 on Topoisomerase II and I Mediated Activities. *Biochim. Biophys. Acta* **1992**, *1131* (1), 53 - 61.

(220) Hasinoff, B. B.; Wu, X.; Nitiss, J. L.; Kanagasabai, R.; Yalowich, J. C. The Anticancer Multi-Kinase Inhibitor Dovitinib Also Targets Topoisomerase I and Topoisomerase II. *Pharmacol.* **2012**, *84* (12), 1617 - 1626.

(221) Seaton, A.; Higgins, C.; Mann, J.; Baron, A.; Bailly, C.; Neidle, S.; van den Berg, H. Mechanistic and Anti-Proliferative Studies of Two Novel, Biologically Active Bis-Benzimidazoles. *Eur. J. Cancer* **2003**, *39* (17), 2548–2555.

(222) Tolner, B.; Hartley, J. A.; Hochhauser, D. Transcriptional Regulation of Topoisomerase II␣ at Confluence and Pharmacological Modulation of Expression by Bis-Benzimidazole Drugs. *Mol. Pharmacol.* **2001**, 59 (4), 699 - 706.

(223) Chamberlin, J.; Story, S.; Ranjan, N.; Chesser, G.; Arya, D. P. Gram-Negative Synergy and Mechanism of Action of Alkynyl Bisbenzimidazoles. *Sci. Rep.* **2019**, *9* (1), 14171.

(224) Bell, C. A.; Dykstra, C. C.; Naiman, N. A.; Cory, M.; Fairley, T. A.; Tidwell, R. R. Structure-Activity Studies of Dicationically Substituted Bis-Benzimidazoles against Giardia Lamblia: Correlation of Antigiardial Activity with DNA Binding Affinity and Giardial Topoisomerase II Inhibition. *Antimicrob. Agents Chemother.* **1993**, *37* (12), 2668 - 2673.

(225) Dale, A. G.; Hinds, J.; Mann, J.; Taylor, P. W.; Neidle, S. Symmetric Bis-Benzimidazoles Are Potent Anti-Staphylococcal Agents with Dual Inhibitory Mechanisms against DNA Gyrase. *Biochemistry* **2012**, *51* (29), 5860–5871.

(226) Nimesh, H.; Sur, S.; Sinha, D.; Yadav, P.; Anand, P.; Bajaj, P.; Virdi, J. S.; Tandon, V. Synthesis and Biological Evaluation of Novel Bisbenzimidazoles as *Escherichia Coli* Topoisomerase IA Inhibitors and Potential Antibacterial Agents. *J. Med. Chem.* **2014**, *57* (12), 5238–5257.

(227) Smith, P. J.; Anderson, C. O. Modification of the Radiation Sensitivity of Human Tumour Cells by a Bis-Benzimidazole Derivative. *Int. J. Radiat. Biol.* **1984**, *46* (4), 331 - 344.

(228) Tawar, U.; Jain, A. K.; Dwarakanath, B. S.; Chandra, R.; Singh, Y.; Chaudhury, N. K.; Khaitan, D.; Tandon, V. Influence of Phenyl Ring Disubstitution on Bisbenzimidazole and Terbenzimidazole Cytotoxicity: Synthesis and Biological Evaluation as Radioprotectors. *J. Med. Chem.* **2003**, *46* (18), 3785–3792.

(229) Bhattacharya, S.; Chaudhuri, P. Medical Implications of Benzimidazole Derivatives as Drugs Designed for Targeting DNA and DNA Associated Processes. *Curr. Med. Chem.* **2008**, *15* (18), 1762–1777.

(230) Darii, M. V.; Rakhimova, A. R.; Tashlitsky, V. N.; Kostyuk, S. V.; Veiko, N. N.; Ivanov, A. A.; Zhuze, A. L.; Gromova, E. S. Dimeric Bisbenzimidazoles: Cytotoxicity and Effects on DNA Methylation in Normal and Cancer Human Cells. *Mol. Biol.* **2013**, *47* (2), 259–266.

(231) Wu, H.; Huang, X.; Yuan, J.; Kou, F.; Chen, G.; Jia, B.; Yang, Y.; Lai, Y. Synthesis, Crystal Structure and DNA-Binding Properties of a Nickel(II) Complex with 2, 6-Bis(2-Benzimidazolyl)Pyridine. *Zeitschrift für Naturforschung B* **2010**, *65* (11), 1334–1340.

(232) Wu, H.; Huang, X.; Yuan, J.; Kou, F.; Jia, F.; Liu, B.; Wang, K. A V-Shaped Ligand 2,6-Bis(2-Benzimidazolyl)Pyridine and Its Picrate Mn(II) Complex: Synthesis, Crystal Structure and DNA-Binding Properties. *Eur. J. Med. Chem.* **2010**, *45* (11), 5324–5330.

(233) Wu, H.-L.; Huang, X.; Liu, B.; Kou, F.; Jia, F.; Yuan, J.; Bai, Y. Copper(II) Complex Based on a V-Shaped Ligand, 2,6- *Bis* (2-Benzimidazolyl)Pyridine: Synthesis, Crystal Structure, DNA-Binding Properties, and Antioxidant Activities. *J. Coord. Chem.* **2011**, *64* (24), 4383 - 4396.

(234) Wu, H.-L.; Yuan, J.-K.; Huang, X.-C.; Kou, F.; Liu, B.; Jia, F.; Wang, K.-T.; Bai, Y. Two Zinc(II) and Cadmium(II) Complexes Based on the V-Shaped Ligand 2,6-Bis(2-Benzimidazolyl)Pyridine: Synthesis, Crystal Structure, DNA-Binding Properties and Antioxidant Activities. *Inorg. Chim. Acta* **2012**, *390*, 12 - 21.

(235) Saikia, E.; Dutta, P.; Chetia, B. A Novel Benzimidazolyl-Based Receptor for the Recognition of Fluoride and Cyanide Anion. *J. Chem. Sci.* **2017**, *129* (1), 1–7.

(236) Liu, S.-G.; Zuo, J.-L.; Li, Y.-Z.; You, X.-Z. Syntheses, Crystal Structures of Blue Luminescent Complexes Based on 2,6-Bis(Benzimidazolyl) Pyridine. *J. Mol. Struct.* **2004**, *705* (1–3), 153 - 157.

(237) Chetia, B.; Iyer, P. K. 2,6-Bis(2-Benzimidazolyl)Pyridine Receptor for Urea Recognition. *Tetrahedron Lett.* **2006**, *47* (46), 8115–8117.

(238) Chetia, B.; Goutam, P. J.; Chipem, F. A. S.; Iyer, P. K. Thiourea Recognition by 2,6-Bis(2-Benzimidazolyl)Pyridine Using Spectroscopic Techniques and DFT. *J. Mol. Struct.* **2013**, *1042*, 32–36.

(239) Chetia, B.; Iyer, P. K. 2,6-Bis(2-Benzimidazolyl)Pyridine as a Chemosensor for Fluoride Ions. *Tetrahedron Lett.* **2008**, *49* (1), 94–97.

(240) Badiei, A.; Razavi, B. V.; Goldooz, H.; Mohammadi Ziarani, G.; Faridbod, F.; Ganjali, M. R. A Novel Fluorescent Chemosensor Assembled with 2,6-Bis(2-Benzimidazolyl)Pyridine-Functionalized Nanoporous Silica-Type SBA-15 for Recognition of Hg2+ Ion in Aqueous Media. *Int. J. Environ. Res.* **2018**, *12* (1), 109–115.

(241) Vosough Razavi, B.; Badiei, A.; Lashgari, N.; Mohammadi Ziarani, G. 2,6-Bis(2-Benzimidazolyl)Pyridine Fluorescent Red-Shifted Sensor for Recognition of Zinc(II) and a Calorimetric Sensor for Iron Ions. *J. Fluoresc.* **2016**, *26* (5), 1723–1728.

(242) Rajnák, C.; Titiš, J.; Fuhr, O.; Ruben, M.; Boča, R. Low Spin Fe(II) Complexes Formed of Monosubstitued 2,6-Bis(2-Benzimidazolyl)Pyridine Ligands. *Polyhedron* **2017**, *123*, 122–131.

(243) Appukuttan, V.; Zhang, L.; Ha, J. Y.; Chandran, D.; Bahuleyan, B. K.; Ha, C.-S.; Kim, I. Stereospecific Polymerizations of 1,3-Butadiene Catalyzed by Co(II) Complexes Ligated by 2,6-Bis(Benzimidazolyl)Pyridines. *J. Mol. Catal. A Chem.* **2010**, *325* (1–2), 84 - 90.

(244) Gerber, T. I. A.; Mayer, P.; Tshentu, Z. R. Imidazolate Coordination of 2,6-Bis(2-Benzimidazolyl) Pyridine in a Dimeric Rhenium(V) Complex. *J. Coord. Chem.* **2005**, *58* (15), 1271 - 1277.

(245) Liu, S.; Pan, R.; Li, G.; Su, W.; Ni, C. Synthesis of Ruthenium Complex Based on 2,6-Bis(1-(Phenyl)-1H-Benzo[d]Imidazol-2-Yl)Pyridine and 2-(1-Phenyl-1H-Benzo[d]Imidazol-2-Yl)Benzoate and Catalytical Oxidation Property of 1-(1H-Benzo[d]Imidazol-2-Yl)Ethanol to 1-(1H-Benzo[d]Imidazol-2-Yl)Ethanone with H_2O_2. *J. Chem.* **2017**, *2017*, 1–7.

(246) Wojtecki, R. J.; Wu, Q.; Johnson, J. C.; Ray, D. G.; Korley, L. T. J.; Rowan, S. J. Optimizing the Formation of 2,6-Bis(N-Alkyl-Benzimidazolyl)Pyridine-Containing [3]Catenates through Component Design. *Chem. Sci.* **2013**, *4* (12), 4440.

(247) Zhang, W.; Sun, W.-H.; Zhang, S.; Hou, J.; Wedeking, K.; Schultz, S.; Fröhlich, R.; Song, H. Synthesis, Characterization, and Ethylene Oligomerization and Polymerization of [2,6-Bis(2-Benzimidazolyl)Pyridyl]Chromium Chlorides. *Organometallics* **2006**, *25* (8), 1961–1969.

(248) Deng, Z.; Yu, L.; Cao, W.; Zheng, W.; Chen, T. Rational Design of Ruthenium Complexes Containing 2,6-Bis(Benzimidazolyl)Pyridine Derivatives with Radiosensitization Activity by Enhancing P53 Activation. *ChemMedChem* **2015**, *10* (6), 991–998.

(249) Chetia, B.; Iyer, P. K. Utilization of 2,6-Bis(2-Benzimidazolyl)Pyridine to Detect Toxic Benzene Metabolites. *Tetrahedron Lett.* **2007**, *48* (1), 47–50.

(250) Peng, C.-C.; Li, Z.; Deng, L.-Q.; Ke, Z.-F.; Chen, W.-H. 2,6-Bis(Benzimidazol-2-Yl)Pyridine as a Potent Transmembrane Anion Transporter. *Bioorg. Med. Chem. Lett.* **2016**, *26* (10), 2442–2445.

Vita

Name	*Leonard Barasa*
Baccalaureate Degree	*Bachelor of Education (Science)*, *Egerton University, Nakuru* *Major: Mathematics/Chemistry*
Date Graduated	*November, 2001*
Other Degrees and Certificates	*Master of Science, University of Nairobi, Nairobi, Major: Chemistry*
Date Graduated	*September, 2011*